

POLITECNICO DI TORINO

Corso di Laurea Magistrale

in Ingegneria per l'ambiente e il territorio

Tesi di Laurea Magistrale

Degradation of bioplastics (polylactic acid-PLA and thermoplastic starch-TPS) in the marine environment



Relatori

Silvia Fiore

Nicolas Kalogerakis

Evdokia Syranidou

Candidato

Giorgia Barale

Anno Accademico 2021-2022

Giorgia Barale S288174

Supervisors: Prof.ssa S. Fiore, Politecnico di Torino, Prof. N. Kalogerakis and E. Syranidou, Technical University of Crete, Greece

Degradation of bioplastics (polylactic acid-PLA and thermoplastic starch-TPS) in the marine environment

Abstract

This master thesis was conducted in collaboration with the Biochemical Engineering & Environmental Biotechnology lab of the Technical University of Crete within an Erasmus+ mobility (February-September 2022, most of experimental activity) and the Circular Economy lab of the Politecnico of Torino (data analysis and some experimental activity).

Bioplastics are biodegradable and/or biobased polymers that are attracting increasing interest in the marketplace and in the literature as sustainable alternatives to conventional fossil-based plastics. Bioplastics undergo the same degradation mechanisms as conventional plastics, and their degradation depends on their physico-chemical properties as well as on the exposure environment. Biopolymers are often biodegradable only under specific and controlled conditions, therefore their behavior in the marine environment is still unclear and raises concerns in the scientific community. The aim of this work is the study of the degradation of two common and, so-called “biodegradable”, bioplastics, namely polylactic acid (PLA) and thermoplastic starch (TPS), in the coastal and pelagic zones of the marine environment. Accelerated weathering (indoor conditions) and natural light (outdoor conditions) were simulated in the BEEB lab of the Technical University of Crete. Pellets degradation over a 5-months period was studied. Weight and size variations of pellets were monitored; Scanning Electron Microscope (SEM) for surface topography changes, and spectroscopy, such as X-ray fluorescence (XRF) and Fourier Transform Infrared (ATR-FTIR) for elemental composition and chemical bonds variations, were used. Microplastics (MPs) formation was described and quantified using fluorescence microscope and Nile Red, Dynamic Light Scattering (DLS), and Nanoparticle Tracking Analysis (NTA). Degradation (visible as surface cracks, topography changes, weight and size differences, surface bonds and elemental variations) was much more evident in pelagic pellets (in seawater) than in coastal ones (on sand). Weight reduction for PLA in indoor conditions was 7.6% in the coastal zone and 33.2% in the pelagic one. Weight reduction for TPS in indoor conditions was negligible in the coastal zone and 16.8% in the pelagic one. An increase in the concentration of Si, S, and Cl was observed on the pellets surface, especially for the pelagic ones. Due to the TPS porous structure, these concentrations were up to two orders of magnitude higher than PLA (from 10^2 to 10^4 mg/kg). Biofilm formation for TPS in the outdoor pelagic environment likely enhanced elements uptake. The Carbonyl Index (CI) increased from 0.30 to 0.85 and 0.47 for PLA indoor and outdoor coastal, respectively; while decreased from 5.60 to 3.40 and 4.90 for TPS indoor and outdoor coastal, respectively. MPs formation (mainly in the form of fibers) was similar for the pelagic zone under indoor and outdoor conditions (from 10^4 MPs/ml of the pure seawater to 10^6) and its increase over the time was two orders of magnitude higher than in the coastal zone. To conclude, degradation effects and microplastics generation were more visible for pelagic zone with respect to coastal zone, likely due to hydrolysis effect. Photo-oxidation, along with its degradation effects, was more powerful for indoor conditions (concentrated UV light) compared to outdoor conditions.

Index

INDEX OF FIGURES	6
INDEX OF TABLES	8
1. INTRODUCTION	11
2. PLASTIC DEGRADATION IN THE MARINE ENVIRONMENT: GENERAL OVERVIEW	13
2.1. THE APPROACH	13
2.2. RESEARCH ARTICLES & REVIEW PAPERS	15
2.3. PLASTIC TYPES	15
2.3.1. <i>Bioplastics</i>	17
2.4. MICROPLASTICS AND NANOPLASTICS	20
2.5. SECONDARY KEYWORD ATTRIBUTION	23
2.5.1. <i>UV weathering and Schwarzschild's law</i>	24
2.6. NATURAL OR ARTIFICIAL SEAWATER	25
2.7. NOVELTY OF THE RESEARCH	26
3. MATERIALS & METHODS	27
3.1. COASTAL ZONE SET UP	28
3.1.1. <i>Outdoor conditions</i>	29
3.1.2. <i>Indoor conditions: accelerated weathering</i>	29
3.2. PELAGIC ZONE SET UP	29
3.3. INSTRUMENTS AND MATERIALS	31
3.3.1. <i>Plastic pellets</i>	32
3.3.2. <i>Calcium Chloride solution for density separation</i>	33
3.3.3. <i>Fluorescence microscopy for MPs/NPs detection and quantification</i>	33
3.3.4. <i>Dynamic light scattering (DLS) to measure MPs/NPs size distribution</i>	34
3.3.5. <i>Nanoparticle Tracking Analysis (NTA) for MPs/NPs concentration and size distribution</i>	35
3.3.6. <i>Energy Dispersive X-ray Fluorescence (EDXRF) spectroscopy for pellets elemental composition</i>	35
3.3.7. <i>Attenuated Total Reflectance – Fourier Transform Infrared Spectroscopy (ATR-FTIR) for Carbonyl Index evaluation</i>	36
3.3.8. <i>Scanning electron microscope (SEM): morphological and elemental characterization</i>	36
3.3.9. <i>Flow Cytometry (FCM) for cells quantification</i>	37
3.3.10. <i>Spectrophotometry and Crystal violet for biofilm quantification</i>	38
3.4. COASTAL ZONE ANALYSIS METHODS	38
3.4.1. <i>Pellets</i>	39
3.4.2. <i>Sand</i>	39

3.5.	PELAGIC ZONE ANALYSIS METHODS	41
3.5.1.	<i>Pellets</i>	41
3.5.2.	<i>Water</i>	42
3.6.	SENSITIVITY ANALYSIS	43
3.6.1.	<i>Pellets weight standard deviation and scale error.</i>	43
3.6.2.	<i>Regression analysis and R² for Schwarzcild's law</i>	43
3.6.3.	<i>Pearson coefficient correlation</i>	44
4.	RESULTS AND DISCUSSION	45
4.1.	DEGRADATION OF THE PLASTIC PELLETS	45
4.1.1.	<i>Weight, size, and macroscopic changes</i>	45
4.1.2.	<i>Surface topography and elemental composition</i>	50
4.2.	SEAWATER PROPERTIES AND BIOLOGICAL PRESENCE	68
4.3.	MPS/NPS FORMATION	71
4.4.	SENSITIVITY ANALYSIS	78
6.	CONCLUSIONS	81
	BIBLIOGRAPHY	83

Index of Figures

Section 2

<i>Figure 2.1. Scheme of the bibliographic research.</i>	14
<i>Figure 2.2. Frame of the Excel file with the bibliographic research.</i>	14
<i>Figure 2.3. Type of documents over the years.</i>	15
<i>Figure 2.4. Percentage of the different plastic types in the global market and main sectors of application (Plastics Europe, 2021).</i>	16
<i>Figure 2.5. Plastic type investigated over the years.</i>	16
<i>Figure 2.6. Global production capacities of bioplastics 2021 and 2026 (European Bioplastics, 2021c).</i>	18
<i>Figure 2.7. Global production capacities of bioplastics in 2021.</i>	19
<i>Figure 2.8. Microplastics and nanoplastics investigation over the years.</i>	22
<i>Figure 2.9. Investigation of plastic toxicity in the marine environment over the years.</i>	23
<i>Figure 2.10. Investigated aspects over the years.</i>	24
<i>Figure 2.11. Example of photoresponse obeying to the Schwarzcild's law.</i>	25
<i>Figure 2.12. Type of seawater (real or artificial) used for research during the years.</i>	26

Section 3

<i>Figure 3.1. Experimental setup scheme.</i>	28
<i>Figure 3.2. Coastal setup: metallic cups filled with sand and plastic pellets.</i>	28
<i>Figure 3.3. Indoor experimental setup.</i>	29
<i>Figure 3.4. Pelagic zone setup (outdoor and indoor conditions).</i>	30

Figure 3.5. PLA and TPS virgin pellets.	33
Figure 3.6. Fluorescence microscope.	34
Figure 3.7. SALD-7500nano by Shimadzu for Dynamic Light Scattering.	34
Figure 3.8. Malvern Panalytical NanoSight NS300 for Nanoparticle Tracking Analysis.	35
Figure 3.9. Rigaku NEX DE (picture by Applied Rigaku technologies, n.d.).	36
Figure 3.10. Thermo Scientific's Nicolet iS50 (picture from Thermo Scientific, n.d.).	36
Figure 3.11. Scanning electron microscope (FEI Inspect S50).	37
Figure 3.12. Flow cytometer CytoFLEX by Beckam Coulter.	37
Figure 3.13. Spectrophotometer UVmini-1240 by Shimadzu.	38
Figure 3.14. Coastal zone experiment methods.	38
Figure 3.15. Pelagic zone experiment methods.	41
Figure 3.16. Weight difference: comparison between 1 day and 1 week after the sampling day.	42

Section 4

Figure 4.1. Timeline of PLA pellets exposed in the coastal zone.	46
Figure 4.2. Timeline of TPS pellets exposed in the coastal zone.	46
Figure 4.3. Timeline of TPS pellets exposed in the pelagic zone. Pellets were cleaned and dried before pictures.	47
Figure 4.4. Differences between virgin TPS pellets, exposed and cleaned pellets, and pellets with biofilm after 90 days exposure (outdoor pelagic).	47
Figure 4.5. Timeline of PLA pellets exposed in the pelagic zone.	47
Figure 4.6. PLA INDOOR coastal weight reduction.	48
Figure 4.7. Schwarzschild's law for PLA INDOOR coastal.	48
Figure 4.8. Weight variation for pelagic pellets.	49
Figure 4.9. Timeline of pellets size variations,	49
Figure 4.10. Virgin pellets of PLA and TPS.	51
Figure 4.11. Virgin TPS detail.	51
Figure 4.12. Spectrum of a virgin pellet.	51
Figure 4.13. SEM pictures for PLA coastal in INDOOR and OUTDOOR conditions.	52
Figure 4.14. SEM pictures for TPS coastal in INDOOR and OUTDOOR conditions.	52
Figure 4.15. Detail of PLA INDOOR coastal pellet surface.	53
Figure 4.16. PLA INDOOR and OUTDOOR coastal surface.	53
Figure 4.17. TPS INDOOR and OUTDOOR coastal surface.	53
Figure 4.18. TPS coastal outdoor detail at 800x.	54
Figure 4.19. Spectra of the particles in A and B.	54
Figure 4.20. Spectra of the particles in C and D.	54
Figure 4.21. Spectrum of the particles in E.	55
Figure 4.22. TPS coastal indoor. Detail to highlight differences between the surface and the blackish spots.	56
Figure 4.23. SEM pictures for PLA pelagic in INDOOR and OUTDOOR conditions.	56
Figure 4.24. SEM pictures for TPS pelagic in INDOOR and OUTDOOR conditions.	57
Figure 4.25. PLA INDOOR and OUTDOOR pelagic. Different surface degradation with same magnification (200x).	57
Figure 4.26. TPS INDOOR and OUTDOOR pelagic. Different surface degradation with same magnification (200x).	58
Figure 4.27. TPS OUTDOOR pelagic detail and spectrum.	58
Figure 4.28. PLA INDOOR pelagic surface detail.	59
Figure 4.29. PLA OUTDOOR pelagic detail.	59
Figure 4.30. Sulfur concentration variation over the time for coastal and pelagic zone.	61

Figure 4.31. Fe concentration variation over the time for TPS INDOOR and OUTDOOR.	61
Figure 4.32. Si concentration variation over the time.	61
Figure 4.33. P concentration variation over the time.	62
Figure 4.34. ATR-FTIR virgin PLA and TPS spectra and main peaks.	63
Figure 4.35. Carbonyl Index for PLA coastal.	64
Figure 4.36. Carbonyl Index for TPS coastal.	64
Figure 4.37. Spectra of PLA INDOOR coastal.	65
Figure 4.38. Spectra of TPS INDOOR coastal.	65
Figure 4.39. Carbonyl Index for PLA pelagic.	66
Figure 4.40. Carbonyl Index for TPS pelagic.	66
Figure 4.41. Spectra of PLA INDOOR pelagic.	67
Figure 4.42. Spectra of PLA OUTDOOR pelagic.	67
Figure 4.43. Spectra of TPS INDOOR pelagic.	68
Figure 4.44. Optical density from Crystal Violet test for biofilm quantification of pelagic pellets.	68
Figure 4.45. Total nitrogen (on the right) and Nitrate (on the left) concentration in seawater.	69
Figure 4.46. Cells concentration over sampling days.	70
Figure 4.47. Flow cytometer results at the beginning and at the end of the experiments for PLA OUTDOOR.	70
Figure 4.48. Microplastics under the microscope.	72
Figure 4.49. MPs concentration with Fluorescence Microscope for coastal zone.	72
Figure 4.50. MPs concentration with Fluorescence Microscope for pelagic zone.	73
Figure 4.51. Schwarzschild's law applied to pelagic outdoor samples.	73
Figure 4.52. Schwarzschild's law applied to pelagic indoor samples.	74
Figure 4.53. Box plot of the mean MPs length for coastal samples at 31 days of exposure.	74
Figure 4.54. Particles concentration over the time for pelagic zone (NTA results).	76
Figure 4.55. Particles diameter over the time for pelagic zone (NTA results).	76
Figure 4.56. Pearson correlation coefficient for PLA and TPS indoor coastal.	78
Figure 4.57. Pearson correlation coefficient for PLA and TPS outdoor coastal.	79
Figure 4.58. Pearson correlation coefficient for PLA and TPS indoor pelagic.	80
Figure 4.59. Pearson correlation coefficient for PLA and TPS outdoor pelagic.	80

Index of Tables

Section 2

Table 2.1. Plastics characterization according to the size (Sangkham et al., 2022).	20
Table 2.2. Primary and secondary microplastics origin (National Geographic Society, 2022).	20
Table 2.3. Toxicity of MPs/NPs on animals (Pizzino et al., 2017; Sangkham et al., 2022).	21
Table 2.4. Exposure routes (Sangkham et al., 2022).	22
Table 2.5. Table Summary for novelty of the research.	27

Section 3

Table 3.1. Coastal zone instruments and materials.	31
Table 3.2. Pelagic zone instruments and materials.	32

Section 4

<i>Table 4.1. Light intensity recorded by Hobo data loggers for coastal zone.</i>	45
<i>Table 4.2. Light intensity recorded by Hobo data loggers pelagic zone.</i>	45
<i>Table 4.3. Macroscopic variations for PLA pellets.</i>	50
<i>Table 4.4. Macroscopic variations for TPS pellets.</i>	50
<i>Table 4.5. Elemental composition of TPS coastal outdoor (last sampling day).</i>	55
<i>Table 4.6. Elemental concentration in mg/kg for PLA indoor coastal pellets covered by sand (with XRF).</i>	55
<i>Table 4.7. XRF for virgin pellets.</i>	60
<i>Table 4.8. Main PLA peaks. Wavenumbers and their corresponding assignment for PLA virgin pellets IR spectrum (Chaplin, 2013; Nasir & Othman, 2022; Smith, 2021).</i>	63
<i>Table 4.9. Main TPS peaks. Wavenumbers and their corresponding assignment for PLA virgin pellets IR spectrum (del Rosario Salazar-Sánchez et al., 2019; Umamaheswari & Murali, 2013).</i>	63
<i>Table 4.10. Fluorescence microscope efficiency tested with beads.</i>	71
<i>Table 4.11. Mean diameter values from DLS analysis for coastal zone.</i>	75
<i>Table 4.12. Mean diameter values from DLS analysis for pelagic zone.</i>	75
<i>Table 4.13. Advantages and limitation of the different techniques used for MPs/NPs detection and quantification. Table readapted from Fu et al., 2020.</i>	77

1. Introduction

Despite the decline in production in the first months of 2020 due to the Covid-19 pandemic, the plastics industry has already recovered, even stronger than before (Plastics Europe, 2021), confirming itself as indispensable for the economy and for the everyday life.

While globally it continues to grow very fast, except for the pandemic period, virgin plastic production is slowly decreasing during the past years in EU27+3. However, with 55Mt of plastic produced in 2020, 29.5Mt of post-consumer plastic collected and a recycling rate of less than 35% (Plastics Europe, 2021), the fate of the plastic waste is nowadays of utmost concern due to its persistence and impact on several ecosystems (Webb et al., 2012).

The packaging sector, followed by the construction sector and the automotive industry, represents the largest end-use markets with a share of 45.5% in the EU27+3 sector plastic demand (Plastics Europe, 2021). Thus, PE and PP, which are among the most used plastics for packaging purposes, lead the market (Plastics Europe, 2021). Packaging sector is by its nature devoted to design products that have a short life into the economy and become trash after a very short period if compared with the persistence of these plastics into the environment (Gewert et al., 2015). Thus, the high rates of plastic production and its accumulation into the environment, along with its very low degradability, led the topic and its threats, especially on the marine environment and human health (European Commission, n.d.) , to be discussed at European level. Indeed, many EU directives, in the frame of the EU plastics strategy, aim nowadays to face plastic pollution and marine litter, accelerating the transition towards a circular plastics economy. They mainly aim to act on the replacement of the most widespread single-use items with more sustainable options (Single-use plastics Directive, 2019/904, (European Commission, n.d.-b), and on the unsustainable consumption of plastic carrier bags (The Plastic Bags Directive 2015/720, European Commission 2022).

Since the most widespread plastics are made from fossil fuels, that not only accumulate into every environment but also contribute to increased greenhouse gas emissions (European Commission, 2022a), the topic of alternative bio-based, biodegradable and compostable plastics is rising interest over the years, reaching also a place in the policy framework of the European Green Deal and new circular economy action plan (European Commission, 2022a). Indeed, plastic durability is no longer seen as a virtue in many sectors.

While bioplastics, that are entirely or partially made from biological resources, instead of fossil material, are not necessarily biodegradable, biodegradable and compostable plastics are supposed to biodegrade (European Commission, 2022a). However, the degradation often occurs under controlled and specific conditions, such as enzymatic biodegradation in industrial composting (Martin et al., 2014). Thus, being the degradation a property that is influenced by many physical and chemical factors (Kliem et al., 2020), the fate of bioplastics left into uncontrolled environments, both terrestrial and aquatic, is still uncertain and under discussion. Filling the knowledge gap on this topic in the near term

is strategic since these alternative plastics already constitute an important part of the plastic economy and will see a further grow in the next years being important contributors into the European Union climate goals (European Bioplastics, 2021c). Life cycle assessments and toxicological studies of the bioplastic items, empathizing material sources and in particular the fate and effect at their end-of-life in several environments, are important to ensure the effectiveness and efficacy of these materials or assess all their potential threats (Martin et al., 2014), such as microplastic formation or heavy metal absorption and transport.

Microplastics are pieces of plastics, smaller than 5 mm and in various shape, that are raising concerns over the years due to their growing volume found in the sea, in food and drinking water (European Commission, 2022b). Currently there is not a specific and comprehensive European law on microplastics related issues. However, in the framework of the European Green Deal and the new circular economy action plan, the European Commission claimed its purpose of facing the unintentional release of microplastics in the environment and closing the scientific knowledge gaps concerning microplastics risk and presence in different environments (European Commission, 2022b).

The experiments presented in this thesis fit in the over-mentioned problems and aimed at filling the scientific knowledge gaps for bioplastics degradation and microplastics formation, specifically in the marine environment. In particular, the alteration of the physicochemical properties of two bioplastics, polylactic acid (PLA) and a biodegradable thermoplastic starch (TPS), due to exposure to UV radiation in the coastal and in the pelagic zone of the marine environment, has been monitored. Since in the recent years the biopolymers, such as PLA and TPS, entered into the market as alternative solutions to fossil-based plastics production and plastic waste problems, their investigation is fundamental to fill the lack of scientific knowledge regarding their fate and MPs formation in non-controlled conditions such as the marine environment (Deroiné et al., 2014). Thus, two different marine compartments have been simulated. The coastal zone has been simulated placing plastic pellets over beach sand. For the simulation of the pelagic zone, the plastic pellets have been immersed in aquariums filled with real seawater. The objective is to assess, by analyzing samples every two weeks, the changes in the pellets physico-chemical properties, and the MPs/NPs formation of the two different plastics in the two environments and under two different weathering conditions: natural light weathering in a greenhouse and accelerated weathering due to the exposure to UV lamps.

The experiments lasted 5 months (March – July 2022) and were performed in the laboratory of Biochemical Engineering & Environmental Biotechnology (BEEB) at the Technical University of Crete (Greece), in collaboration with the Circular Economy lab of the Politecnico di Torino, in the context of the Erasmus+ exchange.

2. Plastic degradation in the marine environment: general overview

Since plastic waste is responsible for the 80% of the marine litter, consisting in particular of single-use plastic items, carrier plastic bags and fishing gear (European Commission, 2022d), the study of the degradation mechanisms and the fate of plastic in such an important environment is fundamental. Indeed, the final destination of plastics that are not landfilled, incinerated, or recycled is usually the ocean. This chapter analyzes the current state of research on plastic degradation in the marine environment.

Conventional plastics, that are fossil based, have a great stability and durability that allow them to be useful in a wide range of applications. Due to these properties, they do not usually degrade fast in the environment in where they are released (Catarci Carteny & Blust, 2021).

Natural degradation of plastic in the environment is a mix of mechanisms that usually requires decades and can be divided in four main mechanisms that are:

- photodegradation
- thermo-oxidation
- hydrolysis
- biodegradation

The exposure to sunlight and ultraviolet light lead to the fragmentation of the polymer and to a decrease of the molecular weight in a way that microorganisms can metabolize them. The pace of these processes depends on the plastics type and on the exposure environment. For example, the plastic physical and chemical properties (mobility, degree of crystallinity, molecular weight, hydrophobicity and functional group presence) influence the decomposition time and conditions (Atiwesh et al., 2021). Also, usually in seawater a polymer degrades in a slower way than if exposed to the air due to lower temperatures and oxygen content (Webb et al., 2012). That's why the study of plastic degradation and its mechanism in the marine environment is of utmost importance.

2.1. The approach

The bibliography research to assess the state of the art of the plastic degradation in the marine environment has been performed in January 2022 and updated in October 2022, using Scopus database searching within “Article title, Abstract, Keywords” the following words: ‘Plastic’ or ‘Polymer’ or ‘Plastic waste’, ‘Marine environment’ or ‘Seawater’, ‘Degradation’. Further selection has been made selecting *Article* and *Reviews* as Document type, *English Language*, and a time period between the year 2011 and 2022.

Over a list of 284 documents sorted on *Relevance*, 138 documents have been selected and transferred into an excel sheet containing *Authors*, *Title*, *Year*, *Source title*, *Citation number*, *DOI*, *abstract*, and *Author Keywords*.

A scheme is showed in Figure 2.1.

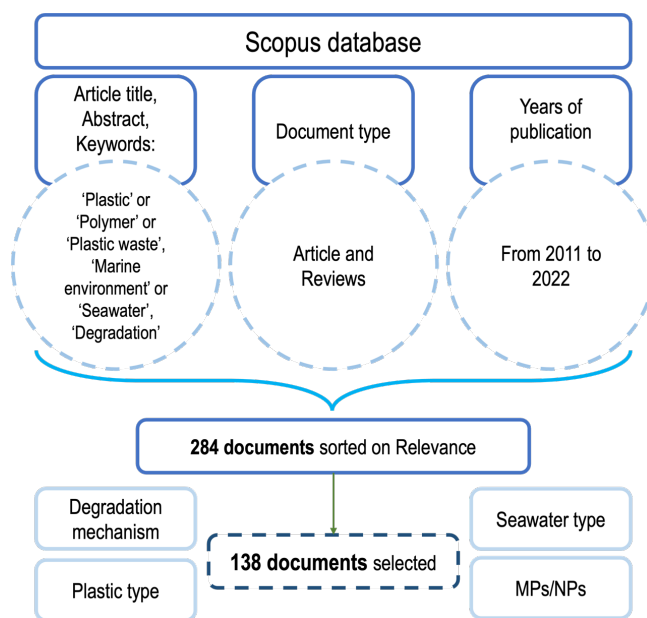


Figure 2.1. Scheme of the bibliographic research.

Reading the abstracts, the document type, a secondary keyword (or my keyword) regarding the main focus of the document, the plastic types analyzed, and the type of seawater used (natural or artificial), have been added. A frame of the Excel file is visible in Figure 2.2.

Authors	Title	Year	Source title	Cited by	DOI	Link	Abstract	Document Type	Author Keywords	My keyword	Plastic type	Seawater type
Wang G.-X., Huang D., Ji J.-H., Völker C., Wurm F.R.	Seawater-Degradable Polymers—Fighting the Marine Plastic Pollution	2021	Advanced Science	25	10.1002/adv.202001121	https://www.scopus.com/inward/record.uri?doi=10.1002/adv.202001121	Polymers shape human life but they also have been identified as pollutants in the oceans due to their long lifetime and low degradability. Recently, various researchers have studied the impact of (micro)plastics on marine life, biodiversity, and potential toxicity. Even if the consequences are still heavily discussed, prevention of unnecessary waste is desired. Especially, newly designed polymers that degrade in seawater are discussed as potential alternatives to commodity polymers in certain applications. Biodegradable polymers that degrade in vivo (used for biomedical applications) or during composting often exhibit too slow degradation rates in seawater. To date, no comprehensive summary for the degradation performance of polymers in seawater has been reported, nor are the studies for seawater-degradation following uniform standards. This review summarizes concepts, mechanisms, and other factors affecting the degradation process in seawater of seawater-degradable polymers or polymer blends. As most of such materials cannot degrade or degrade too slowly, strategies and innovative routes for the preparation of seawater-degradable polymers with rapid degradation in natural environments are reviewed. It is believed that this selection will help to further understand and drive the development of seawater-degradable polymers. © 2020 The Authors. Published by Wiley-VCH GmbH	Review	biodegradability ; biodegradability ; biodegradable polymers ; marine plastic pollution ; seawater-degradable polymers	mechanism overview;	biodegradable	-
Tang C.-C., Chen H.-I., Brimblecombe P., Lee C.-L.	Textural, surface and chemical properties of polyvinyl chloride particles degraded in a simulated environment	2018	Marine Pollution Bulletin	17	10.1016/j.marpolbul.2018.05.062	https://www.scopus.com/inward/record.uri?doi=10.1016/j.marpolbul.2018.05.062	Virgin polyvinyl chloride (PVC) particles were exposed to heat, ultraviolet B (UVB) and solar radiation either in artificial seawater or in air for different periods of time. The surface and chemical properties of fresh and degraded particle surfaces were determined via image analysis using scanning electron micrographs, a Brunauer-Emmett-Teller (BET) specific surface area analyzer and infrared spectroscopy. Thermal and UVB degradation resulted in unique PVC morphologies. In addition, the increased presences of functional groups were evident as dehydrochlorination and oxidation during the degradation process, which altered the chemical properties of PVC. In contrast, under solar exposure with or without seawater, unevenness to the surface was noted that seems to originate from degradation of the PVC surface; in addition, no new functional groups were found. This suggests that the chemical properties of PVC are stable over extended periods in the marine environment. © 2018 Elsevier Ltd	Article	Environmental degradation; Marine debris; Surface morphology; Thermal degradation; Ultraviolet B (UVB) radiation	photo/thermal; oxidation;	PVC	lab
Tang C.-C., Chen H.-I., Brimblecombe P., Lee C.-L.	Morphology and chemical properties of polypropylene pellets degraded in simulated terrestrial and marine environments	2019	Marine Pollution Bulletin	17	10.1016/j.marpolbul.2019.10626	https://www.scopus.com/inward/record.uri?doi=10.1016/j.marpolbul.2019.10626	The morphology and chemical properties of polypropylene pellets degraded in the terrestrial and marine environments reveal their interaction between marine pollutant and biota and help us understand the fate of plastic debris. © 2019 Elsevier Ltd Polypropylene (PP) pellets exposed to solar radiation, ultraviolet B (UVB) radiation and heat in four simulated treatments: dry-air, seawater-air, seawater-darkness, and dry-darkness for 0.5–1.5 years to investigate morphology and chemical change under various environmental conditions. Scanning electron microscopy and infrared spectroscopy were employed to characterize the virgin and degraded pellets. The degraded PP pellets under solar and UVB irradiation revealed 35% and 12% cracks, respectively. Moreover, carbonyl and hydroxyl groups formed on the surface gradually extended to the interior. However, under photo-irradiation, PP pellets floating in seawater showed less degradation than those in a dry environment. The formation of biofilm may retard the	Article	Environmental degradation; Marine debris; Photo degradation; Surface cracking; Thermal degradation	photo/thermal; oxidation;	polypropylene	real

Figure 2.2. Frame of the Excel file with the bibliographic research.

In the following, the results of the bibliographical analysis will be shown and discussed.

2.2. Research articles & review papers

Looking at the number of documents over the years it is evident that the study of plastic degradation in marine environments has attracted an increasing interest. Looking at Figure 2.3 it is visible that both scientific articles and reviews have increased over the years. In particular, the high increase in 2020 and 2021 of review papers can be due to the pandemic situation that forced people outside the laboratories. Since the research has been made until October 2022, there are less documents for the year 2022.

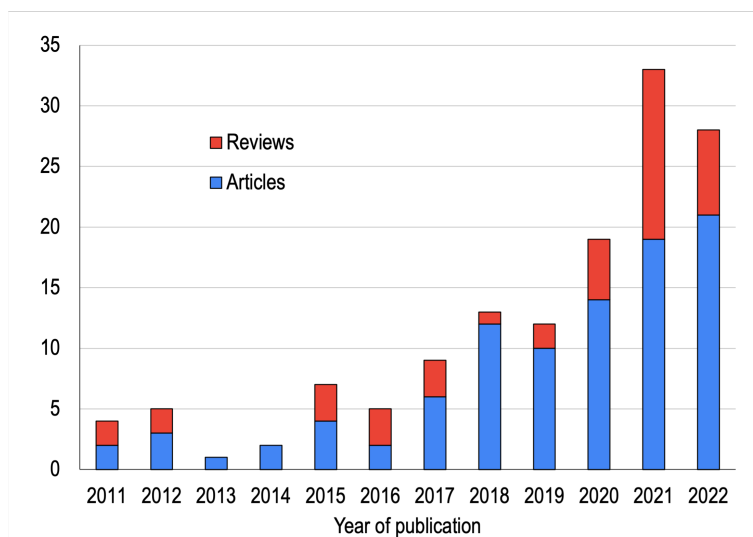


Figure 2.3. Type of documents over the years.

Being these experiments located in the landscape of this hot topic, it is evident how research is important to provide innovation and speed up the gaps closure.

2.3. Plastic types

A look at the different plastic types analyzed in the scientific literature over the years can highlight the market trends and the materials that are arising more interest or concern in the research landscape. PE, PET and PP are among the most common plastics (Figure 2.4) used mainly for food packaging and thus have been and currently are highly investigated (Figure 2.5).

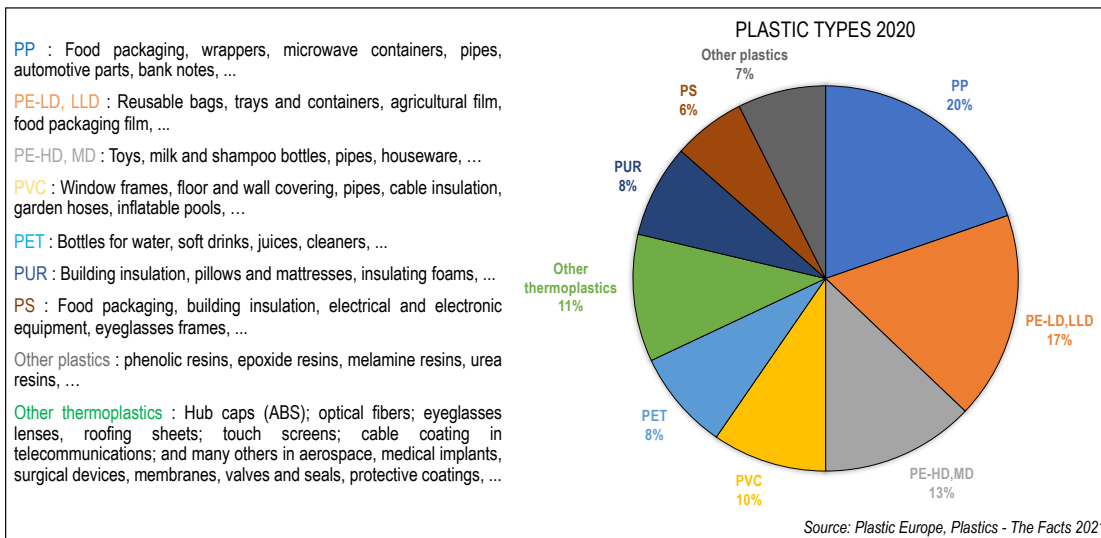


Figure 2.4. Percentage of the different plastic types in the global market and main sectors of application (Plastics Europe, 2021).

From the Figure 2.5, it is also visible that bioplastics began to be highly investigated in the last years along with their increased affirmation on the market as alternative materials to common plastics to face plastic pollution environmental problems. Under the label ‘bioplastics’, plastics that are biodegradable, or plastics produced from biological materials (in this case that can or cannot be biodegradable) are considered (Atiweh et al., 2021).

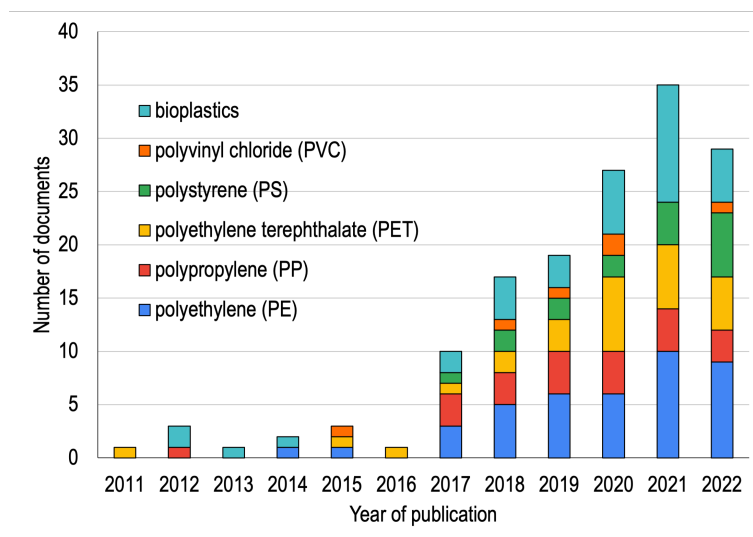


Figure 2.5. Plastic type investigated over the years.

2.3.1. Bioplastics

Being produced from non-renewable resources, with prices very dependent on oil prices and leading to huge amounts of waste accumulation due to its short use lifespan (Deroiné et al., 2014), common plastics, along with their unique and precious characteristics, have several drawbacks. Developed as alternatives of fossil-based plastics, bioplastics represent a wide range of biodegradable or renewable feedstock-based polymers, with a degradability that, like the other polymeric materials, depends on the surrounding environment and physico-chemical characteristics and can range from days to years (Atiwesh et al., 2021).

During recent years, despite the slow decrease in plastic production (Plastics Europe, 2021), bioplastics have followed a continuously growing trend (Figure 2.6). However, bioplastics still represent less than 1% of the total annual production (307Mt in 2020, 55Mt at European level) (Plastics Europe, 2021; European Bioplastics, 2021). This trend is expected to grow in the future, with a bioplastics production around 2.42 Mt in 2021 to around 8 Mt in 2026, overcoming the 2% share in the global plastic production (Plastics Europe, 2021; European Bioplastics, 2021).

While polylactic acid (PLA) is expected to continue to grow thanks to investments in its production (led by Asia that is the main bioplastics producer), the main drivers of the growth are biodegradable bioplastics such as biodegradable PBAT (polybutylene adipate terephthalate) and PBS (polybutylene succinate). However, also the production of bio-based non-biodegradable bioplastics, such as bio-PE (polyethylene) and bio-PP (polypropylene), will increase (European Bioplastics, 2021c). Currently, 64% of the bioplastics production accounts for biodegradable plastics (PLA, PHA, starch blends) and it is expected to reach 70% by 2026, reaching 5.3 Mt produced. At the same time, the share of bio-based non-biodegradable plastics will decrease, despite a production growth (European Bioplastics, 2021c).

The growth in bioplastics production goes with the increasing possibility of their applications to several markets, such as (European Bioplastics, 2021a):

- Packaging
- Consumer goods
- Fibers
- Agriculture and horticulture
- Automotive and transport
- Coating and adhesives
- Construction
- Consumer electronics and electrics

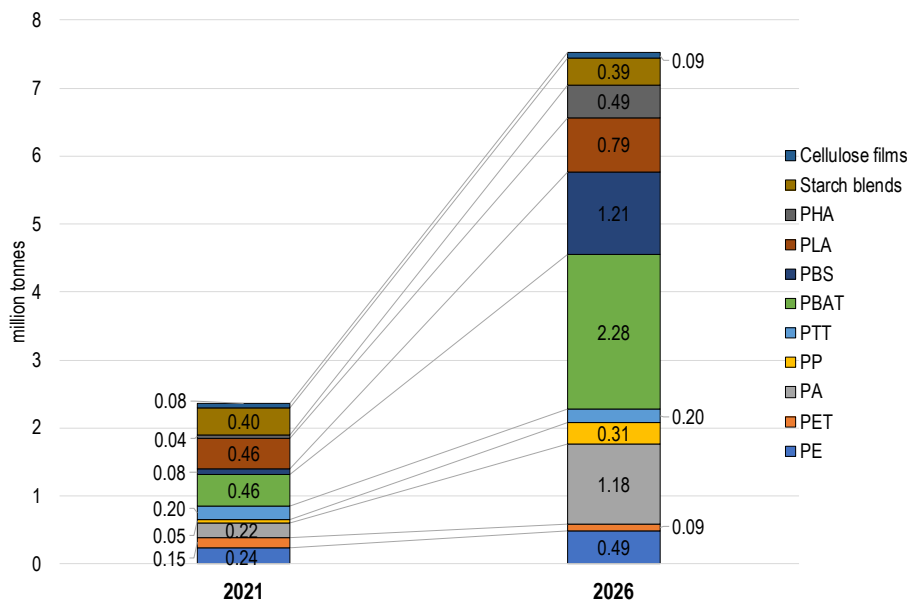


Figure 2.6. Global production capacities of bioplastics 2021 and 2026 (European Bioplastics, 2021c).

In Figure 2.7, the share for the different market segments is reported.

There are many factors that are responsible for the success of bioplastics on the market. Being promoted as materials that can face climate change and that can enhance the independence from fossil fuels, bioplastics have a high consumer acceptance. On a more technological point of view, bioplastics often have the same properties as conventional plastics with an additional possibility for waste management that is composting and a source that is renewable and easily available. For all these reasons, bioplastics are nowadays often seen as environmentally friendly substitutes to conventional fossil-based polymers.

However, there is still a lack of knowledge about the effects of bioplastic pollution in some environments, such as in the marine ecosystems. Indeed, most bioplastics can only degrade under specific controlled conditions; for some of them the decomposition process leads to a release of greenhouse gasses contributing to a change in the ecosystem equilibriums (Atiwesh et al., 2021) and some studies highlight that they can accumulate heavy metal, toxic compounds, antibiotic resistance and metal resistance genes (Di Cesare et al., 2021). Life cycle assessment, the study of degradation mechanisms and toxicological analysis play an important role in order to have a comprehensive idea of the similarities and differences between conventional polymers and bioplastics and their impacts on the environment and human health.

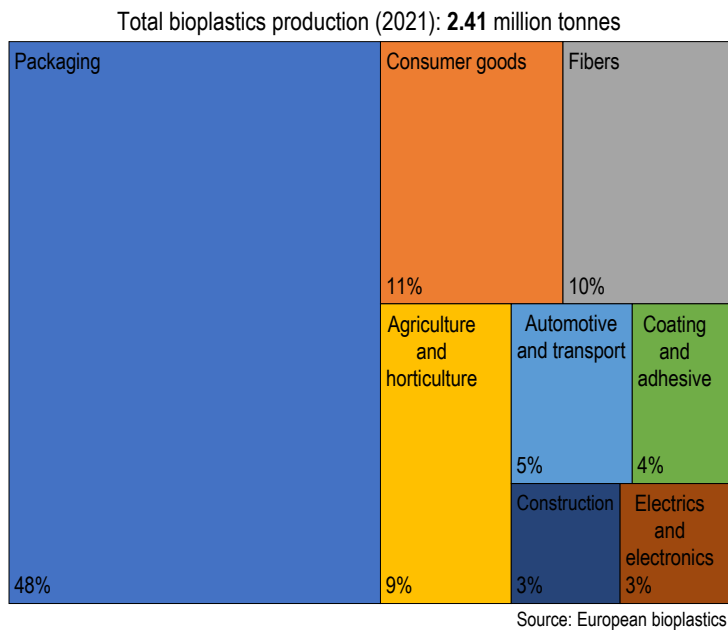


Figure 2.7. Global production capacities of bioplastics in 2021.

Polylactic acid (PLA)

Polylactic Acid (PLA) is a thermoplastic that can be produced using the conventional melting technologies for fossil-based polymers, but using a plant-based feedstock, such as corn, sugar cane, tapioca or potato starch (Atiwesh et al., 2021).

It has broad application possibilities (packaging, plastic bags, fibers, bottles) due to its high melting point and mechanical strength, along with its high degree of transparency that make it be comparable with traditional fossil-based polymers (Martinez Villadiego et al., 2022). Its production as a short-life and disposable product has therefore increased over the years, along with its competitiveness of the price on the market, despite the still quite high production prices (Prieto, 2016; Sin et al., 2012). It is thus receiving attention also from the research community. However, there is still a knowledge gap on how it concerns its behaviour in marine environments (Webb et al., 2012). Like Webb et al., 2013, have assessed, PLA does seem to have a low degradation rate in the water Webb et al., 2012).

Thermoplastic starch (TPS)

The Thermoplastic starch (TPS) is a biodegradable bioplastic that, like PLA, can be obtained using conventional technologies, from plant resources, water and/or other plasticizers (e.g., glycerol, and glucose) and sometimes compounds containing nitrogen (Atiwesh et al., 2021).

Starch-based thermoplastics are cheap materials usually used almost only for packaging, due to their high sensitivity to moisture (they have high hydrophilicity), and low thermal stability (Martinez Villadiego et al., 2022).

2.4. Microplastics and nanoplastics

Oceans and seas are polluted by plastics that can have very different shapes (fragments, pellets, fibers, beads, films,...) and present a wide range of sizes from large (such as macroplastics (>25 mm), and mesoplastics (5-25 mm)) to very small brittles (microplastics (1–5 mm) and nanoplastics (1–1000 nm)) (Bhatt et al., 2021; Sangkham et al., 2022). The dimension of what is called micro or nanoplastics can differ according to different definitions, so there is not a univocal characterization. Table 2.1 reports the most widespread plastics characterization according to the size.

Table 2.1. Plastics characterization according to the size (Sangkham et al., 2022).

Plastic name	Diameter	Shape
Nanoplastics (NPs)	1-1000nm, <20 μm	Fragments, pellets, beads, granules, foam, fibers, films
Microplastics (MPs)	1μm-5mm	
Mesoplastics (MSPs)	5-25mm	
Macroplastics (MCPs)	>25mm	

As highlighted in Table 2.2, microplastics can be manufactured to be of microscopic size for commercial products, such as pharmaceuticals, cosmetics, textiles (primary MPs), or can result from the fragmentation and degradation of larger plastics due to environmental exposure (secondary MPs) (National Geographic Society, 2022).

Table 2.2. Primary and secondary microplastics origin (National Geographic Society, 2022).

Primary MPs	Secondary MPs
<p>Manufactured for indirect or direct use as raw materials for consumer polymer goods:</p> <ul style="list-style-type: none"> - facial cleansers, cosmetics, scrubs, microbeads, - toothpaste, exfoliants, and abrasives - washing synthetic clothes and rubbers - tea bags 	<p>Produced from the breakdown, cracking, and/or degradation of larger plastic fragments:</p> <ul style="list-style-type: none"> - physical, chemical, and/or biological action

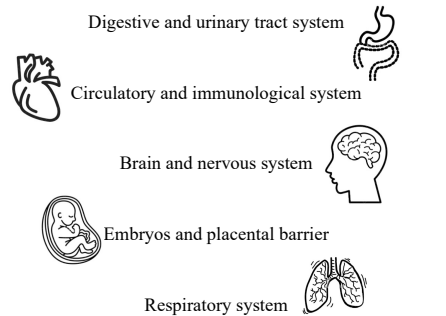
The effects of these plastics on the living systems are linked with their pervasivity, abundance, size, shape, and physico-chemical properties. Bigger-size plastics can have consequences on movement, feeding and breathing. Smaller-size plastics can reach the digestive system causing gastrointestinal and secretion blockage. That's why the assessment of the microplastics size distribution can be crucial to understand their

behavior and potential hazard in the different environments (Yang et al., 2022). The proven presence of toxic chemicals (such as polychlorinated biphenyls (PCBs), organic pesticides, organic pesticides, dyes, heavy metals) on the plastic particles found in the ocean increases the risk that can occur after their ingestion (Webb et al., 2012). The bioaccumulation and biomagnification of these compounds, in addition to damaging marine flora and fauna (listed in Table 2.3), can also enhance the risk to human health (Bhatt et al., 2021). The toxic chemicals that can be found on oceanic plastics are linked with several health issues, such as chronic inflammations, neurological problems, growth of abnormalities, hormonal imbalances, different types of cancer, arthritis, diabetes, obesity (Table 2.4) (Bhatt et al., 2021; Schirinzi et al., 2017; Webb et al., 2012). In this context, also microplastics produced from biodegradable plastics (BMPs) cannot go unnoticed. Indeed, BMPs can act as contaminants carriers until their complete degradation, leading to the same environmental threats as conventional MPs (Bao et al., 2022).

Table 2.3. Toxicity of MPs/NPs on animals (Pizzino et al., 2017; Sangkham et al., 2022).

Toxicity of MPs/NPs on animals	
- Effects on cell viability (number of live, healthy cells)	- Cytotoxicity
- Oxidative stress (imbalance between production and accumulation of oxygen reactive species).	- Alterations in the expression of some genes, and other DNA damages,
- Histological abnormalities	- Metabolism changes
- Decreased immune response	- Neurotoxicity
- Inflammation	- Effects on reproductive activity
	- Tumors

Table 2.4. Exposure routes (Sangkham et al., 2022).

Exposure routes		
Ingestion (oral intake) 	Inhalation 	Dermal contact 
→ through food, water, beverages, drug capsule, salt	→ through indoor/outdoor air	→ through textiles, cosmetics, skincare products, toothpaste
- High risk of biphenyl exposure - Serious health risk for long-term exposure	- Short and long-term acute and chronic respiratory problems - Inflammation	- Skin discomfort and deeper absorption - Irritation
Human body's systems affected by MPs/NPs exposure		
		
 Additional studies are needed to fill the knowledge gap about all the exposure routes and the different effects of MPs/NPs on human health in different concentrations and environments		

Recently, the problem of micro/nano-plastics contamination of marine environments has arisen with increasing concern. The increasing importance of MPs/NPs presence and fate is reflected in the amount of their investigation in the literature, as highlighted in Figure 2.8.

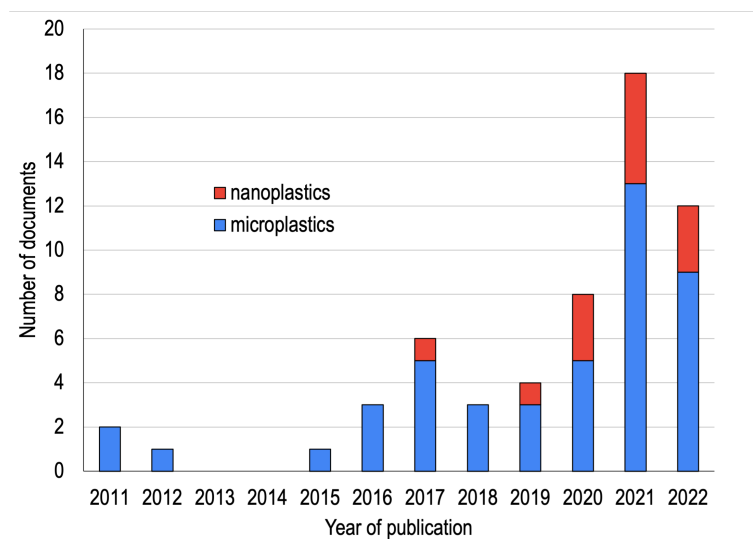


Figure 2.8. Microplastics and nanoplastics investigation over the years.

This trend is visible also in the investigation of plastics negative effects on marine biota and human health, the contaminants interaction and transport (Figure 2.9).

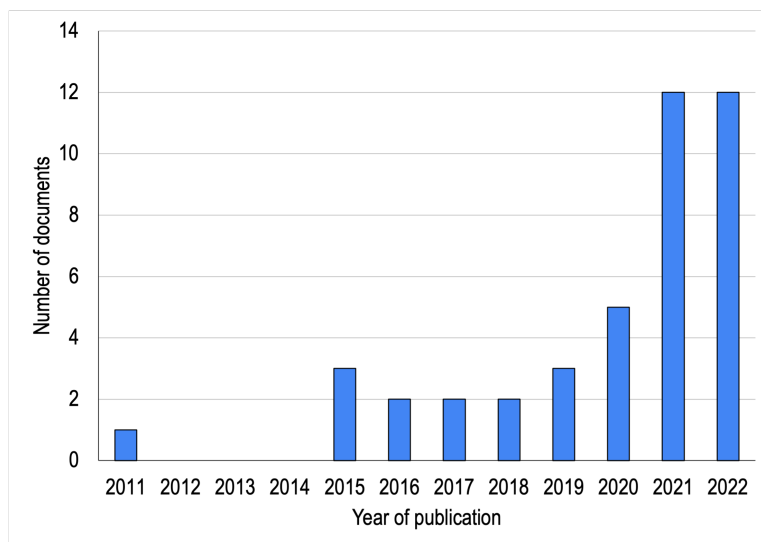


Figure 2.9. Investigation of plastic toxicity in the marine environment over the years.

2.5. Secondary keyword attribution

To highlight which topics are mainly investigated in the literature of the plastics degradation in the marine environment a secondary keyword (or My keyword) has been associated with the documents.

The selected keywords are:

- *weathering*: it refers to degradation led by abiotic factors, such as sunlight, air, heat, moisture, wind (Pickett, 2018).
- *biodegradation*: it is the conversion of a polymer firstly into its monomers, and then into carbon dioxide, water, and methane (mineralization) performed by microorganisms (Bahl et al., 2021).
- *photo/thermal oxidation*: it is the degradation of a polymeric material due to the action of light or heat and oxygen (Gardette et al., 2013).
- *hydrolysis*: it occurs when water breaks down the chemical bonds of a polymer (Gewert et al., 2015). Main point of hydrolysis: diffusion of water toward the polymer interior, scission of ester linkages, reduction of chains into soluble fragments resulting in lower molar mass. Temperature, pH, molecular weight, crystallinity are the main driving factors (Gorrasi & Pantani, 2018).
- *mechanisms overview*: it refers to the description of the different degradation pathways that a polymer can undergo in different environments and conditions, and their effects on it and its properties.

A keyword has been associated with a total of 92 documents out of the initial 112. The results are shown in Figure 2.10. The documents without a keyword are mainly focused on plastics characterization and detection into different environments, while the review papers mainly focus on the effects of the different mechanisms on the degradation (mechanisms overview).

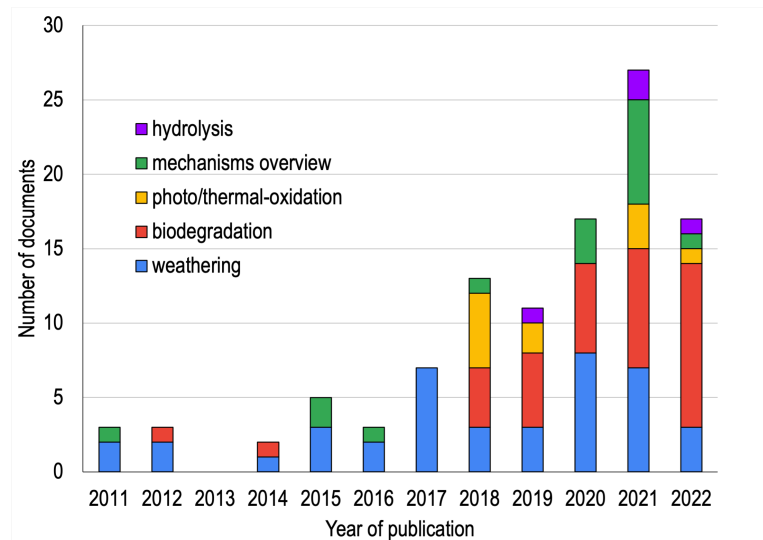


Figure 2.10. Investigated aspects over the years.

The experiments conducted for this thesis are mostly focused on the investigation of the photo-oxidation effects on the degradation of bioplastics.

2.5.1. UV weathering and Schwarzschild's law

Ultraviolet radiation is usually considered one of the most important drives of degradation. UV light can break molecular bonds that generate free radicals, leading to the formation of hydroxyl acids and carbonyl acids. This can also lead to the scission of molecular chains, and thus morphological changes of the material. Since the breaking of bonds is due to photons with an energy higher than the bond, the rate of degradation of a material increases with the level of UV irradiation (Yang et al., 2022).

Accelerating the degradation of plastics, by the photodegradation effect of UV light (reciprocity law experiments), can be useful in the research on weathering and durability of materials. However, since the accelerated condition obtained through lab experiments does not match with the solar spectrum, these kinds of experiments experience sometimes a lack of acceptance by the scientific community (J. W. Martin et al., 2003).

Specifically, reciprocity law experiments consist in experiments where the photoresponse of the material analyzed is a function of the irradiance to which is exposed (Eq 2.1):

$$I \cdot t = constant,$$

(2. 1)

where I is the radiant intensity and t is the exposure time.

Divergences from this law are called *reciprocity law failures* and often occur for very high or very low values of irradiance (J. W. Martin et al., 2003).

The Schwarzschild's law in Eq. 2.2 is a generalization of the reciprocity law, that accounts also for low intensity experiments:

$$I \cdot t^p = \text{constant}, \quad (2. 2)$$

Where p is the Schwarzschild coefficient, and it is different according to the material studied and the irradiance values.

The Schwarzschild's law has been seen to model adequately the photoresponse (weight loss, color and properties changes, MPs generation) as functions of the irradiance for a large variety of materials during degradation experiments. The law is obeyed when a linear relationship between the logarithm of the photoresponse chosen and the logarithm of light intensity is found (Figure 2.11) (Yang et al., 2022).

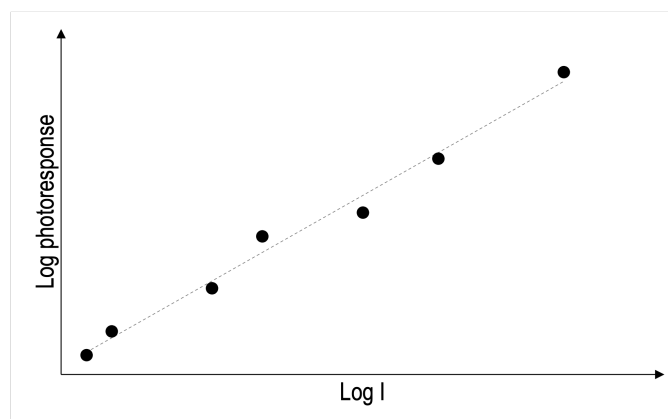


Figure 2.11. Example of photoresponse obeying to the Schwarzschild's law.

2.6. Natural or artificial seawater

Another important aspect to evaluate is the type of seawater that has been used to perform the experiments. Artificial seawater is purer, containing salts and minerals, while natural seawater can contain several contaminants depending on the area of collection and, if not sterilized, microorganism and algae that can grow fast under certain conditions.

The experiments conducted in literature have been reviewed according to the seawater type used. Results are shown in Figure 2.12.

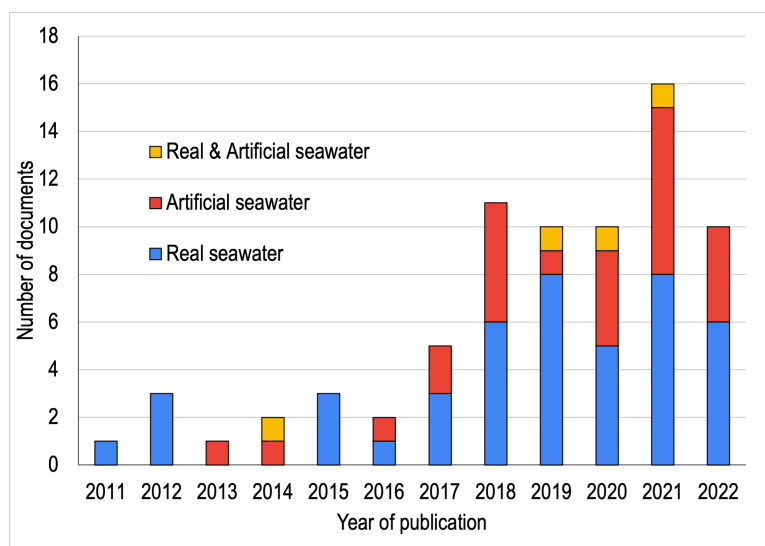


Figure 2.12. Type of seawater (real or artificial) used for research during the years.

Dealing with natural seawater is important when the fate of plastic waste must be explored, since the main ending of plastics not recycled or landfilled or thermovalorized is the sea. Thus, the experiments conducted in this work will be collocated in the real seawater context. However, having real seawater conditions in a laboratory context is challenging, concerning especially the temperature control and the sea waves simulation.

2.7. Novelty of the research

Literature research was conducted using Scopus to evaluate the state of the art in the study of the degradation of bioplastics (specifically PLA and starch-based) in the marine environment. Scopus database was used. The documents containing within “Article title, Abstract, Keywords” the following words, have been selected: ‘bioplastic’ or ‘biopolymer’ or ‘biodegradable, ‘marine environment’ or ‘seawater’, ‘degradation’ or ‘weathering’ or ‘ageing’. Further selection has been made selecting *Article* and *Reviews* as Document type, *English Language*, and a time period between the year 2011 and 2022. Over a list of 197 documents, only 31 research papers were found concerning PLA and/or TPS, and only 22 research articles were found to be compliant with the same plastic types and aim of the experiments: the study of degradation of bioplastics (PLA or starch-based) in the marine environments. The results are summarized in Table 2.5.

The study of these two bioplastics became in the last years a landscape of increasing interest as visible from the years of publication. PLA was more investigated than TPS, and only two papers studied the two plastics together. Janik et al., 2018 studied the two polymers separately, while Guzman-Sielicka et al., 2013 as blended-polymers.

Simulating coastal and pelagic zone, the effect of hydrolysis can be evaluated. While simulating indoor and outdoor conditions, the effect of photodegradation can be analyzed. No articles were found examining both pelagic and coastal zone of the marine environment in both natural and accelerated weathering. Pinto et al., 2022 and Al-Salem

et al., 2020 were the only one that studied UV degradation, but natural degradation was not investigated.

Table 2.5. *Table Summary for novelty of the research.*

Authors	PLA	TPS	Accelerated degradation	MPs/NPs formation	Days of exposure	Type of seawater	Sediments or sand	Elemental composition variation
Cheng et al. 2022	x					real		
Pinto et al. 2022		x	with UV (photo-degradation)			artificial		x
Al-Salem 2022		x			82 days			
Phosri et al. 2022	x					real	x	
Pokora et al. 2022	x							
Miksch et al. 2022	x		with temperature (thermal-oxidation)			real		
Li et al. 2022	x		with temperature (thermal-oxidation)		468 days	artificial		
Cañado et al. 2022	x							
Mroczkowska et al. 2021		x						x
Eich et al. 2021		x					x	
Rheinberger et al. 2021	x		with enzymes (enzymatic degradation)			artificial		
Niu et al 2021	x							
Catarci Carteny & Blust 2021	x				180 days			
Jacquin et al. 2021	x				134 days			
Delacuvellerie et al. 2021	x				82 days	real	x	
Beltrán-Sanahuja et al. 2020	x						x	
Al-Salem 2020	x		with UV (photo-degradation)				x	
Janik et al. 2018	x	x				real		
Pauli et al. 2017		x				real		
Pelegriini et al. 2016	x				600 days	artificial		
Guzman-Sielicka et al. 2013	x	x						
Accinelli et al. 2012		x				real	x	
Total	16	8		0			6	2

No articles had investigated the formation of micro-/nano-plastics and only two (Mroczkowska et al., 2021; Pinto et al., 2022) investigated the elements uptake and thus the possibility of these plastics to become contaminants carriers. In this context, the use of real seawater and real sand is important because they contain pollutants and toxic elements.

Thus, up to date, this work is the only one giving a 360° vision on the degradation of PLA and TPS in the marine environment with several different techniques. It is the first one simulating both pelagic (with real seawater) and coastal (with real sand) zones, in natural and accelerated weathering, being able to evaluate the effect of photo-degradation and hydrolysis. It is also the first one analyzing the secondary MPs generated from the exposure to the different environments.

3. Materials & methods

In the following paragraphs the experimental setup (schematized in Figure 3.1) will be clarified, along with all the materials and instruments used.

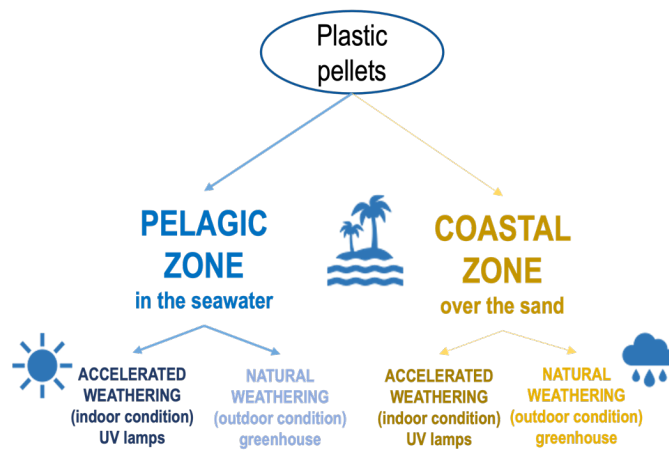


Figure 3.1. Experimental setup scheme.

In Sections 3.1 and 3.2 the setups of the two different environments will be described, followed by the description of the materials and instruments used (Section 3.3). Also, a detailed description of the methods used at every sampling day and along all the experimental period is reported (Sections 3.4 and 3.5).

3.1. Coastal zone set up

To simulate the coastal zone metallic cups were filled with 10g of Cretan beach sand, sieved with 1mm-pores sieve and dried in the oven for 1 day to remove humidity. Each cup contained 20 pellets of one plastic type. Half of the cups were placed in the greenhouse, and the other half cups were placed in closed chambers and irradiated with UV lamps (Figure 3.1). One cup per plastic type and per environment (4 cups in total per sampling day) was removed for further analysis every two weeks.



Figure 3.2. Coastal setup: metallic cups filled with sand and plastic pellets.

All the 20 pellets were weighted prior to their addition on the surface of the sand in each cup. The cup number and the initial weight were reported in an Excel file. Every two weeks one cup per plastic type and environment was removed from the exposition environment and the contained sand and pellets were analyzed. Pellets diameter and

weight were monitored. Fourier transform infrared (FTIR), X-ray fluorescence (XRF) and scanning electron microscope (SEM) were used to analyze the pellets surface composition and changes. Microplastics (MPs) presence and concentration within the sand were assessed through Fluorescence microscope and Dynamic Light Scattering (DLS), after density separation. The day 0 of the experiments was 25th February 2022.

3.1.1. Outdoor conditions

Cups were positioned in a greenhouse, located in the Technical University of Crete campus. A data logger (HOBO) was placed near the samples to monitor temperature and radiation with an hourly time interval.

3.1.2. Indoor conditions: accelerated weathering

UV lamps were used for accelerated weathering in boxes insulated with aluminum foil (Figure 3 3). For the first two months of the experiments, UVB lamps were used, before their substitution with more powerful UVC lamps (after around 70 days from the beginning of the experiments).



Figure 3 3. Indoor experimental setup.

3.2. Pelagic zone set up

The pelagic zone was simulated using 4 aquariums, one per plastic type and environment. Pellets were weighted one by one to obtain weight averages and around 250 pellets were placed in each aquarium. Approximately 10.25 g of PLA and 7 g of TPS per aquarium were used. Twenty liters of natural seawater for each aquarium was collected from Agios Onoufrios bay and was further filtered and sterilized. The sterilization process was performed with an autoclave at 121°C and 100bar. Oxygen in the aquariums was provided through an air-pump, to maintain real seawater oxygen concentration, and to provide movement in the aquariums. Every few days the water level was checked, and deionized water was added if needed to keep a stable total volume. Every two weeks, 20 pellets per environment were removed and were analyzed: pellets diameter and weight were

assessed, biofilm quantification, X-ray fluorescence analysis (XRF), Fourier transform infrared (FTIR) and scanning electron microscope (SEM) were performed.

Temperature and radiation were continuously monitored with data loggers. Every two weeks water pH, salinity, conductivity, Dissolved Oxygen, Redox Potential (ORP), Nitrogen, Nitrate, Ammonia, Phosphorous contents were measured. Secondary MPs were detected using Fluorescence microscope, Dynamic Light Scattering (DLS), and Nanoparticle Tracking Analysis (NTA), and cells were quantified with flow cytometry. The day 0 of the experiments is Wednesday 9th March 2022. As for the coastal zone, an aquarium per plastic type was placed under UV lamps and in the greenhouse (Figure 3.4).



Figure 3.4. Pelagic zone setup (outdoor and indoor conditions).

3.3. Instruments and materials

In Table 3.1 and Table 3.2, the instruments and materials used for the experiments are summarized. A large amount of Falcon tubes, Eppendorf tubes, slimed pipets, glass bottles, aluminum foil were used but was not reported.

Table 3.1. Coastal zone instruments and materials.

COASTAL ZONE			
Objective	Technique	Model	Additional materials
Experimental setup			Metallic cups Sand Plastic pellets (PLA by Plastika Kritis and TPS by BIOTEC)
UV weathering	Exposure to UV lamps	Sylvania F36 T8 BLB lamps Geyer HT8UVC36 254 nm	Boxes covered in aluminum foil
Temperature and radiation monitoring	Recording with data logger	HOBO data logger	
Pellets' weight	Precision weighting balance	Kern PNJ precision balance	
Pellets' cleaning	Immersion in ethanol	Honeywell Ethanol denaturated with MEK, IPA and Bitrex, absolute, >98% (GC grade)	
Pellets' drying	Drying in incubator		
Pellets' size	Graphic image analysis	ImageJ	Ruler
Pellets' elemental composition	Fluorescence spectroscopy (XRF)	Rigaku NEX DE	
	Infrared spectroscopy (FTIR)	Thermo Scientific's iS50	
	Scanning electron microscopy (SEM)	FEI Inspect S50 SEM	
MPs/NPs separation from sand	Density separation with CaCl ₂	Honeywell Fluka Calcium Chloride Desiccant, ACS Reagent, 96.0%	dH ₂ O
MPs/NPs concentration	Fluorescence microscopy	Leica DMLB + ebq 1000 isolated	Nile Red, Invitrogen, Thermo Fisher diluted in Acetone
MPs/NPs size distribution	Spectroscopy: Dynamic light scattering (DLS)	Sald-7500nano Shimadzu	

Table 3.2. Pelagic zone instruments and materials.

PELAGIC ZONE			
Objective	Technique	Model	Additional materials
Experimental setup			Glass aquariums Seawater Plastic pellets (PLA by Plastika Kritis and TPS by BIOTEC) Air pumps (Seta air 275R plus)
UV weathering	Exposure to UV lamps	Sylvania F36 T8 BLB lamps Geyer HT8UVC36 254 nm	Boxes covered in aluminum foil
Temperature and radiation monitoring	Recording with data logger	HOBO data logger	
Pellets' weight	Precision weighting balance	Kern PNJ precision balance	
Pellets' drying	Drying in incubator		
Pellets' size	Graphic image analysis	ImageJ	Ruler
Biofilm quantification	Spectrophotometry	UVmini-1240 Shimadzu	Sigma, Crystal Violet Solution, 1% aqueous solution
Water analysis	Probe measurements for Conductivity, Dissolved Oxygen, pH, redox potential	Hach DR2800 portable spectrophotometer	
	Spectrophotometry for Nitrogen, Phosphate, Ammonia, Nitrates	Hach cuvette tests (LCK138, LCK349, LCK304, LCK339)	
Cells quantification	Flow cytometry	Beckman Coulter CytoFLEX	Thiazole Green: by Biotium, Thiazole Green (SYBR® Green I), 10,000X in DMSO
Pellets' elemental composition	Fluorescence spectroscopy (XRF)	Rigaku NEX DE	
	infrared spectroscopy (FTIR)	Rigaku NEX DE	
	Scanning electron microscopy (SEM)	Thermo Scientific's iS50	
MPs/NPs concentration	Fluorescence microscopy	Leica DMLB + ebq 1000 isolated	
	Nanoparticle tracking analysis (NTA)	NanoSight NS300	Whatman, Glass Microfiber Filters GF/A, diameter 47 mm, pore size 1.6 µm
MPs/NPs size distribution	Spectroscopy: Dynamic light scattering (DLS)	Sald-7500nano Shimadzu	

3.3.1. Plastic pellets

The fate of plastic pellets in the different environments and conditions was studied using virgin plastic pellets (Figure 3.5). Polylactic acid (PLA) and thermoplastic starch (TPS) were used, being nowadays polymers of great interest that have entered the bioplastics market as good alternatives to replace fossil-based polymers and with a production that has increased and is projected to increase even more over the years (Zaaba & Ismail, 2019).



Figure 3.5. PLA and TPS virgin pellets.

Polylactic acid (PLA)

The PLA pellets used in the experiments were purchased from Plastika Kritis. They have a density of about 1.25 kg/m^3 and an average diameter of 3 mm.

Thermoplastic starch (TPS)

The TPS pellets used (BIOPLAST GF 106/02) in the experiments are produced by BIOTEC. They are plasticizer-free and GMO-free thermoplastic containing natural potato starch. Their density is 1.25 kg/m^3 , they have a cylindrical shape with a height of about 3 mm.

3.3.2. Calcium Chloride solution for density separation

The separation of micro-/nanoplastics from the sand was performed with a density separation method using Calcium chloride. Calcium chloride is a salt with chemical formula CaCl_2 , that appears as a white crystalline solid at room temperature. It is highly soluble in water and when it is dissolved in water the temperature of the solution rises, because of its very high enthalpy change.

3.3.3. Fluorescence microscopy for MPs/NPs detection and quantification

A fluorescence microscope is an optical microscope equipped with ultraviolet light. It eases the procedure of distinguishing the nature of what is being observed using the fluorescent response of materials.



Figure 3.6. Fluorescence microscope.

For this experiment the seawater (from the pelagic experiment) and the calcium chloride solution after density separation (for the coastal experiment) were dyed with Nile Red. Nile Red is a dye that has been seen to selectively bond to plastics, helping in their identification and quantification (Sancataldo, 2020). Plastic surfaces can adsorb the dye making the fragments fluorescent when irradiated with blue light (Maes et al., 2017). The fluorescence microscope DMLB by Leica and the power supply ebq 1000 have been used (Figure 3.6).

3.3.4. Dynamic light scattering (DLS) to measure MPs/NPs size distribution

Dynamic light scattering (DLS) is a technique that can be used to determine the particle size distribution of particles or polymers in a liquid. SALD-7500nano by Shimadzu was used for this purpose (Figure 3.7). This instrument can detect changes in particle size and particle size distribution at one-second intervals of particles in a range from 7 nm to 800 μm (Shimadzu, n.d.).



Figure 3.7. SALD-7500nano by Shimadzu for Dynamic Light Scattering.

3.3.5. Nanoparticle Tracking Analysis (NTA) for MPs/NPs concentration and size distribution

Nanoparticle tracking analysis (NTA) is a technology for the analysis of particles in liquids to retrieve particle size distribution and concentration for particles with size up to 2000 nanometers. It uses the particles properties of light scattering and Brownian motion (Malvern Panalytical, n.d.). In this experiment the instrument Malvern Panalytical NanoSight NS300 was used (Figure 3.8). The seawater samples were filtered with filters with a pore size of 1.6 μm before being used for NTA analysis to avoid clogging the thin tubes of the instrument. This is the reason why the high density CaCl_2 solution was not used for NTA.

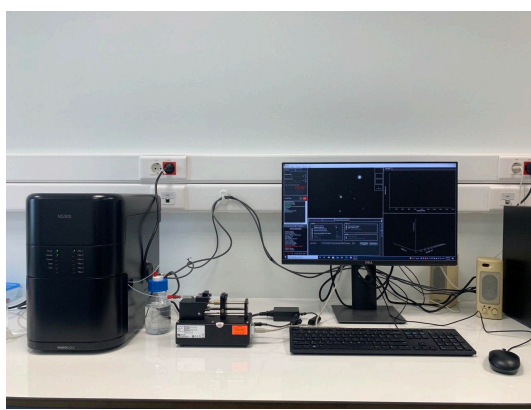


Figure 3.8. Malvern Panalytical NanoSight NS300 for Nanoparticle Tracking Analysis.

3.3.6. Energy Dispersive X-ray Fluorescence (EDXRF) spectroscopy for pellets elemental composition

The analysis with Energy Dispersive X-ray Fluorescence (EDXRF) spectroscopy provides a non-destructive method to determine the elemental composition of a material in solid, liquid or powder. It can measure a wide range of atomic elements, starting from Sodium to Uranium. Smaller atoms, having too little energy, cannot be detected directly with this technique. Using this method, it is possible to detect what kind of elements, such as heavy metals, have been adsorbed by the plastic pellets during their degradation (Applied Rigaku technologies, n.d.). For this experiment the instrument NEX DE by Rigaku was used (Figure 3.9).



Figure 3.9. Rigaku NEX DE (picture by Applied Rigaku technologies, n.d.).

3.3.7. Attenuated Total Reflectance – Fourier Transform Infrared Spectroscopy (ATR-FTIR) for Carbonyl Index evaluation

Changes in the chemical structure of the surface of the polymers can be examined using Attenuated Total Reflectance - Fourier-Transform Infrared Spectroscopy (ATR-FTIR). The instrument used in our case is Thermo Scientific's Nicolet iS50 (Figure 3.10), equipped with the diamond crystal ATR module. Spectrum acquisition is done with the OMNIC software, provided from Thermo Scientific.



Figure 3.10. Thermo Scientific's Nicolet iS50 (picture from Thermo Scientific, n.d.).

3.3.8. Scanning electron microscope (SEM): morphological and elemental characterization

Scanning electron microscopy is a very powerful tool to produces images of the surface of a sample, using a concentrated electrons beam. Information about the

surface topography and elemental composition can be retrieved. The instrument Inspect S50 by FEI was used (Figure 3.11).



Figure 3.11. Scanning electron microscope (FEI Inspect S50).

3.3.9. Flow Cytometry (FCM) for cells quantification

Flow cytometry (FCM) is a technique used for the qualitative and quantitative measurement of biological and physical properties of cells and other particles in liquid solutions, with rapid analysis based on scattering of light and emission of fluorescence occurring when a laser beam hits the cells moving in the pipes of the instrument (Manohar et al., 2021). The instrument used was CytoFLEX by Beckman Coulter (Figure 3.12).



Figure 3.12. Flow cytometer CytoFLEX by Beckman Coulter.

Sheath, a high-density liquid, was used to separate the cells so that they go through the system one by one. Sybr Green dye was used to ease the procedure of cells recognition. The 488nm blue laser was used, and the forward scattering (FSC, related to the size of the particle) and the side scattering (SSC, related to the complexity of the cell) were considered. The seawater samples were filtered with filters with a pore size of 20 μm to avoid tubes blockages.

3.3.10. Spectrophotometry and Crystal violet for biofilm quantification

The crystal violet test was performed to determine the extent of biofilm on the plastic pellets. The pellets were dyed with crystal violet dye and the optical density (OD) of the cleaning solution was measured using a spectrophotometer (Ebert et al., 2021). This is an instrument that can measure the intensity of light absorbed by the analyzed solution. The spectrophotometer UVmini-1240 by Shimadzu was used in this experiment (Figure 3.13).



Figure 3.13. Spectrophotometer UVmini-1240 by Shimadzu.

3.4. Coastal zone analysis methods

Every two weeks one cup (containing the sand and the pellets) per environment and per plastic type (4 in total) was removed. The analysis of the sand and the pellets was performed separately and in parallel. In the following a description of the methodology (schematized in Figure 3.14) is provided.

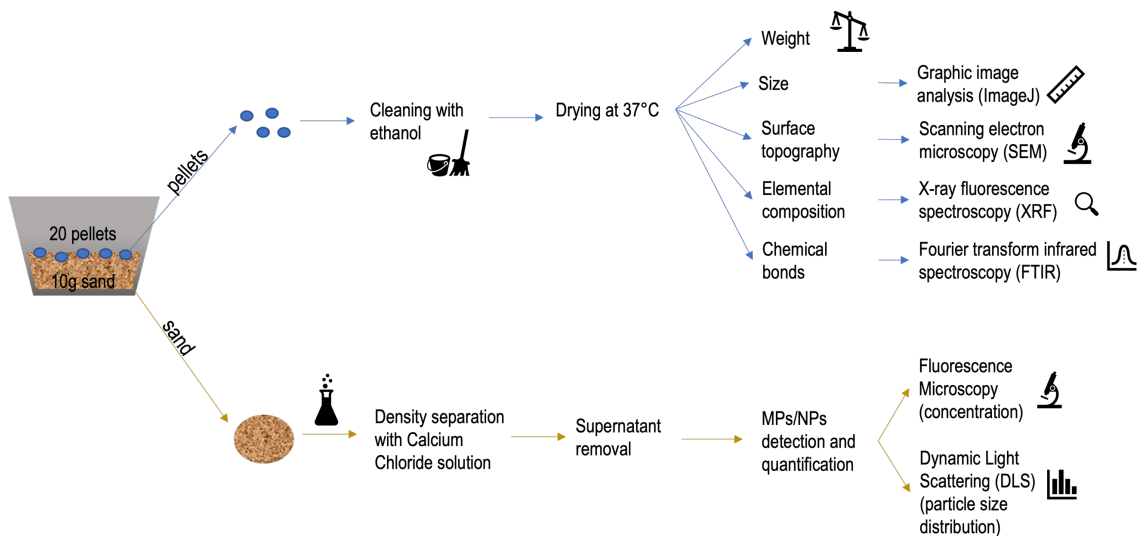


Figure 3.14. Coastal zone experiment methods.

3.4.1. Pellets

The pellets were immersed in ethanol and then let dry before the weighting process in order to remove the sand particles that remain attached to the surface. A small part of sand is thus lost during this process. However, the pellets and the sand were mixed to spread the possible secondary MPs within the sand to reduce the losses at a minimum level. The losses were more abundant for the PLA that exhibits an attractive effect towards sand.

The pellets were placed in an incubator at 37°C overnight. When they were dry, their weight can be assessed, and pictures were taken to monitor dimension changes. In every picture a ruler was placed next to the pellets to set the scale in ImageJ. With ImageJ mean, min, max and standard deviation of the pellets area and Feret diameter were calculated, and these data was used to highlight possible size changes over the months. Since the procedure highly depends on the precision of the user, light condition and pellet color, only macroscopic changes can be monitored.

Moreover, some pellets undergo X-ray fluorescence (XRF) analysis to assess the elemental composition of their surface (with particular focus on Chlorine, Sulfur, Silicon, Iron, Nickel and Phosphorous). This allows monitoring of possible element adsorption, leaching or changing on the pellet surface. For every sample the analysis was repeated three times. Fourier Transform Infrared spectroscopy was used to highlight plastic blends and the effect of the degradation process. Virgin pellets and the pellets of the last sampling day were also analyzed with Scanning Electron Microscopy (SEM) to obtain images of the degradation effects and the elemental composition of their surface.

3.4.2. Sand

Once the pellets were removed from the cup, a density separation process was performed to separate the MPs/NPs on the liquid surface and ease the process of analysis. Thus, in the first phases of the experiment several solutions were tested in order to find the appropriate one. The solution must allow the plastic to float on the liquid phase and to create a clear separation with the sand, in order to obtain trustable results regarding the concentration of the particles.

Selection of the proper solution for the density separation

Since some PLA pellets were sometimes observed to flow on the seawater surface, the 1st trial concerned an oversaturated solution of NaCl (concentration). 30ml of solution with 30g of sand were added in glass bottles and mixed, before letting them settle down. However, secondary PLA particles did not float on the solution but remained over the sand.

The second trial was performed with a solution of ZnCl_2 (~1.5 g/mL), according to literature results (Rodrigues et al., 2020). 15 mL of ZnCl_2 solution were mixed with 10 g of sand for one hour and then left to settle overnight. The density separation was clear, and the plastic particles floated on the surface. Also, MPs were well detectable using Fluorescence microscope with supernatant droplets.

However, with a zinc chloride solution many problems arise:

- Zinc is a heavy metal and thus must be carefully handled, also for its disposal.
- Chemical reactions occur inside the sand and lead to the formation of bubbles that were trapped into the sand layer, lowering the level of supernatant.
- ZnCl_2 is more expensive than other compounds
- Since zinc is corrosive, it was dangerous to use this solution with some of the instrumentations before further (time consuming) filtration steps.

The 3rd, and last, trial was performed according to Duong et al., 2022 with an oversaturated solution of CaCl_2 (~1.44 g/mL). The bottles with the solution were mixed on the shaker and then let settled. The formation of separated layers was achieved. The procedure for density separation and supernatant collection for microscope analysis was preliminary performed with control bottles containing known concentrations of polystyrene (PS) beads of known size (500 and 200nm with 10^8 and 10^4 concentration). After the shaking and the settling of the sand, the supernatant (where MPs are expected to accumulate) of each bottle was taken. A part of the sample was dyed with Nile Red to highlight the presence of MPs under the fluorescence microscope. The samples were left in the dark with the dye for at least three hours. Longer time of incubation (compared to literature values of 20 minutes) leads to better results. Droplets of 1 μL were analyzed under the microscope. PS beads under the microscope appeared magenta and were recognizable thanks to their round shape.

The use of Fluorescence microscope for MPs detection was repeated at every sampling day for every sample (3 droplets of 1 μL) to assess and monitor over the time the concentration of secondary MPs. Also, during the microscope analysis pictures of the MPs were taken to estimate a preliminary particle size distribution with ImageJ.

The supernatant was then used for Dynamic Light Scattering (DLS) to estimate the particle size distribution and monitor it over the weeks. For both plastic types, the refractive index was set to 1.45 and only results with a correlation higher of 0.900 were considered. Calcium Chloride solution was used as blank. All the data was collected and elaborated in Excel files to ease the procedure of comparing and analyzing the data.

3.5. Pelagic zone analysis methods

Starting from the 21st March 2022, every two weeks seawater samples and 20 pellets from each aquarium were taken for analysis. The scheme of the methods used is reported in Figure 3.15.

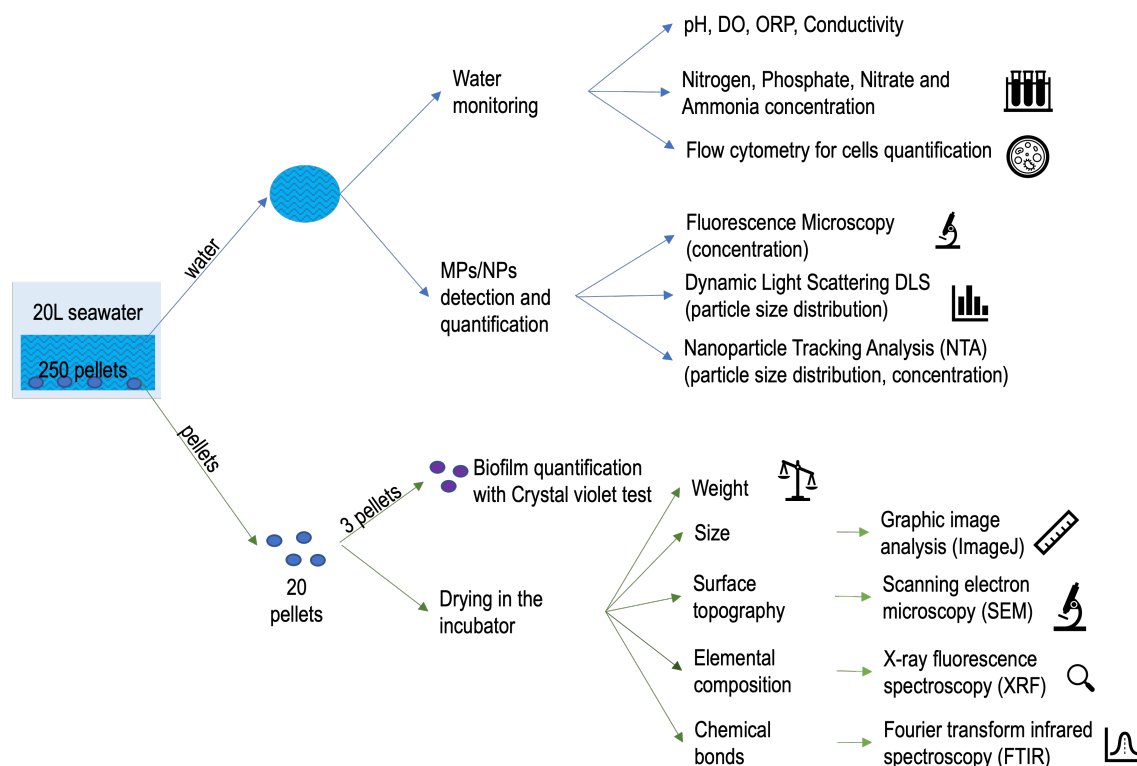


Figure 3.15. Pelagic zone experiment methods.

3.5.1. Pellets

Once removed from the aquarium three of the twenty pellets were collected for biofilm quantification procedure. The followed protocol, from Lobelle & Cunliffe, 2011, was followed:

- drying of pellets under the laminar flow hood
- dyeing with a drop of Crystal Violet
- 45 minutes drying
- pellets washing (three times with DI H₂O)
- 45 minutes drying
- placing the three pellets into a 2 mL Eppendorf tube with 1 mL ethanol (95% v/v) and on the shaker for 10 minutes
- transferring the solution to a cuvette and to the spectrophotometer
- measuring optical density (OD) at 595 nm.

The remaining pellets should be cleaned from possible biofilm presence. Pellets were added in Eppendorf Tubes with pure ethanol. The solution with the pellets was put on a shaker overnight before. Next, the pellets were removed and dry in the incubator (37°C) for one week. Indeed, pellets (especially TPS) tend to absorb water inside their structure and weighting them one week after the sampling day leads to a weight reduction of 3% for TPS (Figure 3.16).

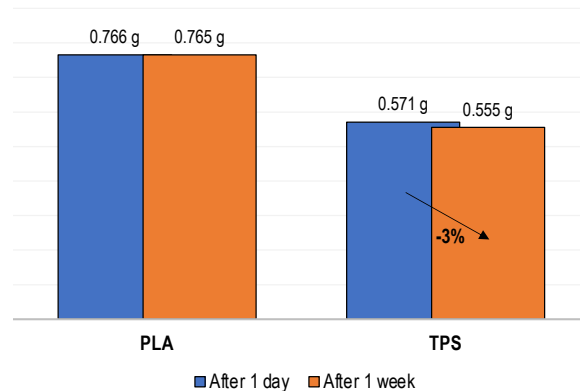


Figure 3.16. Weight difference: comparison between 1 day and 1 week after the sampling day.

At this point, all the pellets (including those treated with Crystal violet) were weighted and pictures were taken to monitor dimension changes (using ImageJ) following the same procedure as coastal zone. As for coastal zone, some of the pellets undergo XRF analysis, FTIR, and SEM to assess the elemental composition of their surface, plastic bonds and surface changes respectively.

3.5.2. Water

During the sampling day in each aquarium the following water properties were monitored with the use of a multimeter and specific probes:

- Temperature
- Conductivity
- Redox potential (ORP)
- Dissolved Oxygen (DO)
- pH

These properties were expected to be as close as possible to the seawater properties (except for temperature) and their monitoring was important to check if some phenomena in the water are occurring. Nitrogen, Phosphate, Ammonia and Nitrates concentrations were also monitored over the weeks, using standard protocols for cuvette tests (LCK 138, LCK 349, LCK 304, LCK 339).

If during the sampling days differences in concentrations were visible, proper solutions can be prepared to restore the initial concentrations. This was the case of Nitrogen that a decrease was noticed during the months and a solution of potassium nitrate (KNO_3 , 43g/L) was added accordingly.

A part of the collected seawater was dyed with Nile Red and left 3 hours before the analysis with the Fluorescence microscope to detect microplastics. For each aquarium 3 drops of $1\mu\text{l}$ were analyzed. Each sample was also analyzed with DLS to determine the particle size distribution, as for coastal zone. In this case, seawater was used as blank. Few milliliters of seawater are filtered with $1.6\mu\text{m}$ filters and NTA was performed to determine the particle size distribution and concentration of NPs. Another part of the Sample was filtered with a 20micrometers Nylon net and was dye with Sybr Green (2ml of samples with $10\mu\text{l}$ of dye for 20 minutes) and the flow cytometer was used for qualitative and quantitative cells determination, using the 488nm blue laser.

3.6. Sensitivity analysis

3.6.1. Pellets weight standard deviation and scale error.

Since for the pelagic zone all the pellets where immersed in the same aquariums and the variability in pellets weight was quite high, problems arise during the weight variation assessment. That's why the standard deviation in the weight of 20 pellets was assessed for 35 samples for each plastic ($0.800 \pm 0.02\text{ g}$ for PLA and $0.566 \pm 0.02\text{ g}$ for TPS). Based on this, a percentage threshold below which the variation could be considered meaningful was set. The threshold was 5.3% for PLA and 6.9% for TPS.

For the coastal zone, the variability of pellets weight was overcome thanks to the weight assessment of the pellets in each cup before the beginning of the experiment. Thus, coastal pellets weight assessment was mainly affected by the accuracy of the scale (0.01g), thus weight losses smaller than 1.2% for PLA and 1.8% for TPS have been considered as no meaningful changes occurred.

3.6.2. Regression analysis and R^2 for Schwarzcild's law

To see if data obeyed to the Schwarzcild's law (linear dose-response fit), regression analysis was used. Regression analysis is a statistical tool for estimating the relationships between a dependent variable (response) and an independent variables (dose) (Gallo, 2015). The goodness of fit to the law was evaluated with the coefficient of determination R^2 , that determines the proportion of the variance in the response that can be explained by the dose (CFI Team, 2022). R^2 can be calculated as (Eq 3.1):

$$R^2 = \frac{SS_{regression}}{SS_{total}}, \tag{3.1}$$

Where $SS_{\text{regression}}$ is the sum of squares due to regression that measures how well the model represents the data analyzed, and SS_{total} is total sum of squares measures that measures the variation in the data (CFI Team, 2022).

3.6.3. Pearson coefficient correlation

Correlation is a statistical method for measuring the strength of the linear relationship between two variables through the correlation coefficient that can vary between 1 and -1 (QuestionPro, 2022).

Correlation between two variables can be a positive correlation (if one variable increases, also the other variable increases), a negative correlation (if one variable decreases, also the other variable decreases), or no correlation (QuestionPro, 2022).

To analyze the results, the Pearson correlation coefficient (r) was used (Eq. 3.2):

$$r = \frac{N \sum xy - (\sum x)(\sum y)}{\sqrt{[N \sum x^2 - (\sum x)^2][N \sum y^2 - (\sum y)^2]}}$$

(3.2)

Where N is the sample size, and x and y are the sample points (QuestionPro, 2022).

4. Results and discussion

4.1. Degradation of the plastic pellets

4.1.1. Weight, size, and macroscopic changes

During the exposure period, lasted around 5 months (around 140 days), plastic pellets underwent to some macroscopic changes that differed according to the plastic type and the exposure environment and condition.

In Table 4.1 and Table 4.2 the light intensity that the pellets received during the experiments is summarized.

Table 4.1. Light intensity recorded by Hobo data loggers for coastal zone.

COASTAL ZONE			
Sampling #	Days of exposure	Sunlight intensity [KWh/m ²]	UV light intensity [KWh/m ²]
0	0	0.00E+00	0.00E+00
1	19	3.36E+04	3.75E+02
2	31	8.45E+04	5.61E+02
3	45	1.67E+05	7.69E+02
4	59	2.64E+05	9.72E+02
5	73	3.47E+05	2.54E+03
6	87	4.59E+05	3.15E+03
7	101	5.71E+05	3.73E+03
8	115	6.75E+05	4.43E+03
9	129	7.81E+05	5.09E+03
10	143	8.85E+05	5.71E+03

Table 4.2. Light intensity recorded by Hobo data loggers pelagic zone.

PELAGIC ZONE			
Sampling #	Days of exposure	Sunlight intensity [KWh/m ²]	UV light intensity [KWh/m ²]
0	0	0.00E+00	0.00E+00
1	12	1.50E+04	1.41E+02
2	26	4.53E+04	2.86E+02
3	40	8.22E+04	3.27E+02
4	54	1.29E+05	3.82E+02
5	68	1.82E+05	5.75E+02
6	82	2.30E+05	1.29E+03
7	96	2.78E+05	2.00E+03
8	110	3.51E+05	2.68E+03
9	124	4.08E+05	3.27E+03
10	138	4.73E+05	3.87E+03

The cumulative light intensity of indoor conditions is lower than outdoor ones, also if only the 4% of the sunlight (UV fraction) is considered. However, sunlight UV fraction

is mostly UVA, that is less powerful than UVB and UVC. UV light of indoor conditions is constituted by UVB light, for one half of the experiment, and UVC light that is the most detrimental for polymers. Therefore, even with lower cumulative radiation, the degradation effects are higher. Also, light intensity for coastal zone is higher than for pelagic zone due to the water absorbance.

To have a more clear and effective data representation the days of exposure were usually used as x-coordinate instead of light radiation that is different for each zone and condition. In the following, visual differences are highlighted, followed by weight and size changes, the microscopic effect of degradation on the surface, and variations in the surface elemental composition.

Pellets degradation timeline

Looking at Figure 4.1 and Figure 4.2 for PLA OUTDOOR coastal there were no changes visible with bare eyes, the INDOOR pellets started to turn yellow and to glue with the sand, with no possibility of removal during the cleaning procedure (the presence of the sand likely affected the weight measurements).

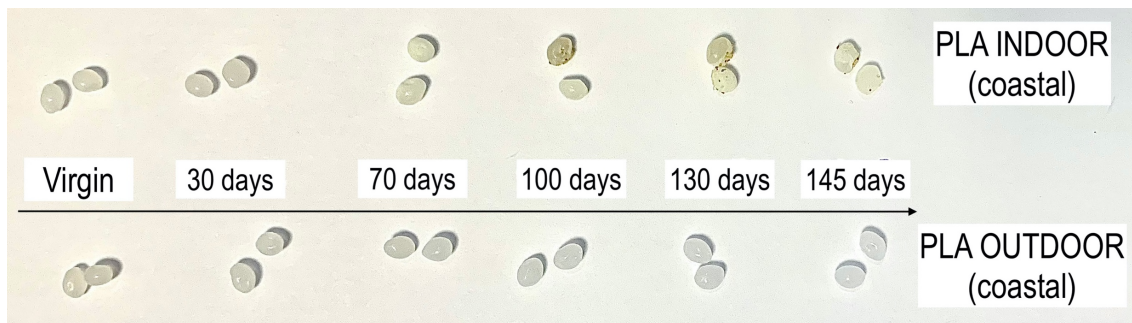


Figure 4.1. Timeline of PLA pellets exposed in the coastal zone.

For the TPS pellets for the coastal experiments, the only macroscopic characteristic that changes during the exposure period was the color (different shadows of yellow, Fig.).

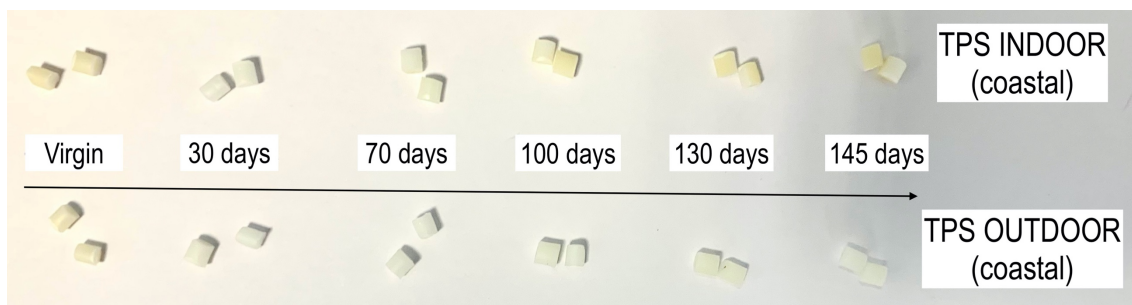


Figure 4.2. Timeline of TPS pellets exposed in the coastal zone.

Concerning the pelagic zone, TPS OUTDOOR pellets were the ones that highlights the most of macroscopic changes (Figure 4.3). Indeed, algal biofilm started to visibly grow on the pellets surface after few weeks from the start of the experiments (Figure 4.4).

No big differences were detectable for TPS INDOOR and PLA OUTDOOR, while for PLA INDOOR a change of the color (from transparent to white, Figure 4.5) and a size reduction were visible.

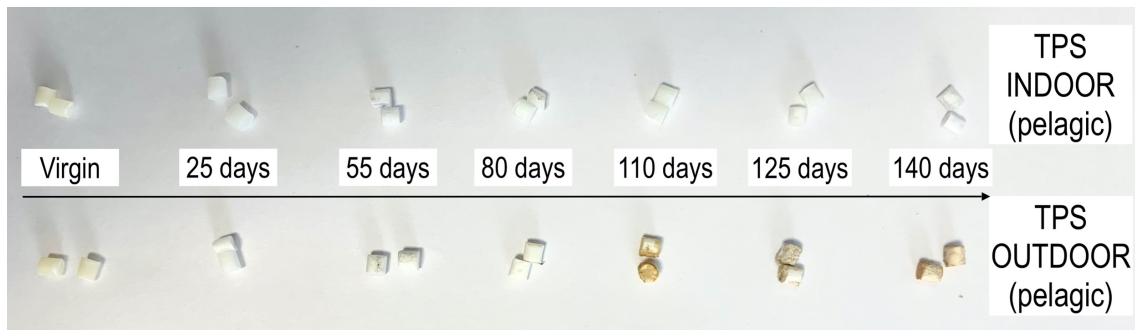


Figure 4.3. Timeline of TPS pellets exposed in the pelagic zone. Pellets were cleaned and dried before pictures.



Figure 4.4. Differences between virgin TPS pellets, exposed and cleaned pellets, and pellets with biofilm after 90 days exposure (outdoor pelagic).

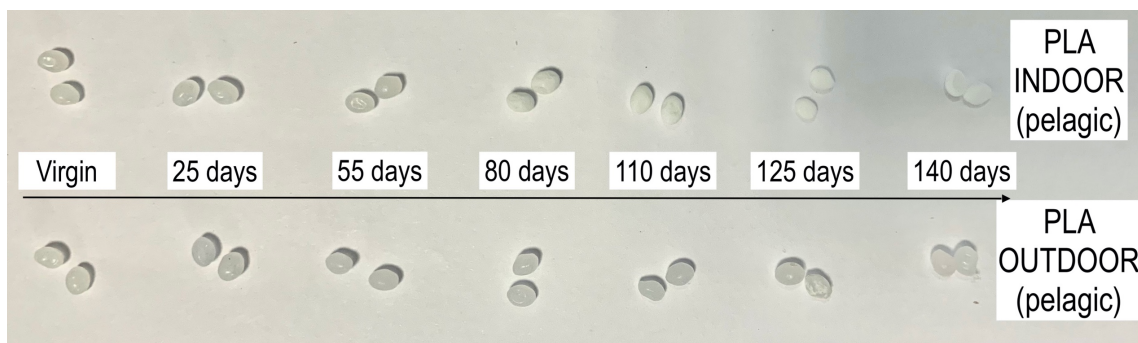


Figure 4.5. Timeline of PLA pellets exposed in the pelagic zone.

Thus, PLA indoor in both exposure conditions had more visible changes (sand adhesion, color change and size reduction). For outdoor conditions changes were almost only detectable for TPS pelagic due to biofilm formation.

Pellets weight variations

The weight differences over the exposure period can highlight signs of degradation. Also, if degradation cannot be justified by weight data alone (Kliem et al., 2020), macroscopic weight decrease is likely linked with pellets weathering. Coastal pellets weight assessment was mainly affected by the accuracy of the scale, thus variations smaller than 1.2% for PLA and 1.8% for TPS cannot be considered as meaningful changes.

Regarding pellets in coastal environment significant weight differences were visible only for PLA INDOOR (Figure 4.6), with a weight reduction up to 7.6% for the last sampling day. However, due to the impossibility to remove some sand particles from the surface, this reduction could be more accentuated. Also, analyzing size differences with ImageJ, no macroscopic changes were highlighted. However, for PLA INDOOR the presence of sand particles could have affected the results.

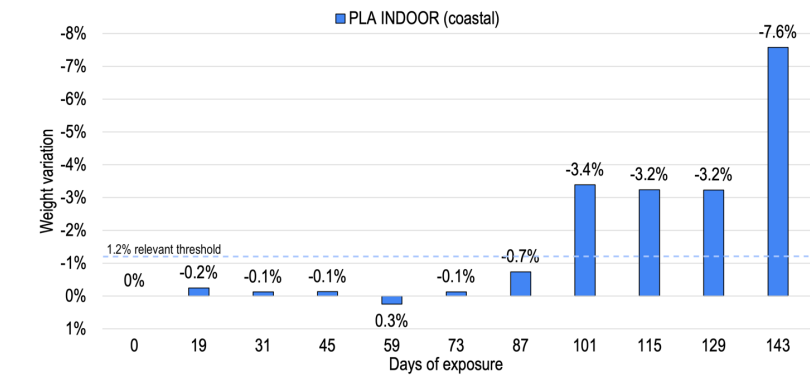


Figure 4.6. PLA INDOOR coastal weight reduction.

Using the weight variations of coastal pellets as photoresponse in the Schwarzschild's law a clear linear dose-response was not visible. However, two different trends were visible for PLA INDOOR corresponding to the two different types of lamps (UVB before and UVC after, Figure 4.7). Weight variations after lamps change had a goodness of fit to the law of $R^2=0.70$.

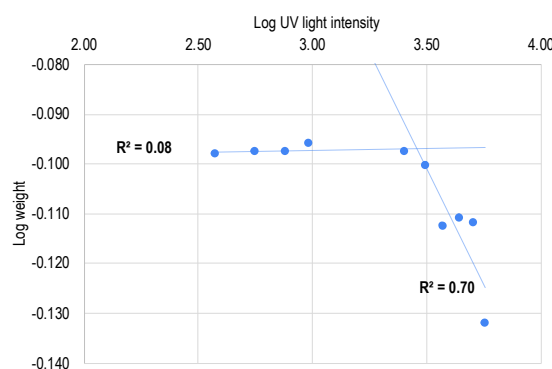


Figure 4.7. Schwarzschild's law for PLA INDOOR coastal.

Regarding pelagic zone, weight losses were detectable for each plastic type with different magnitudes (Figure 4.8). Pellets weight variation for indoor conditions was higher than for outdoor one, with more effect on PLA than TPS. PLA INDOOR manifested a weight reduction up to 33.2% (visible also with bare eye), while TPS INDOOR up to 16.8%.

Due to the errors in weight assessment linked with the variability of the pellets size, the standard deviation obtained from the weighting procedure of the pellets was used and a significant threshold of 5.3% for PLA and 6.9% for TPS was retrieved.

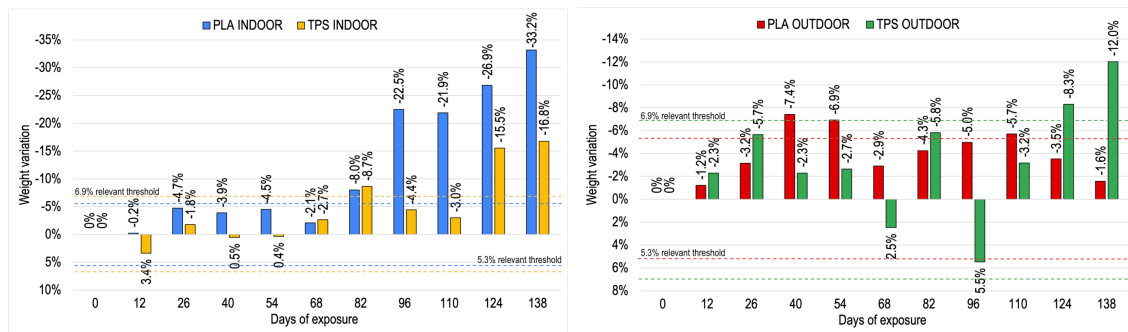


Figure 4.8. Weight variation for pelagic pellets.

Also, the size reduction confirmed the trend (Figure 4.9), that was more appreciable for PLA INDOOR than TPS INDOOR. However, TPS OUTDOOR shows a size increase, that could be due to biofilm accumulation on the surface, water intrusion and change of the structure (the water intrusion occurs also for INDOOR conditions, but the effect of external degradation is higher than the size increase).

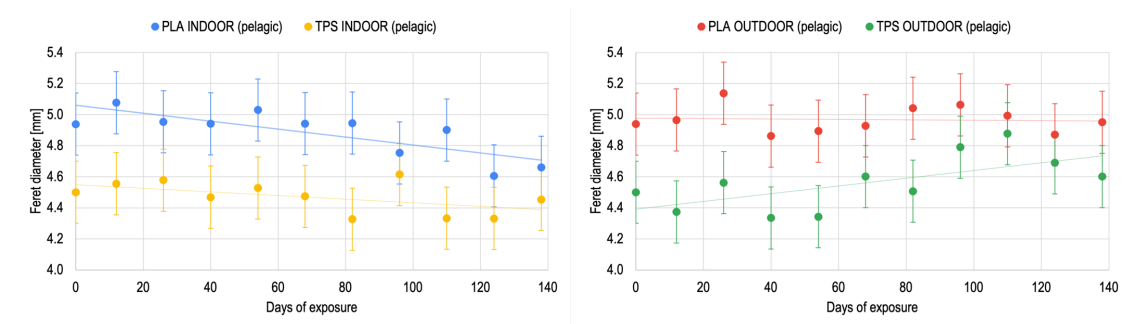


Figure 4.9. Timeline of pellets size variations,

Erosion of plastics in water can follow two different pathways: bulk erosion and surface erosion. Bulk erosion is the predominant degradation mechanism when water diffusion into the polymer structure is faster than its degradation, leading to homogeneous degradation of the sample. When plastic degradation is faster than water diffusion, surface erosion occurs: the polymer is eroded starting from the surface towards the interior (Gorrasi & Pantani, 2018).

Surface erosion could be the main mechanism for PLA due to its less porous structure, and for the indoor condition, due to the aggressiveness of the UV light. On the other hand, bulk erosion could be the main mechanism for TPS in outdoor conditions because it is more porous.

In Table 4.3 and Table 4.4 the main macroscopic variations are summarized.

Table 4.3. Macroscopic variations for PLA pellets.

PLA				
	COASTAL		PELAGIC	
	INDOOR	OUTDOOR	INDOOR	OUTDOOR
Weight loss	X		X	
Size			X (reduction)	
Surface visible changes	X (sand glued)		X (size reduction, color change)	

Table 4.4. Macroscopic variations for TPS pellets.

TPS				
	COASTAL		PELAGIC	
	INDOOR	OUTDOOR	INDOOR	OUTDOOR
Weight loss			X	
Size			X (reduction)	X (increase)
Surface visible changes	X (color change)			X (biofilm formation)

Briefly:

- For outdoor conditions in the coastal zone there were no macroscopic signs of degradation over 5 months of experiments.
- For outdoor conditions in the pelagic zone there were no macroscopic signs of degradation over 5 months of experiments.
- Indoor conditions led to changes for all plastic types and all environments (with less effect on TPS coastal).

4.1.2. Surface topography and elemental composition

Scanning Electron Microscope

Scanning Electron Microscope allowed to look at the microscopic sign of degradation, otherwise not visible with bare eyes. In Figure 4.10 the surface of virgin PLA and TPS pellets were photographed. From the pictures, the different surface morphologies are visible: PLA surface appears smoother and with a higher crystallinity, while TPS appears more porous and fibrous (as visible in the detail of Figure 4.11 with 1600% magnification).

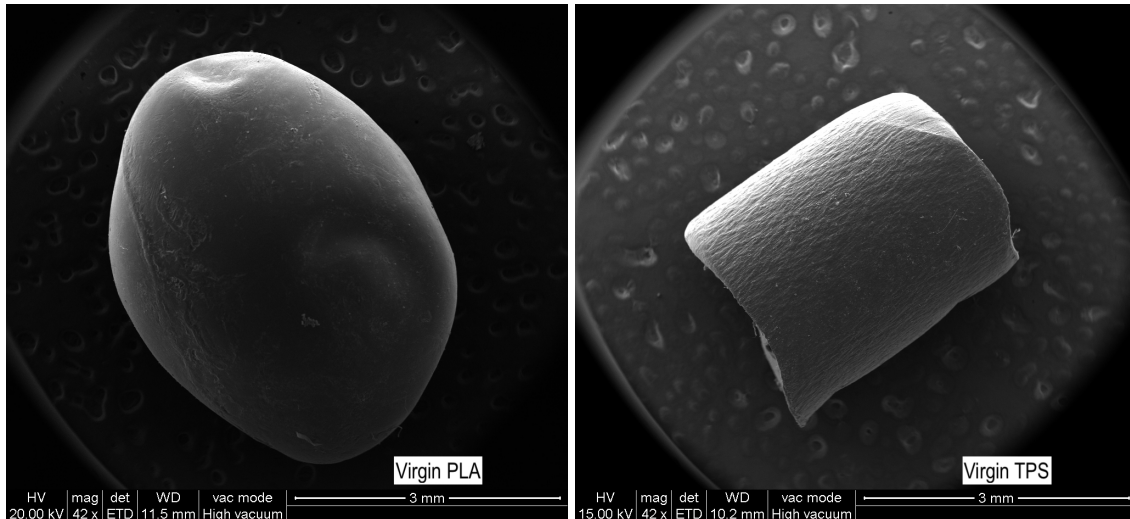


Figure 4.10. Virgin pellets of PLA and TPS.

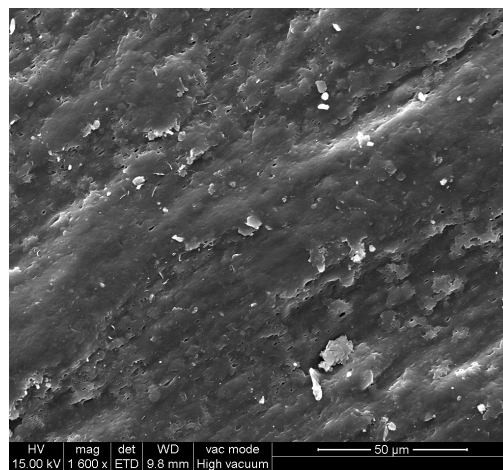


Figure 4.11. Virgin TPS detail.

The spectrum obtained with SEM from the analysis of the virgin pellets surface appears as the one in Figure 4.12, with peaks of C and O that are the main polymeric components, and a peak in correspondence with the gold (Au), used to make pellets conductive. Also, if probably on the pellets surface other elements can be present in small concentrations, the signal of the carbon covers the weak signals of the other compounds.

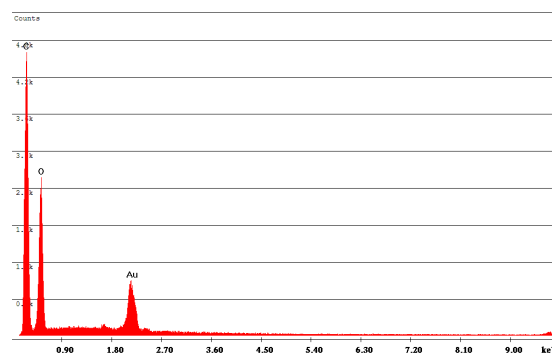


Figure 4.12. Spectrum of a virgin pellet.

From the pictures of the pellets at their last sampling day (Figure 4.13 and Figure 4.14), the signs of degradation of the surface can be analyzed.

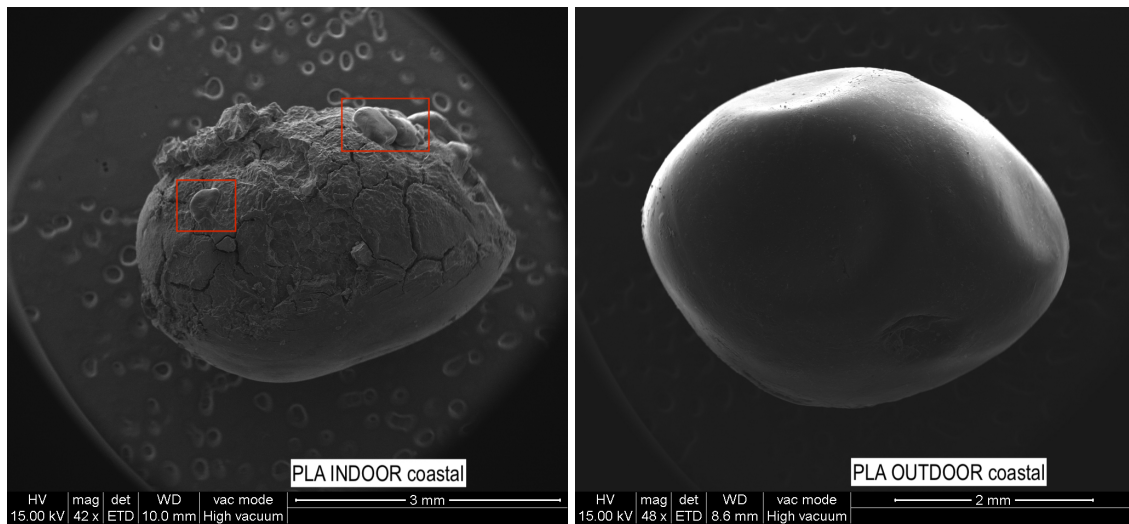


Figure 4.13. SEM pictures for PLA coastal in INDOOR and OUTDOOR conditions.

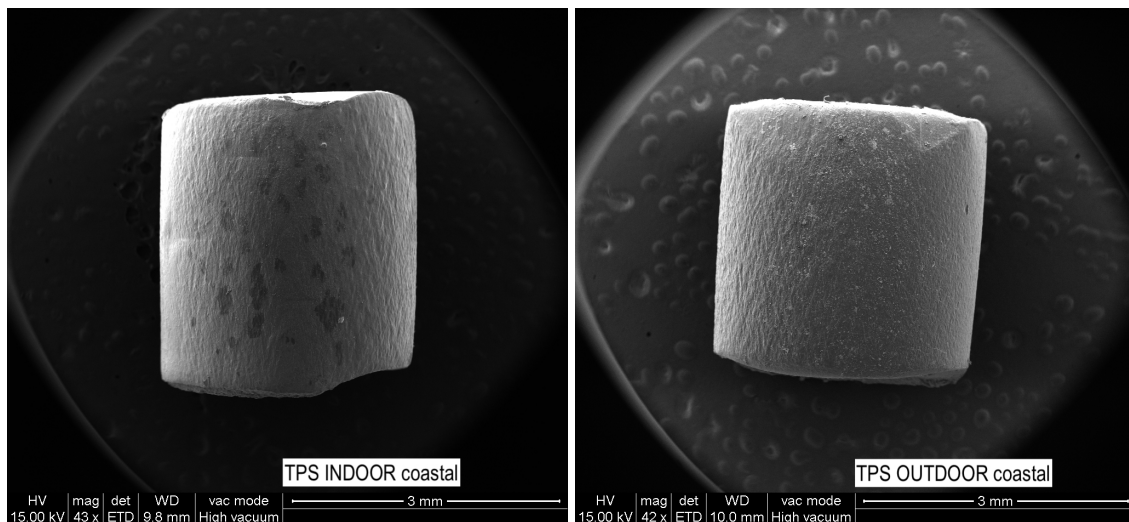


Figure 4.14. SEM pictures for TPS coastal in INDOOR and OUTDOOR conditions.

Strong differences between INDOOR and OUTDOOR conditions were visible, according with the macroscopic changes summarized in Table 4.3 and Table 4.4.

As observed during the pellets cleaning procedure, for PLA INDOOR pellets, sand particles remained stucked to the pellet forming a sort of glue, that is also visible in the detail highlighted in Figure 4.15.

PLA INDOOR presented different degradation effects for the part in contact with sand (upper part in Figure 4.13, more damaged, lot of cracks), compared with the free surface (more homogeneous). A spot analysis (Figure 4.15) on what is supposed to be a sand particle allowed to confirm this hypothesis.

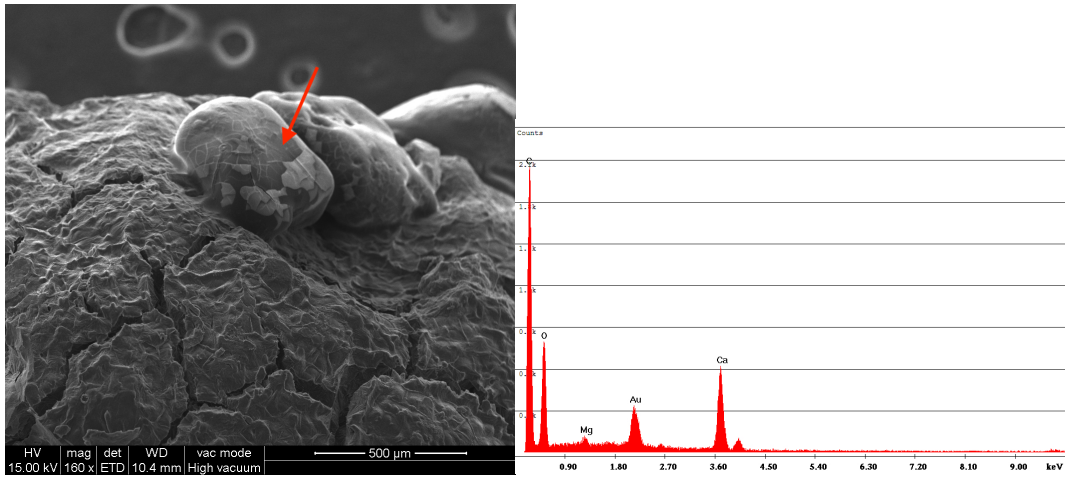


Figure 4.15. Detail of PLA INDOOR coastal pellet surface.

Looking at the pellets surface closer, completely different degradation effects for the different conditions can be observed (Figure 4.16 and Figure 4.17).

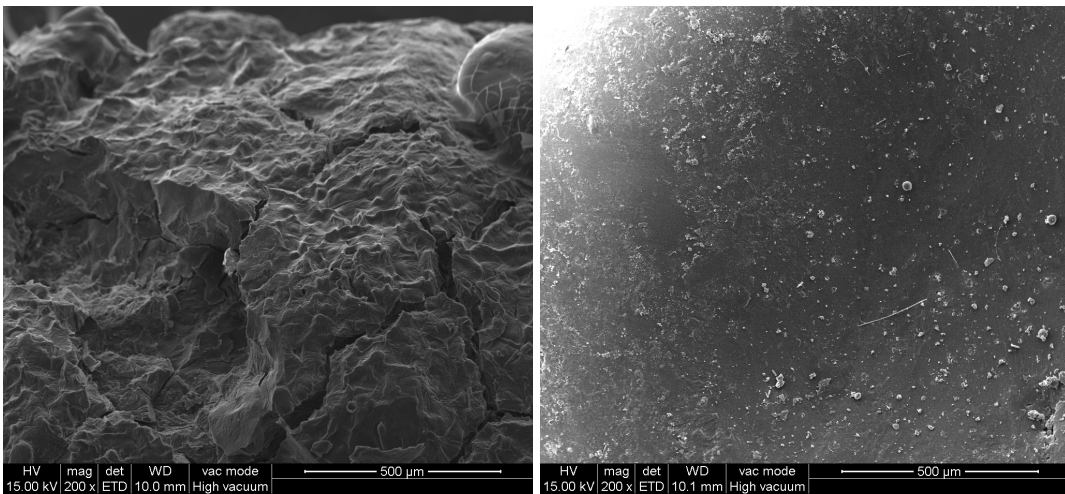


Figure 4.16. PLA INDOOR and OUTDOOR coastal surface.

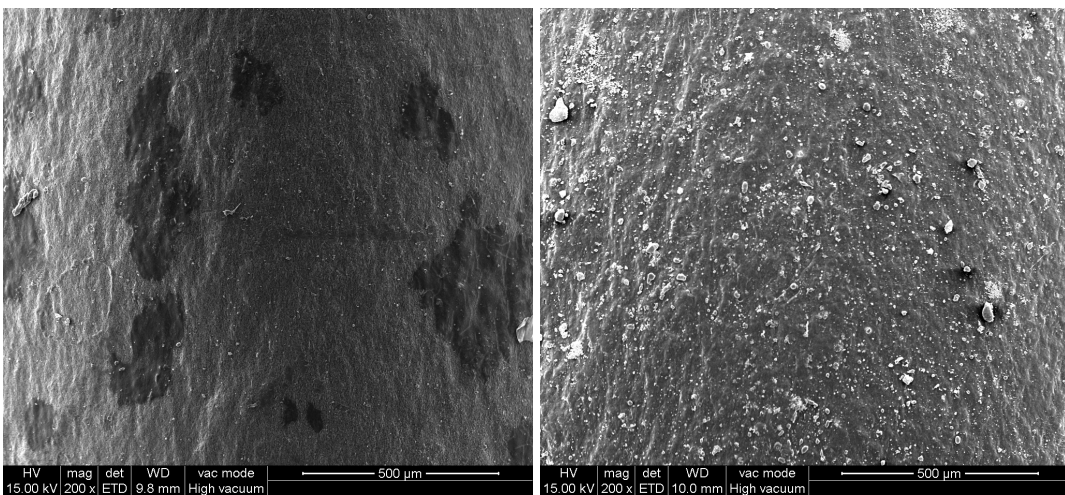


Figure 4.17. TPS INDOOR and OUTDOOR coastal surface.

Despite the cleaning procedure with ethanol, several extraneous bodies were visible on the pellets surface. Using TPS OUTDOOR as reference surface, a spot analysis (EDS) was done in several points to assess the nature of these particles (Figure 4.18).

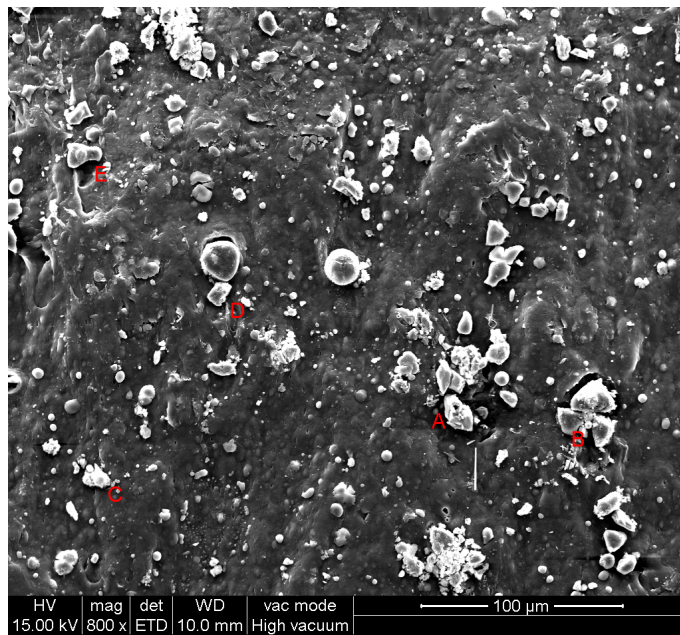


Figure 4.18. TPS coastal outdoor detail at 800x.

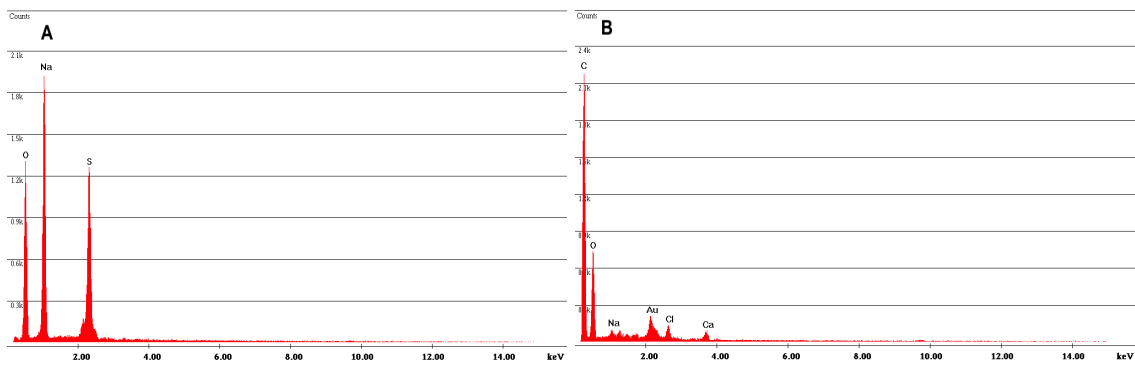


Figure 4.19. Spectra of the particles in A and B.

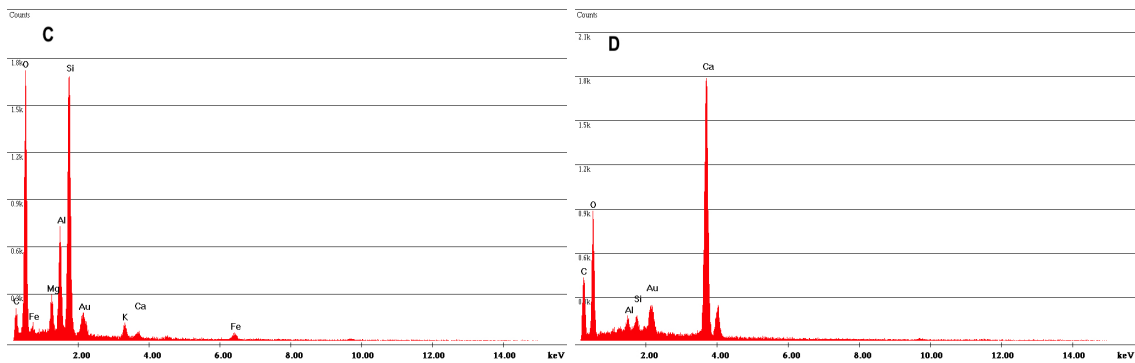


Figure 4.20. Spectra of the particles in C and D.

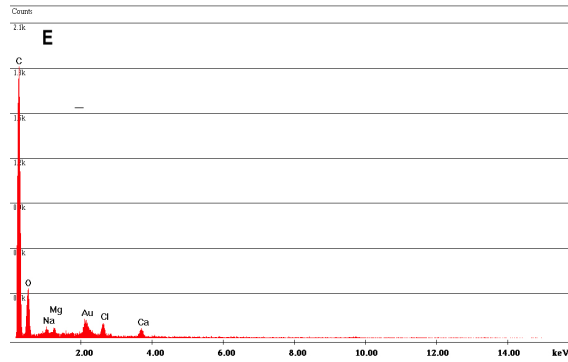


Figure 4.21. Spectrum of the particles in E.

Spectra (Figure 4.19, Figure 4.20, and Figure 4.21) highlighted that these objects were mainly salts and microscopic sand particles. In Table 4.5 the elements present in the various spots are summarized.

Table 4.5. Elemental composition of TPS coastal outdoor (last sampling day).

	A	B	C	D	E
C		X	X	X	X
O	X	X	X	X	X
Na	X	X			X
S	X				
Au		X	X	X	X
Cl		X			X
Ca		X	X	X	X
Fe			X		
Mg			X		X
Al			X	X	
Si			X	X	
K			X		

Also, analyzing the elemental concentration with XRF on the part of the pellets covered by sand (Table 4.6) highlighted the sand composition, that is compliant with SEM EDS results.

Table 4.6. Elemental concentration in mg/kg for PLA indoor coastal pellets covered by sand (with XRF).

Al	Si	S	Cl	Ca	Fe	Ni
2270	64800	194	119	28100	702	53.2

The presence of S, Si, Fe, Cl (also visible with XRF) was assessed. However, Nickel was never detected but the high content of C could have covered the signal.

To better understand the black spots present on TPS INDOOR coastal surface, two magnifications were done (800x and 3000x, Figure 4.22).

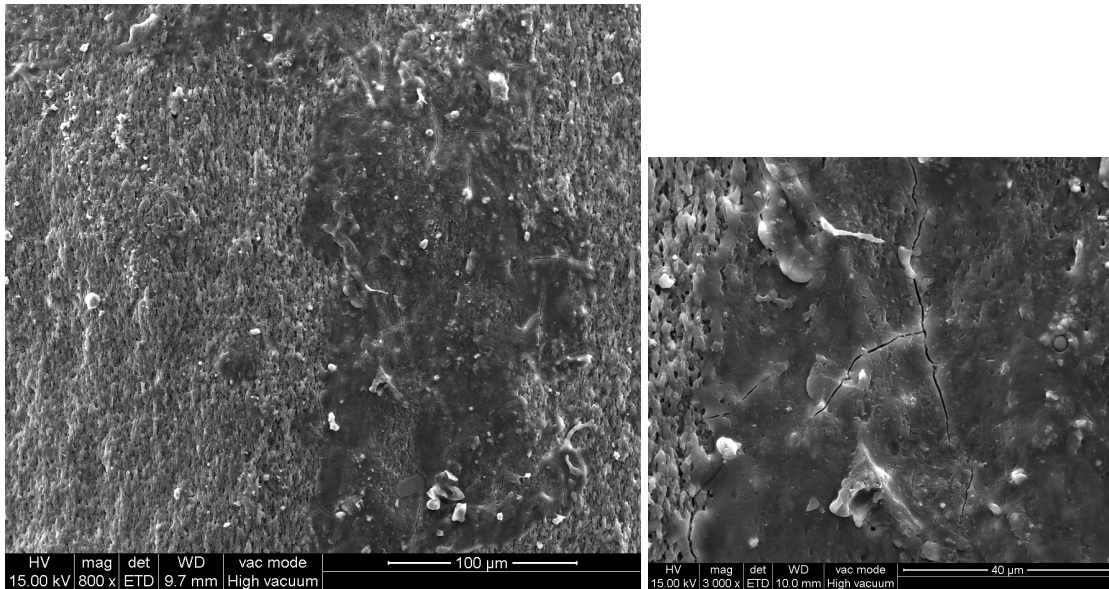


Figure 4.22. TPS coastal indoor. Detail to highlight differences between the surface and the blackish spots.

The black spots visible in TPS INDOOR could be due to different degradation occurred in the part where the surface was in contact with the sand. The porosity of the surface seems to decrease a lot in the black area (the surface seems to have been compacted). This is the area where surface cracks were more visible.

Looking at the pelagic zone (Figure 4.23 and Figure 4.24), the situation appears quite different. Indeed, differences from virgin pellets are visible for all plastic types and condition of exposure, according to the macroscopic changes summarized in Table 4.3 and Table 4.4.

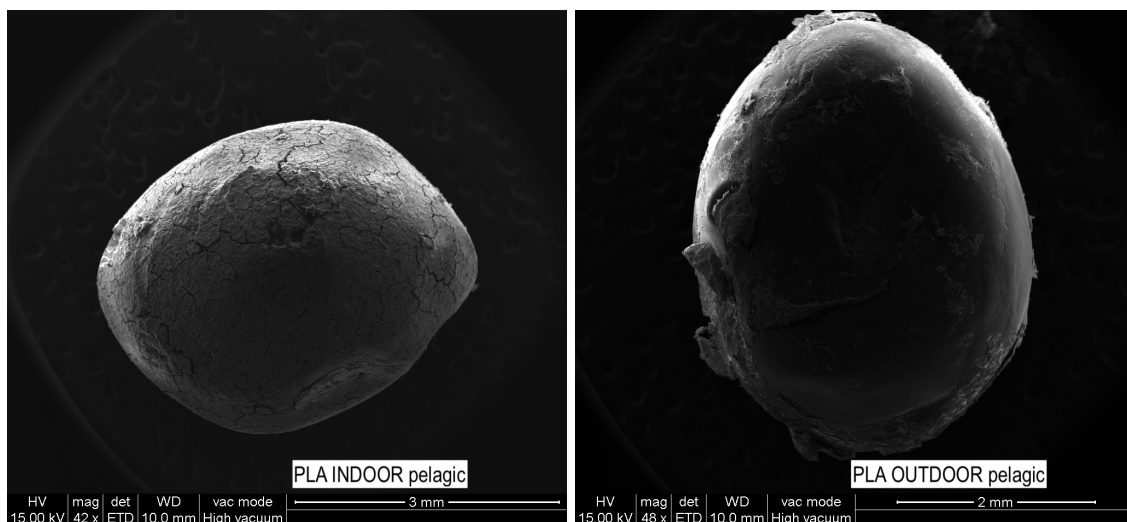


Figure 4.23. SEM pictures for PLA pelagic in INDOOR and OUTDOOR conditions.

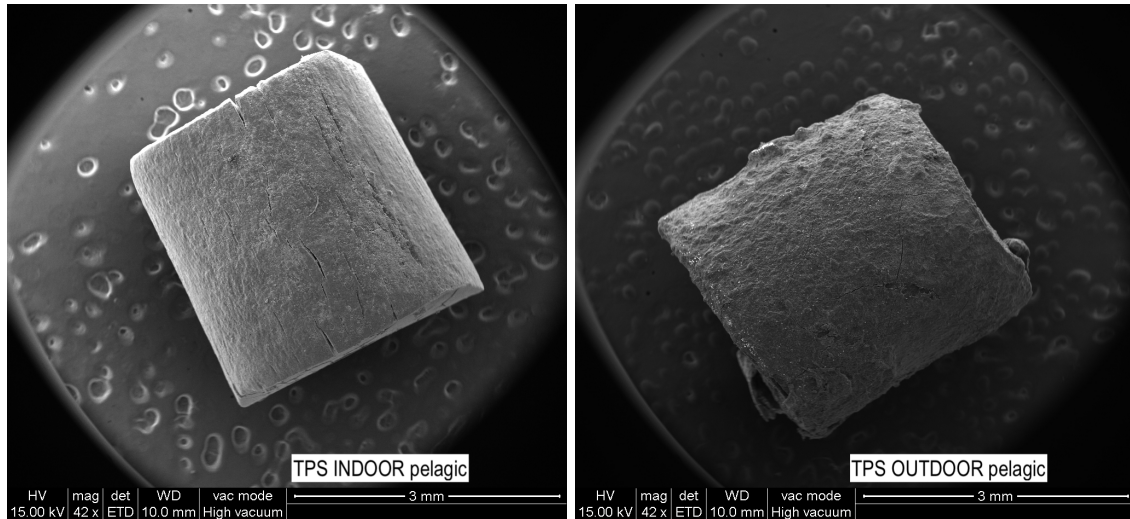


Figure 4.24. SEM pictures for TPS pelagic in INDOOR and OUTDOOR conditions.

For the INDOOR conditions, pellets surface presented a high level of degradation, consisting in cracks and fractures, especially for PLA (Figure 4.25). Pellets in OUTDOOR conditions presented surface inhomogeneities. The surface seemed to be partly covered by biofilm (Figure 4.26).

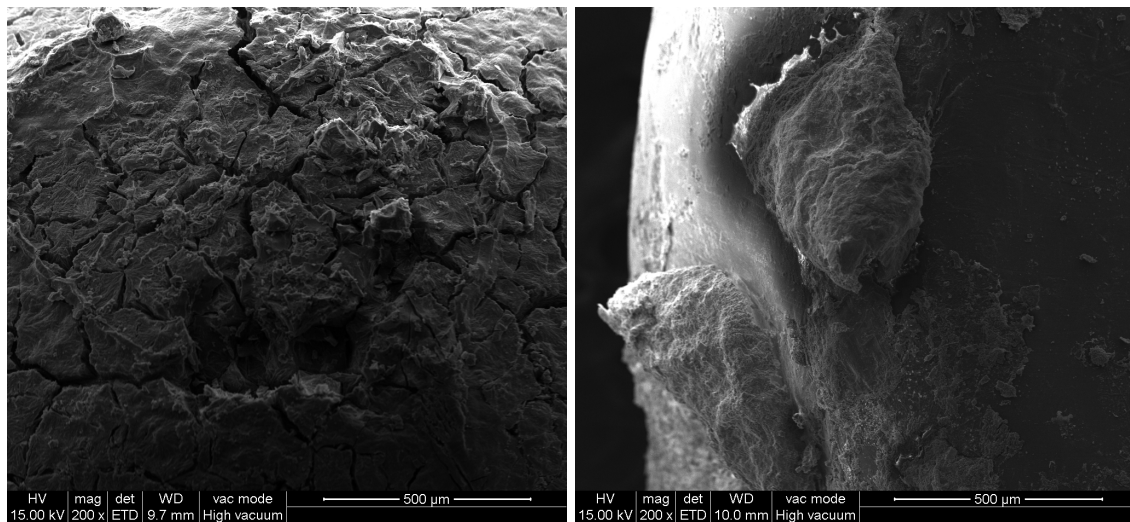


Figure 4.25. PLA INDOOR and OUTDOOR pelagic. Different surface degradation with same magnification (200x).

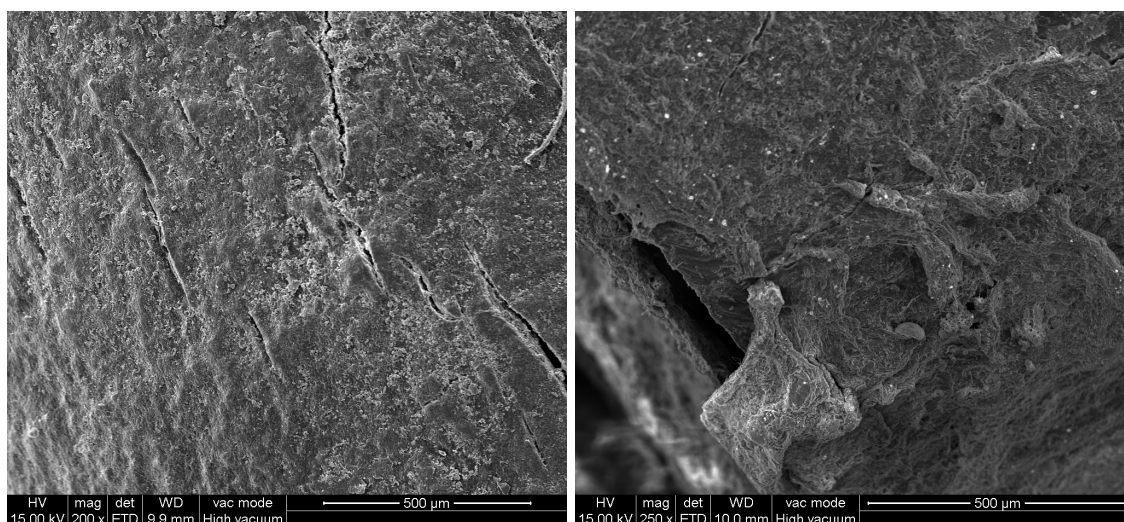


Figure 4.26. TPS INDOOR and OUTDOOR pelagic. Different surface degradation with same magnification (200x).

Looking closer to impurities on the surface of TPS OUTDOOR pelagic, salt crystals were detected (Figure 4.27). Moreover, some fiber-shaped particles (Figure 4.27 in yellow circles) with the same shape and size as the MPs visible with Fluorescence microscope were observable on the surface.

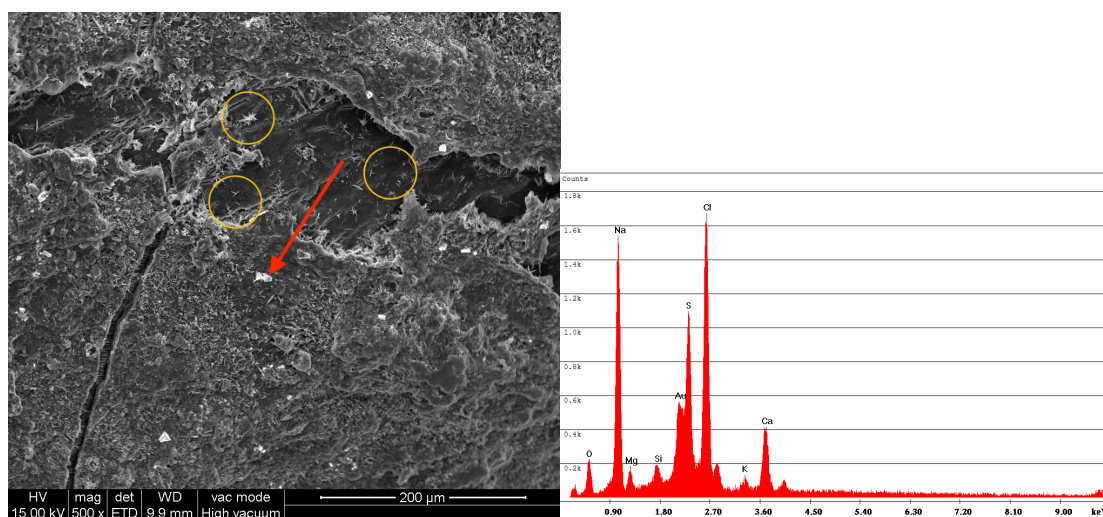


Figure 4.27. TPS OUTDOOR pelagic detail and spectrum.

From an enlargement of the image of PLA INDOOR (Figure 4.28), the spectra of the fragments present on the surface confirmed that it was plastic dethatching. Also, on the polymer surface ruts in the form of fibers (that was the predominant shape in which MPs are visible under the Fluorescence Microscope) were visible.

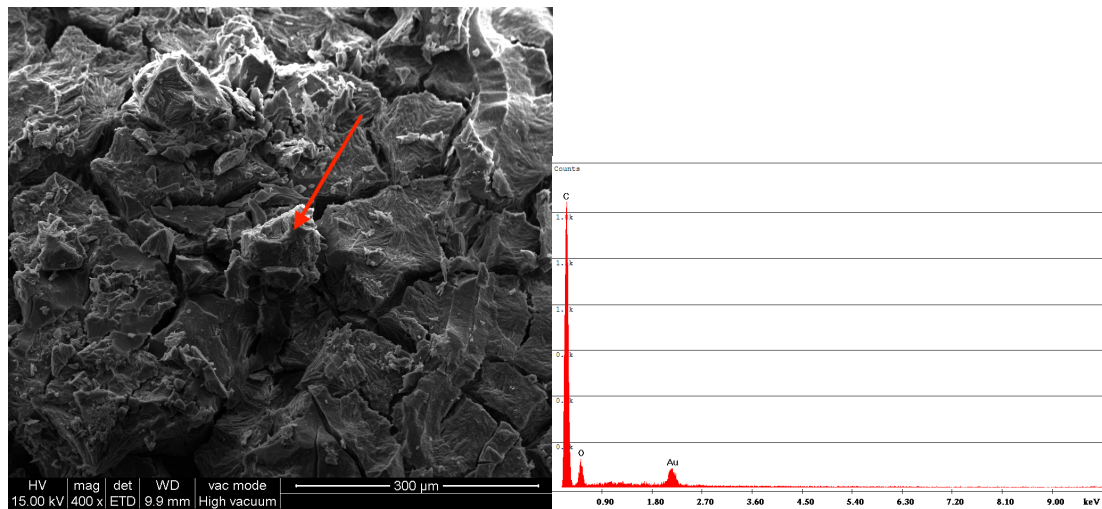


Figure 4.28. PLA INDOOR pelagic surface detail.

Looking closer to an inhomogeneity on PLA OUTDOOR surface the detail of Figure 4.28 was visible. This can be biofilm containing some salts, leftover of seawater evaporation.

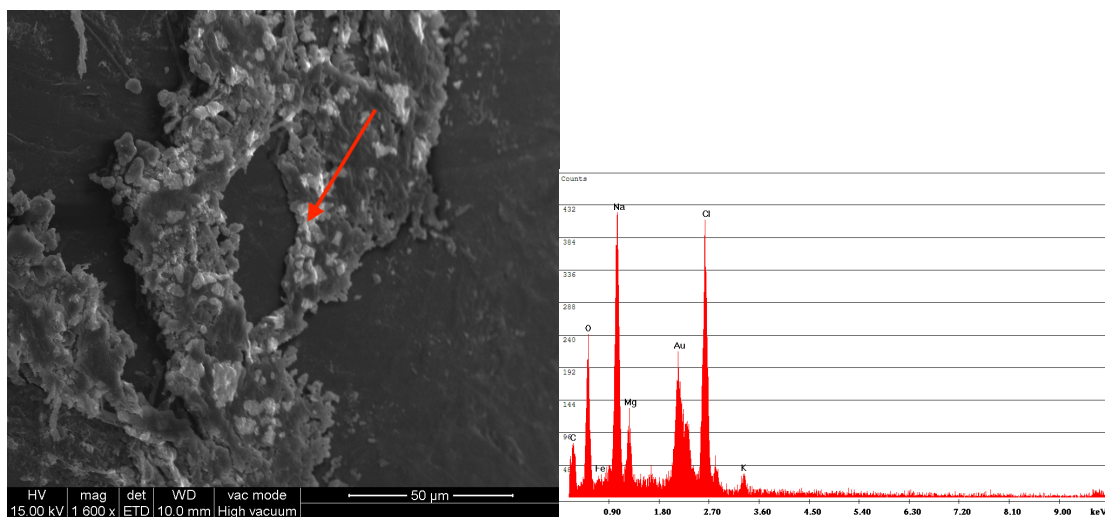


Figure 4.29. PLA OUTDOOR pelagic detail.

Briefly:

- Coastal pellets presented less signs of degradation than pelagic pellets (this is compliant with the observed macroscopic and properties changes). Hydrolysis plays an important role as it accelerates bonds breaking and degradation.
- Pelagic degradation was more homogeneous than coastal one: in water pellets were free to move in water.
- Indoor conditions had a degradation effect higher than outdoor ones. Indoor pellets are exposed 24/7 to concentrated UV light, and this greatly affects the results.

- On some pellets ruts and particles, shaped as MPs visible under the microscope and with the same size, were detectable.
- Some salts/sand particles were detected on the pellets surface for both pelagic and coastal pellets. They become new pellets components and can act as contaminant carriers through the ecosystems.

X-ray Fluorescence spectroscopy

From the XRF analysis 6 elements have been selected to be analyzed: Silicon (Si), Sulfur (S), Iron (Fe), Phosphorous (P), Nickel (Ni), and Chlorine (Cl).

Virgin pellets were analyzed, and their elements concentration is reported in Table 4.7.

Table 4.7. XRF for virgin pellets.

<i>mg/kg</i>	Si	P	S	Cl	Fe	Ni
PLA	0	0	91.7 ±83.5	87.7 ±111.4	100.2 ±3.8	27.1 ±4
TPS	0	187 ±96.2	86.2 ±91.8	60.3 ±104.5	117.0 ±11.5	32.9 ±1.9

Pellets surface of both PLA and TPS presented a low concentration of Iron and Nickel. TPS seem to contain also Phosphorous. For both plastic type, Sulfur and Chlorine concentrations presented high variability due to the inhomogeneity of the samples and the spot analysis of XRF.

The increase of elements concentration on the pellets surface can be linked with the deposition of these elements on the pellet surface or their absorption inside the pellets. Generally, for pellets immersed in water a more enhanced increasing concentration over exposure time was visible, like we can see in Figure 4.30 with the example of Sulfur (they have completely different orders of magnitude for concentration). Especially TPS exhibited the major increase, likely due to its more porous and less crystalline structure (visible also with SEM), compared with PLA. Indeed, the bigger water uptake inside TPS structure can explain these trends: water enters in the polymer along with the elements, but during water evaporation the elements remain trapped inside the pores.

The higher elements increase by TPS OUTDOOR with respect to INDOOR (as visible in Figure 4.31) can be linked with the biofilm presence and differences in the degradation mechanisms occurring under natural outdoor conditions and UVC lights.

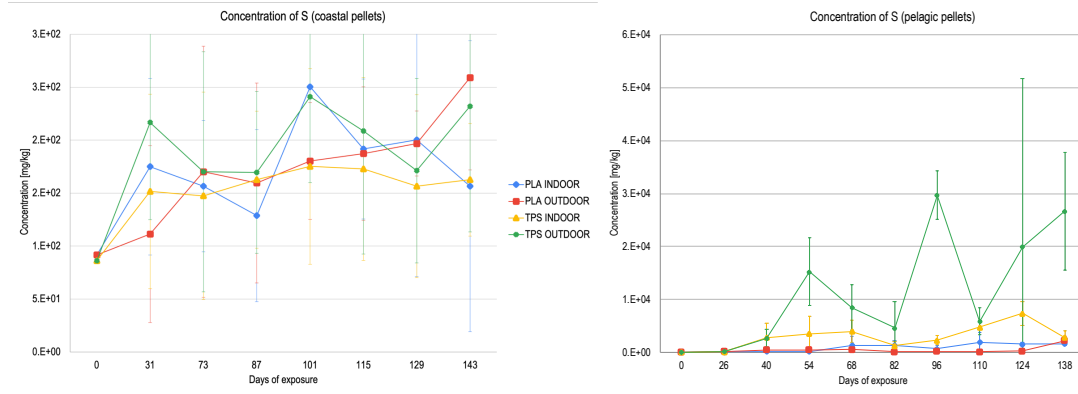


Figure 4.30. Sulfur concentration variation over the time for coastal and pelagic zone.

The concentrations of Silicon, Sulfur, and Chlorine in seawater have not been assessed experimentally. However, in literature, seawater analyses highlight their presence. Being Silicon, Sulfur, and Chlorine seawater components, the increase of these elements concentration in TPS in the aquariums can be justified. Iron and Nickel concentration increase for TPS OUTDOOR in pelagic zone can be explained by the presence of this elements in seawater (5ppm for Iron and 26ppm for Nickel from ICP-MS analysis). Regarding coastal zone, due to the non-homogeneity of the system the variability was very high (Figure 4.32). Silicon was expected to increase because of sand contact. The same thing can be said for Sulfur and Chlorine. However, the Si uptake for pelagic pellets was orders of magnitude higher than coastal pellets.

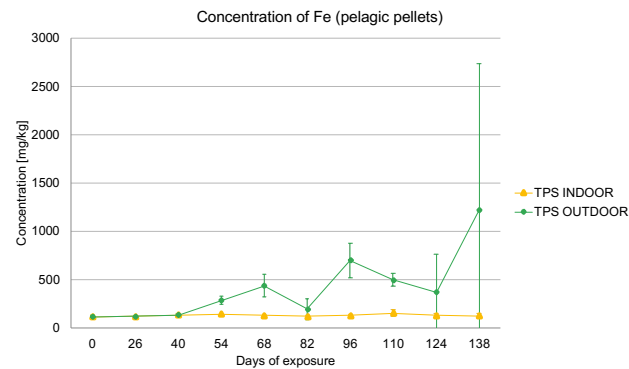


Figure 4.31. Fe concentration variation over the time for TPS INDOOR and OUTDOOR.

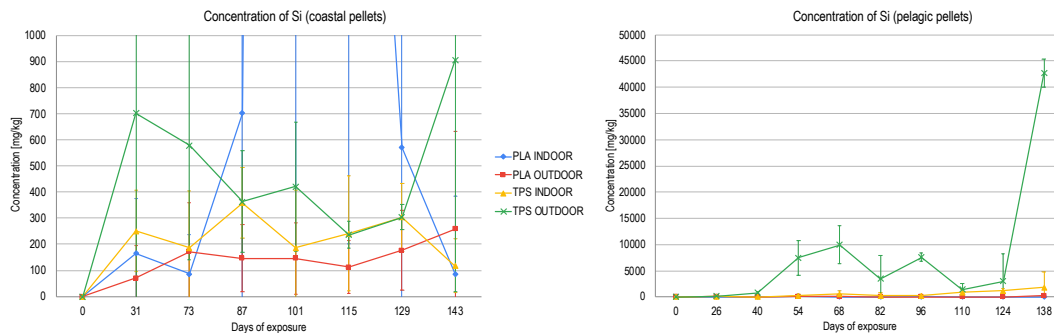


Figure 4.32. Si concentration variation over the time.

Phosphorous (Figure 4.33) is a constituent for TPS, but not for PLA (no P was detected for virgin pellets neither over the exposure time).

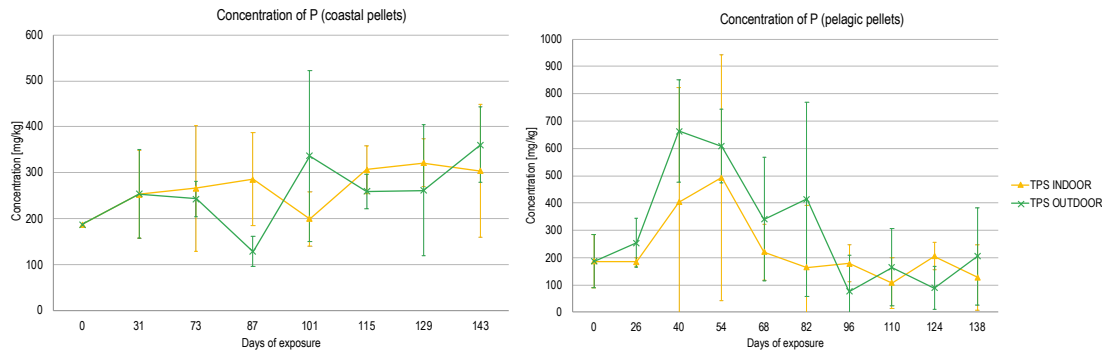


Figure 4.33. P concentration variation over the time.

Briefly:

- Virgin PLA does not contain P and Si. Virgin TPS does not contain Si.
- Elements concentration (Si, S, Cl) for pelagic pellets increased orders of magnitude more than coastal ones.
- TPS pellets have an aptitude to absorb water and they tend to have a rapid increase of elemental concentrations, acting as carrier for toxic compounds.
- The presence of impurity was way higher on coastal surface than on pelagic one (with SEM), but pelagic pellets elemental concentration with XRF was orders of magnitude higher than coastal, we can suppose that they have been sorbed.

Fourier transform infrared spectroscopy with Attenuated total reflectance (ATR-FTIR)

Virgin pellets can be characterized and the variation of chemical bonds over the time can be monitored with ATR-FTIR. In Figure 4.34 the spectra of virgin PLA and virgin TPS is showed. In Figure 4.34 the wavenumbers appear on the x axis, with cm^{-1} as the unit and the absorbance (it can also be transmittance) on the y axis (dimensionless parameter). Each peak corresponds to a specific chemical bond. To associate the peaks to the bonds, tables are available for the conversion. In Table 4.8 and Table 4.9 some peaks were characterized. Deviations from these spectra mean that some changes occurred on the pellets surface. In the $2400\text{-}2000\text{ cm}^{-1}$ region and in the 500 cm^{-1} and below region, there are many tiny peaks. This is noise and instrument artefacts, that must be ignored.

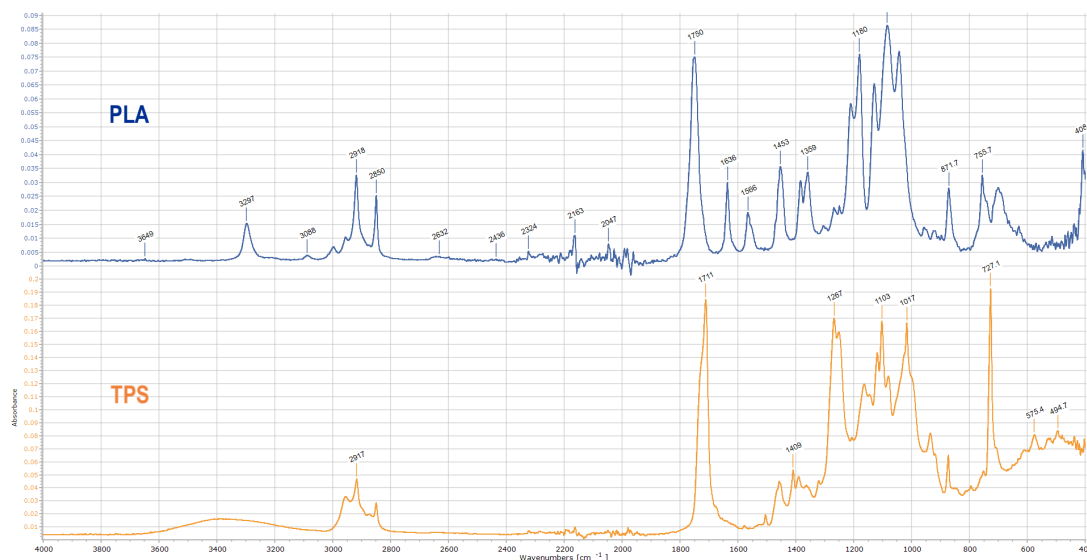


Figure 4.34. ATR-FTIR virgin PLA and TPS spectra and main peaks.

Table 4.8. Main PLA peaks. Wavenumbers and their corresponding assignment for PLA virgin pellets IR spectrum (Chaplin, 2013; Nasir & Othman, 2022; Smith, 2021).

PLA			
Wavenumbers [cm ⁻¹]	Assignments	Wavenumbers [cm ⁻¹]	Assignments
3297	C-H or N-H stretch	1566	
3088	C-H stretching	1453	CH ₃
2918	CH ₂	1359	CH
2850	CH ₂	1180	C-O-C
2632		1070	S=O or C=OH
1750	CH ₃	872	Amorphous phase
1636	C=O	756	Crystalline phase

Table 4.9. Main TPS peaks. Wavenumbers and their corresponding assignment for PLA virgin pellets IR spectrum (del Rosario Salazar-Sánchez et al., 2019; Umamaheswari & Murali, 2013).

TPS			
Wavenumbers [cm ⁻¹]	Assignments	Wavenumbers [cm ⁻¹]	Assignments
2917	CH ₂	1017	C-O bond
1711	C=O	727	C-H bending
1409	S-O stretching	575	
1267	C=O	495	
1103	C-O stretching		

To monitor and describe the degradation of the mechanical properties of polymers with a single number, the carbonyl index (CI), that describes the hydrolyzation of carbonyl groups (C=O) can be useful. There are several ways to define it. The CI is environmental

and exposure conditions dependent and thus can vary a lot for the same plastic exposed in different environments. Thus, the comparisons with the literature results are not meaningful since there are not standardized values (Almond et al., 2020). What was more important for this work was to show another way to justify the pellets physico-chemical properties changes (and thus degradation) over the time. Indeed, the CI changes over the time means that surface chemical bonds are modified.

According to a previous study on PLA /PBAT plastic (Wang et al., 2023), the following Carbonyl Index (Eq. 4.1) was used:

$$CI = \frac{I_{1710}}{I_{1452}}, \tag{4.1}$$

where I is the value of the absorbance at 1710 cm⁻¹ and 1452 cm⁻¹, respectively. The CI of some of the sampling days for the coastal zone are presented in Figure 4.35 and Figure 4.36.

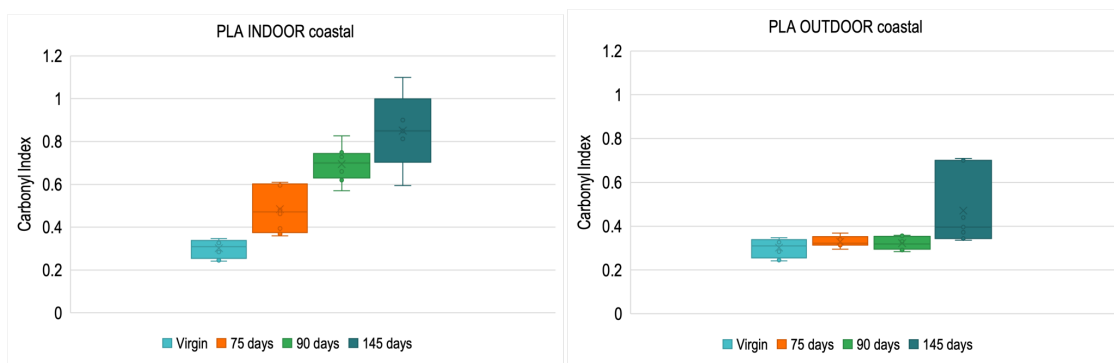


Figure 4.35. Carbonyl Index for PLA coastal.

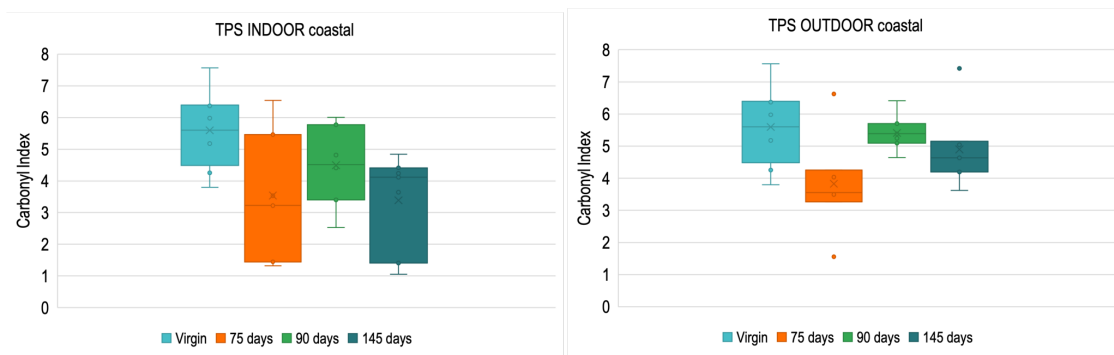


Figure 4.36. Carbonyl Index for TPS coastal.

Differences in CI were bigger for indoor conditions than outdoor ones, and for PLA more than TPS. The CI for PLA increases, while for TPS decreases. PLA INDOOR increased from 0.30 to 0.85, while PLA OUTDOOR from 0.30 to 0.47. For TPS INDOOR a reduction from 5.60 to 3.39 was visible and for TPS OUTDOOR from 5.60 to 4.90. Figure 4.37 and Figure 4.38 highlight the differences occurred in the whole spectrum for the

pellets exposed in the coastal zone for indoor conditions (where the changes were more relevant). For PLA the main changes occurred in the regions 2800-3350 cm^{-1} linked with C-H stretching, and 1550-1650 cm^{-1} corresponding to C=O bonds (carbonyl band). For TPS the main changes occurred in the regions around 3300 cm^{-1} linked with O-H stretching (hydroxyl band), and 2917 cm^{-1} corresponding to CH_2 bonds.

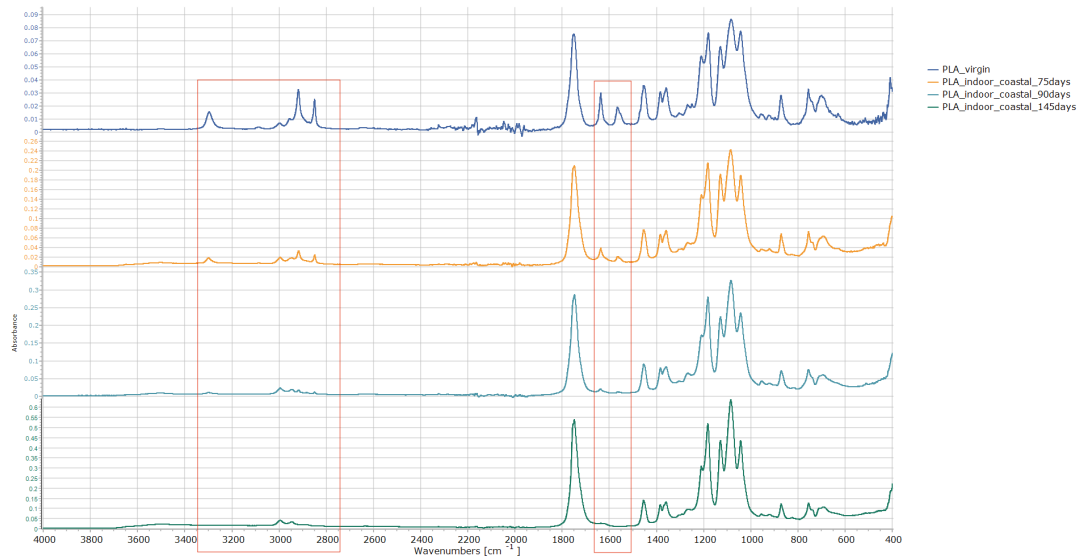


Figure 4.37. Spectra of PLA INDOOR coastal.

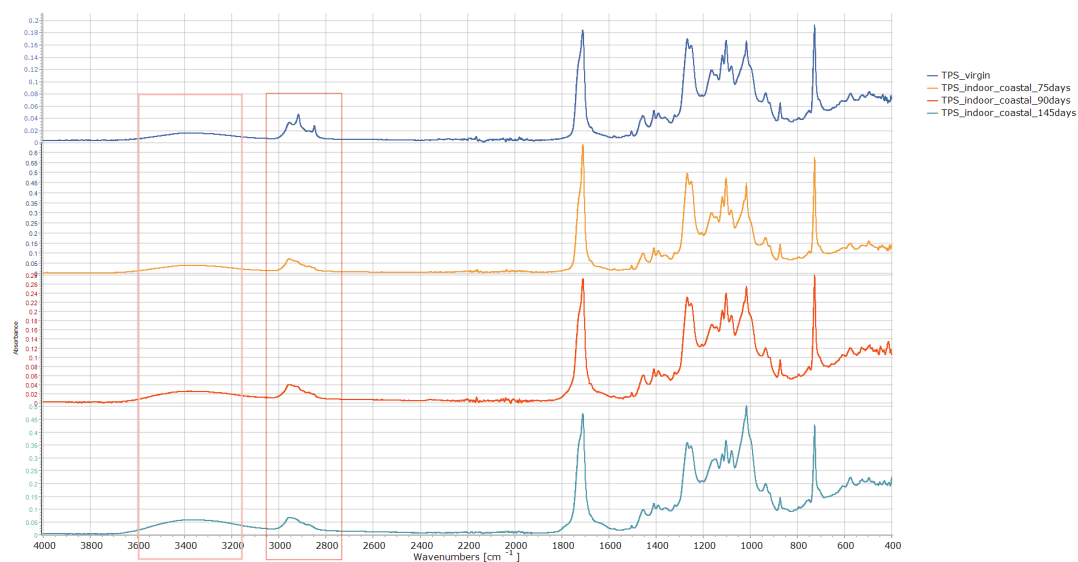


Figure 4.38. Spectra of TPS INDOOR coastal.

The CI of some of the sampling days for the pelagic zone are presented in Figure 4.39 and Figure 4.40. Again, differences in CI were higher for indoor conditions than outdoor ones. Also, CI increase for PLA was lower for pelagic zone than for coastal one. PLA INDOOR moved from 0.30 to 0.44, while PLA OUTDOOR from 0.30 to 0.39. While CI

decrease for TPS was higher for pelagic zone than coastal one. For TPS INDOOR a reduction from 5.60 to 3.2 was visible and for TPS OUTDOOR from 5.60 to 4.74. Figure 4.41, Figure 4.42, and Figure 4.43 highlight the differences along the sampling days in the whole spectrum for the pelagic zone. The main changes occurred in the same regions as for coastal zone. Bigger changes were visible for PLA INDOOR (Figure 4.41) with respect to PLA OUTDOOR (Figure 4.42). Changes were also visible for TPS in the region around $1000\text{-}1200\text{cm}^{-1}$ corresponding to C-O-C bonds (Figure 4.43). The changes in these regions of the spectrum are consistent with literature studies on conventional plastics, as these bonds are more susceptible to oxidation, independently from the plastic type (Benítez et al., 2013; Sandt et al., 2021; Skariyachan et al., 2016).

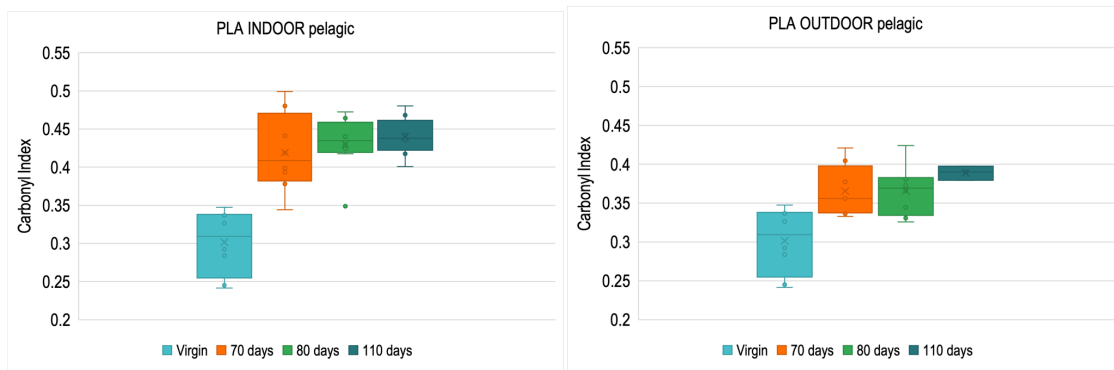


Figure 4.39. Carbonyl Index for PLA pelagic.

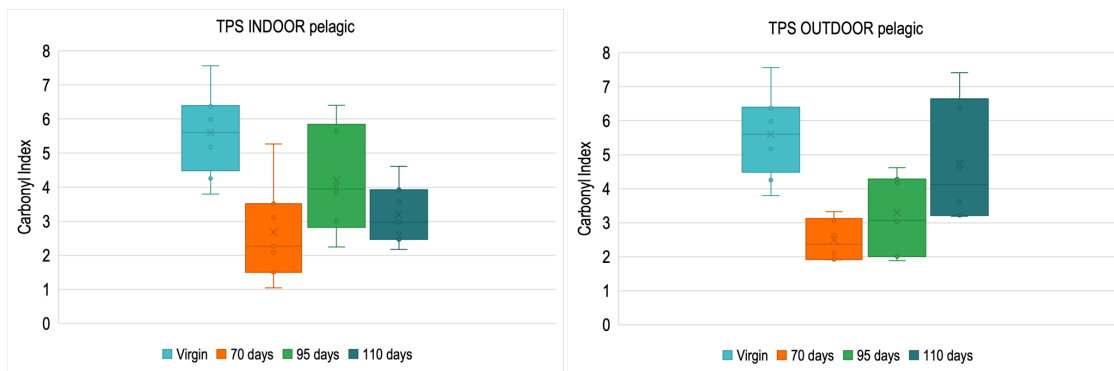


Figure 4.40. Carbonyl Index for TPS pelagic.

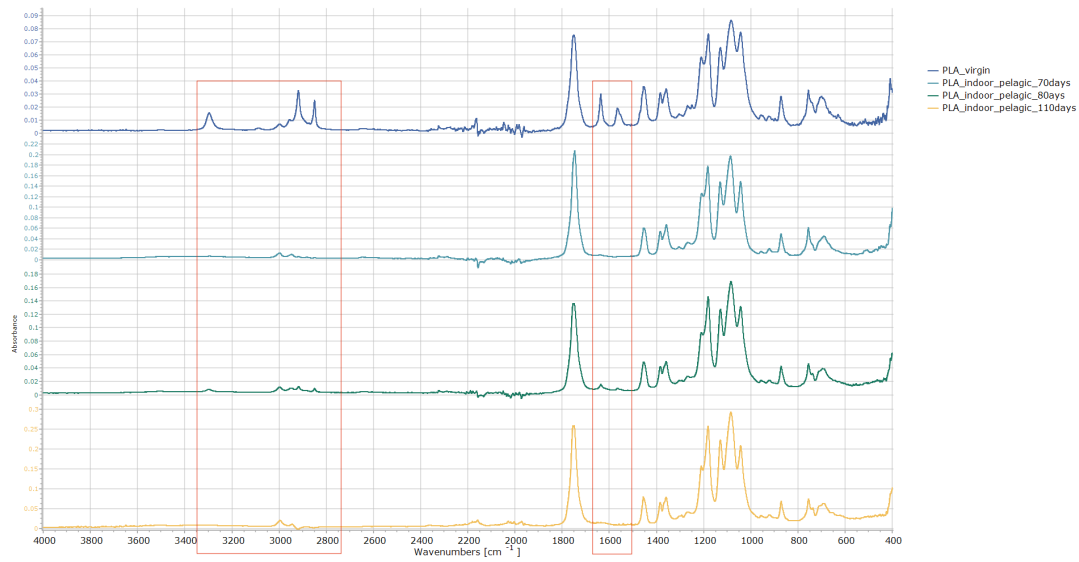


Figure 4.41. Spectra of PLA INDOOR pelagic.

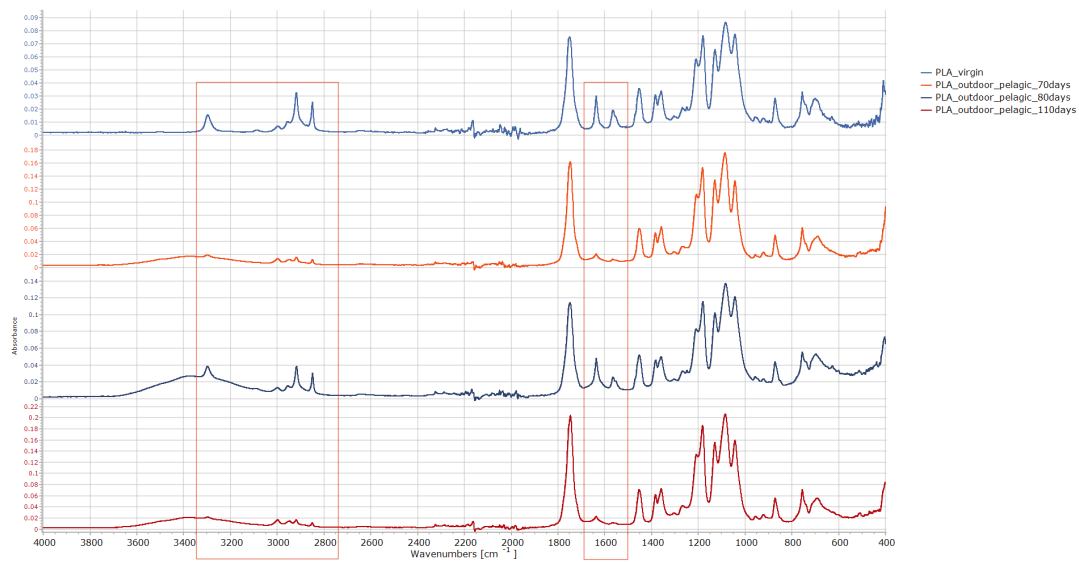


Figure 4.42. Spectra of PLA OUTDOOR pelagic.

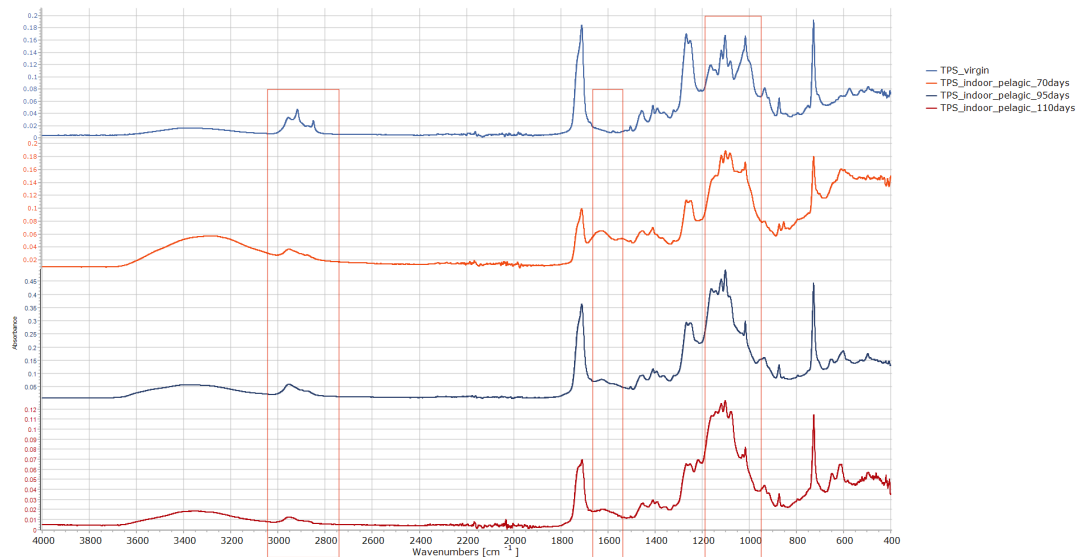


Figure 4.43. Spectra of TPS INDOOR pelagic.

4.2. Seawater properties and biological presence

Biofilm formation

The term biofilm refers to an ensemble of complex communities of bacteria, algae, fungi and protozoa (Mampel et al., 2006). During the exposure period, in the aquarium of the TPS OUTDOOR, the grow of algal biofilm was visible with bare eyes, while the other aquariums didn't show such behavior. Crystal Violet test is a widespread method used for bacterial biofilm quantification. Thus, the algae biofilm development on TPS pellets couldn't be monitored. The biofilm quantification obtained from Crystal Violet test, presented in Figure 4.44, showed that a certain amount of biofilm was present on every pellet type and exposure condition, also on the pellets exposed to UVC lamps (the same lamps used for sterilization purposes).

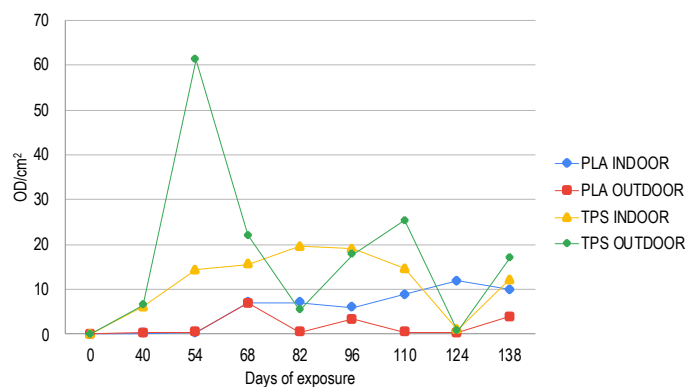


Figure 4.44. Optical density from Crystal Violet test for biofilm quantification of pelagic pellets.

Due to these results, the possibility that Crystal Violet test does not work properly with bioplastics arose. However, Crystal Violet test performed on virgin pellets (4 test for each plastic type) led to OD values one or two orders of magnitude lower than the first analyzed sample (at 40 days), and up to 3 orders of magnitude for the other sampling dates. However, it is not excluded that surface property changes due to degradation could have trapped some dye (or some elements could have bonded with it) leading to misleading results in the biofilm quantification. Indeed, despite the simplicity, time efficiency, and cheapness of the Crystal Violet test, the increase in biofilm detected by the test cannot be directly correlated with the amount of all bacterial cells in the biofilm, even according to Banihashemi & Gil (2022). Indeed, dead cells and some polysaccharide blends could be stained and influence the optical density values (Banihashemi & Gil, 2022).

Water parameters

Nitrogen, Nitrate, Ammonia and Phosphorous concentration in seawater were monitored every two weeks. In Figure 4.45 Total Nitrogen and Nitrate concentrations are reported.

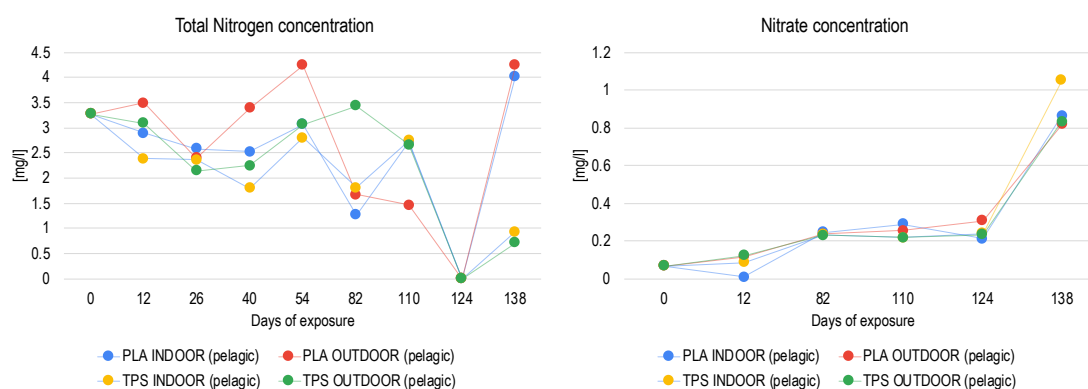


Figure 4.45. Total nitrogen (on the right) and Nitrate (on the left) concentration in seawater.

Nitrogen decreased over the time (until Nitrogen was added to the aquariums), while Nitrate increased over the time. No correlation between Nitrogen and Nitrate was found. Despite the visible presence of biofilm for outdoor conditions, no differences in the Nitrate trends were found. Thus, biofilm did not seem to have a significant role in this increase. The increase could be due to the not sterile environment and to the contact with oxygen. pH, Dissolved Oxygen (DO), Redox Potential (ORP), Conductivity, and Temperature were monitored. pH slowly decreased over the time up to 11% for TPS indoor. DO decrease showed a negative correlation with temperature increase (-0.8) and a reduction around 32-34% for all plastics and conditions, except for TPS outdoor (-14%). ORP decreased over the exposure time, with a reduction around 63-74% for all plastics and conditions, except for TPS outdoor (-24%). Higher Conductivity variations occurred for indoor conditions (26-27%) with respect to outdoor ones (13%). Temperature in indoor conditions rose from 12 in March to 32°C in July, and from 18/19 to 42/43°C for outdoor ones.

Flow cytometry

To quantify the presence of cells inside the seawater of the aquariums flow cytometry was used. Particles detected as cells were the ones that were not background (assessed using a seawater blank) and that were stained by the SYBR green dye, with an intensity higher 10^4 . Particles with lower intensity can be broken cells, plastics, or other compounds. Fig shows that the cells concentration over the time was quite low and did not differ a lot from the blank concentration. Since the aim was to be as close as possible to seawater conditions, these results confirmed that cells concentration was more or less stable over the time (Figure 4.46 and Figure 4.47).

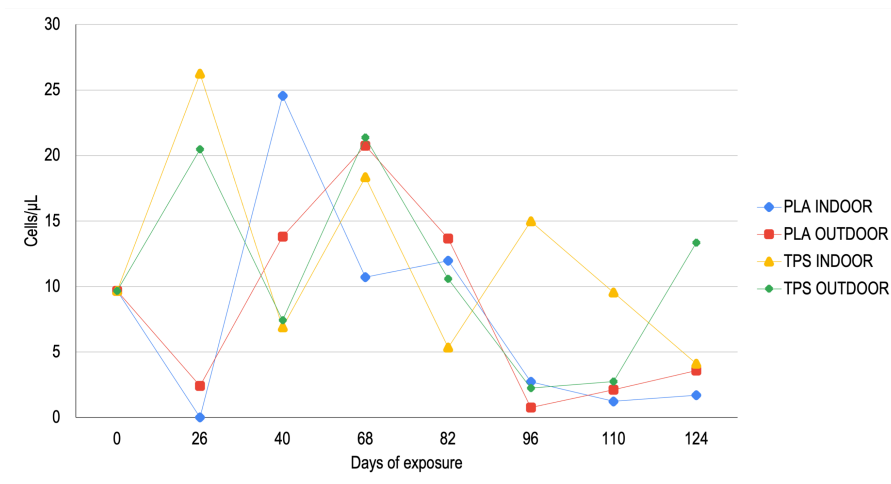


Figure 4.46. Cells concentration over sampling days.

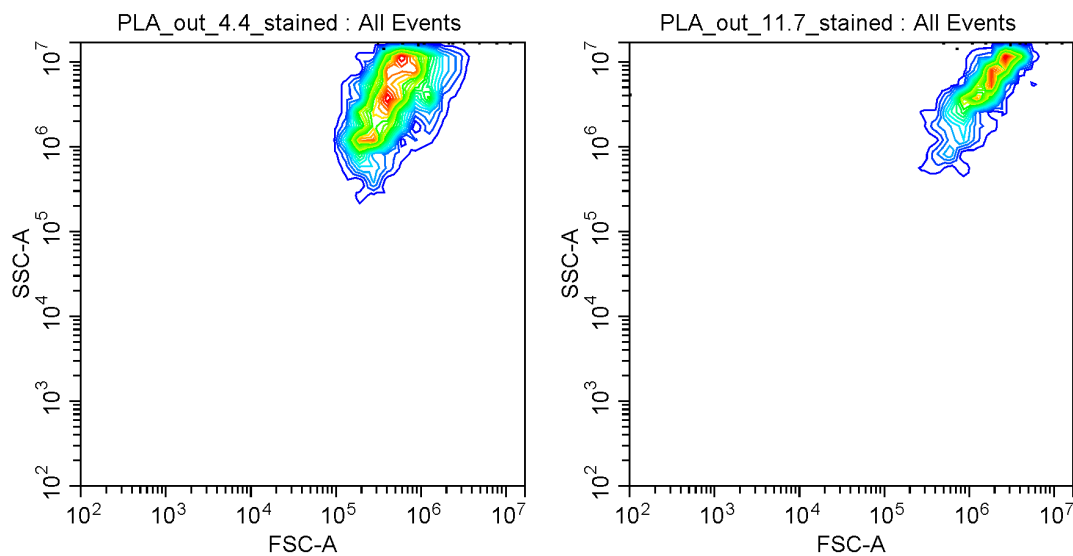


Figure 4.47. Flow cytometer results at the beginning and at the end of the experiments for PLA OUTDOOR.

No correlation was visible between Crystal Violet Optical Density values and cells concentration. However, they seem to be very rarely correlated since Extracellular Polymeric Substances (EPS) produced by microorganisms depends on many factors,

including the type of bacterium producing them. Thus, if the cells in the biofilm are not major EPS producers, a correlation with the Crystal Violet OD is not detectable. Also, since a portion of the samples was discarded due to the 20 μm filtration (necessary to avoid clogging the flow cytometer), while Crystal Violet OD is measured directly on the surface of the pellets, searching for possible correlations can be misleading. No correlations were found between Nitrogen/nitrate and cells concentration (also removing samples after nutrients addition).

4.3. MPs/NPs formation

Secondary micro and nano-plastics result from plastic chain breaking due to the weathering process (Bao et al., 2022). Their presence was quantified using Fluorescence Microscope for both pelagic and coastal zone. The particle size distributions of the particles present in the samples was assessed with Dynamic Light Scattering (DLS). Moreover, for pelagic samples, Nanoparticle Tracking Analysis (NTA) was used to assess concentration, mean diameters and particle size distribution of the particle in the sample smaller than 1.6 micron.

Fluorescence Microscope

Due to the physico-chemical properties of plastics, the presence of other particles, and limitations of the instruments used, the MPs and NPs detection and quantification was challenging. Differences in detection difficulties raised for coastal zone more than pelagic, due to the use of Calcium Chloride solution. Fluorescence Microscope was the most reliable technique. Indeed, the Nile Red dye allows to be sure that only plastics are measured. Using or not the dye resulted in completely different appearance during test performed with polystyrene (PS) beads under the fluorescence microscope. Also, to be sure that there was no overestimation due to Nile Red presence, a solution with water and Nile Red was tested, leading to the conclusion that when the dye is not attached to a plastic its shape and color are different (red squashed droplets instead of magenta fibers). The efficiency of the method was tested using PS beads of 500nm with different concentrations and in different solutions (deionized water, seawater, and CaCl_2 solution). Results are summarized in Table 4.10.

Table 4.10. Fluorescence microscope efficiency tested with beads.

Beads' real concentration	Concentration [particles/ml]		
	dH ₂ O	Seawater	CaCl ₂ solution
1E+08	2.7E+07	2.3E+07	2.1E+04
1E+06	2.4E+05	3.4E+04	4.9E+02

The concentration estimation in seawater differs by one or two orders of magnitude from the original one. While for CaCl₂ solution the detection capacity is very low (4 orders of magnitude less). It was noticed that where the differences were higher the presence of many aggregates impeded the exact enumeration. Also, the fact that beads are very small (around two orders of magnitude less than MPs from samples) made even more difficult their detection. Moreover, PS beads density is around 1 g/cm³ (against 1.3 g/cm³ for PLA and TPS). This density allows a good mixing and homogeneity with water, explaining the good detection. However, due to the big density difference with seawater and even more with calcium chloride solution, the beads likely remain on the liquid surface impeding a good homogeneity of the droplets analyzed. Due to the higher density of PLA and TPS this last point could be relevant, and a test performed with PS beads could underestimate the efficiency of the method. The presence of fluorescence helps the recognition of the polymer, improving the efficacy of the analysis. Plastics mainly appears in the form of fibers and in a magenta color as visible in Figure 4.48.

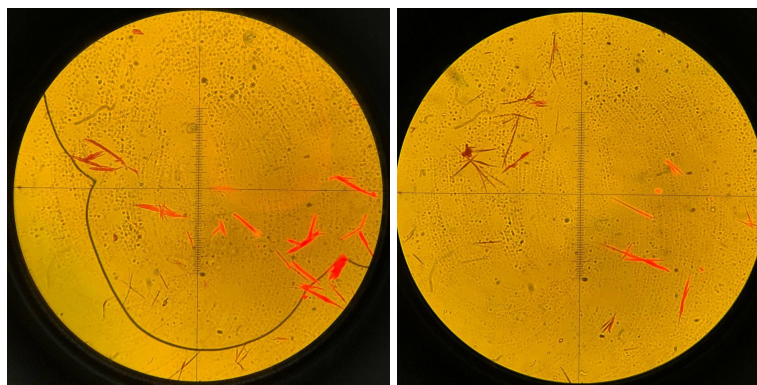


Figure 4.48. Microplastics under the microscope.

The MPs concentration at every sampling day is reported in Figure 4.49 and Figure 4.50 for the different plastic types and zones.

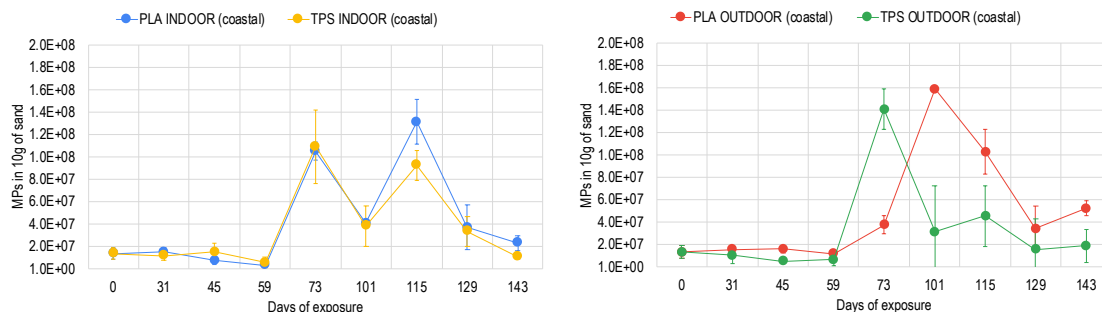


Figure 4.49. MPs concentration with Fluorescence Microscope for coastal zone.

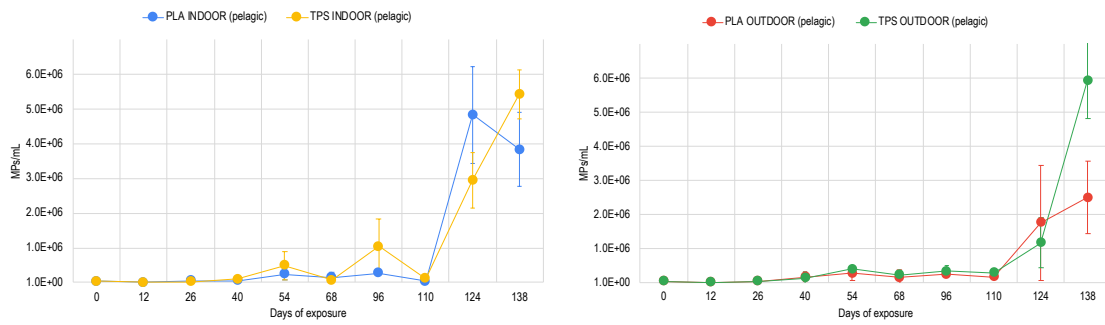


Figure 4.50. MPs concentration with Fluorescence Microscope for pelagic zone.

Despite the different exposure conditions (UV and sunlight) each plastic type for each zone followed the same trend. While pelagic MPs concentration showed a slight increase and a sudden increase towards the end of the experiment, coastal zone one exhibited a peak in the middle of the experiment, followed by a decreased. Also, the increase of MPs concentration for pelagic samples was two orders of magnitude higher than blank solution, while maximum one order of magnitude for coastal. While for coastal zone indoor PLA and TPS followed the same trend, for outdoor conditions the maximum peak in concentration for PLA was delayed for 15 days.

Secondary MPs concentration of the pelagic zone used as photoresponse obeyed to Schwarzschild's law, as visible in Figure 4.51. The correlation was good for outdoor conditions and for the first part of the indoor experiment (UVB lamp), while it was less accurate for the last part, where also the standard deviations (Figure 4.50) were higher. Coastal zone MPs did not obey to Schwarzschild's law.

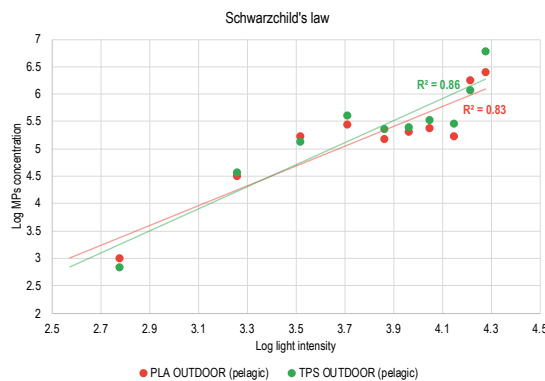


Figure 4.51. Schwarzchild's law applied to pelagic outdoor samples.

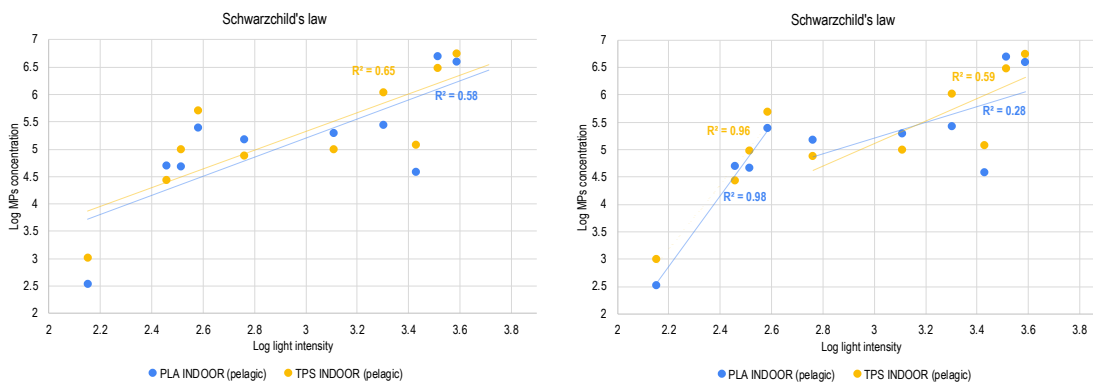


Figure 4.52. Schwarzchild's law applied to pelagic indoor samples.

For the coastal zone, the size of some MPs (of the second sampling day) under the Fluorescence microscope was retrieved by taking pictures and measuring the length with ImageJ. Results are shown in Figure 4.53. The mean size of PLA plastic fibers was 28 μm , while 38 μm for TPS, with higher variability for TPS outdoor.

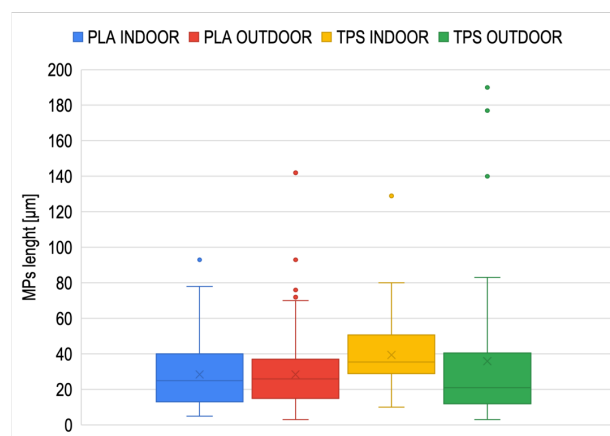


Figure 4.53. Box plot of the mean MPs length for coastal samples at 31 days of exposure.

Dynamic Light Scattering

Beads (500 nm and 200 nm size) were tested with deionized water, seawater and CaCl_2 solution. The peaks for deionized water and seawater were compliant with the size of the beads. However, the intensities were slightly different between deionized and seawater. Probably, the seawater blank hid some of the intensity of the beads. Nevertheless, no results were detectable with the Calcium Chloride solution. This was probably due to the high-density difference, the small size of beads and their aggregation. Indeed, while inserting a certain concentration of beads in the solution, an immediate rise of an aggregate of beads was visible.

Despite the appropriate refractive index (RI) for these plastic types was used, there could be particles other than plastics that have the same RI, and DLS is not able to differentiate MPs from other particles that scatter light (Fu et al., 2020). Since DLS does not provide

concentration values, it is difficult to compare the results with the other techniques to countercheck. Despite the mixing, plastics sedimentation for pelagic zone and flotation for coastal zone, along with aggregation for both compartments, could significantly affect the reliability of what the instrument measures.

In Table 4.11 and Table 4.12 the mean diameters of the samples retrieved from DLS are reported. As visible, the analysis with Calcium Chloride solution was more challenging due to the signals covered by the solution itself and indeed many values were below the detection level (BDL). Coastal zone values didn't have a linear trend over the time, but fluctuations in the values occurred. Pelagic zone pellets (except for PLA indoor) showed a decreasing diameter value over the time.

Table 4.11. Mean diameter values from DLS analysis for coastal zone.

Days of exposure	COASTAL ZONE				Days of exposure	COASTAL ZONE			
	PLA INDOOR		TPS INDOOR			PLA OUTDOOR		TPS OUTDOOR	
	NUMBER [μm]	VOLUME [μm]	NUMBER [μm]	VOLUME [μm]		NUMBER [μm]	VOLUME [μm]	NUMBER [μm]	VOLUME [μm]
31	0.02	1.98	0.88	3.39	31	0.07	8.02	0.26	2.04
45	BDL	BDL	232.60	240.51	45	279.57	303.05	1.14	3.91
59	BDL	BDL	0.38	3.96	59	BDL	BDL	2.95	4.11
73	BDL	BDL	BDL	BDL	73	BDL	BDL	BDL	BDL
101	BDL	BDL	BDL	BDL	101	BDL	BDL	BDL	BDL
115	0.14	11.15	0.07	7.93	115	0.90	15.08	1.27	19.50
129	322.94	343.92	302.62	328.75	129	299.34	325.68	BDL	BDL
143	BDL	BDL	241.83	262.72	143	BDL	BDL	267.63	279.99

Table 4.12. Mean diameter values from DLS analysis for pelagic zone.

Days of exposure	PELAGIC ZONE				Days of exposure	PELAGIC ZONE			
	PLA INDOOR		TPS INDOOR			PLA OUTDOOR		TPS OUTDOOR	
	NUMBER [μm]	VOLUME [μm]	NUMBER [μm]	VOLUME [μm]		NUMBER [μm]	VOLUME [μm]	NUMBER [μm]	VOLUME [μm]
26	BDL	BDL	BDL	BDL	26	54.50	181.03	171.83	198.92
40	212.85	220.69	216.58	227.57	40	154.38	179.67	134.92	165.10
54	BDL	BDL	BDL	3.69	54	BDL	BDL	BDL	BDL
68	0.20	0.20	22.10	22.10	68	BDL	BDL	BDL	BDL
82	BDL	BDL	2.96	64.31	82	BDL	BDL	0.31	13.56
96	0.39	0.65	BDL	BDL	96	0.62	0.71	0.44	55.64
110	396.85	639.64	BDL	BDL	110	0.08	0.36	BDL	BDL
124	1.02	1.18	0.98	1.02	124	0.36	0.59	0.08	0.35
138	BDL	BDL	1.06	2.04	138	BDL	BDL	0.10	2.12

Nanoparticle Tracking Analysis (only for pelagic)

NTA analysis gives back particle concentration and diameter (particle size distribution). A test with beads in dH₂O was performed and the results had the same order of magnitude of the real concentration. A seawater blank was tested and a concentration of $1.7 \cdot 10^7$ particles/mL was obtained. This value was subtracted to all the sample analyzed. The results are shown in Figure 4.54. Particles concentration was one or two orders of magnitude higher than concentration for Fluorescence microscope. PLA samples had the biggest final variation in the concentration values: 400% for PLA INDOOR and 800% for PLA OUTDOOR, against the 250% increase for TPS. A higher concentration variation was observed for TPS instead of PLA for Fluorescence microscope.

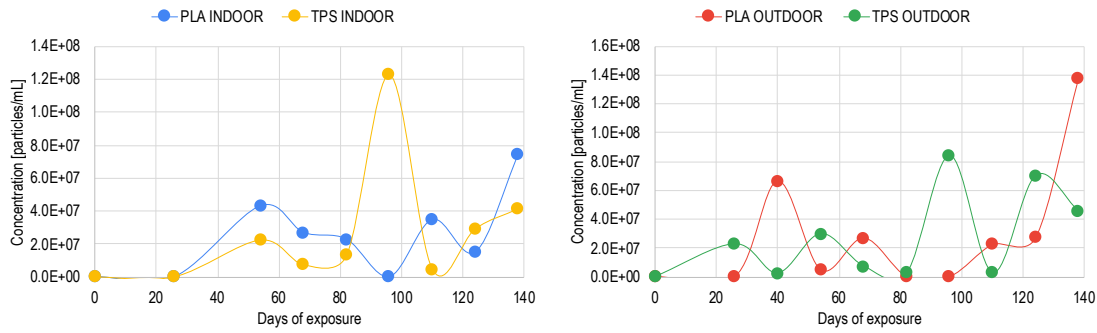


Figure 4.54. Particles concentration over the time for pelagic zone (NTA results).

Particles concentration had an increasing trend over the time and an oscillating behavior. The fluctuations can be linked to the degradation process of the different layers of the plastic pellets. However, it is challenging to confirm that all the particles observed are nanoplastics. The use of fluorescence could help this process, but our instrument did not allow this measurement.

The particles seen could be cells or can be due to contamination. However, contamination was low in the closed box for indoor conditions. Also, microplastics contamination was not influent in the experiments. Cells concentration (and the part that was not cells) retrieved with flow cytometry and OD results from Crystal Violet test were not correlated with NTA results. Also, a low particles concentration was found in the range of 0.5-5 μm , that is the range of bacterial cell size. And since from flow cytometry results cells concentration was stable over the time, the cells were already removed when the seawater particles concentration was removed from the data.

No correlation between Fluorescence microscope and NTA (only 0.74 for PLA OUT) was observed. Fluorescence microscope could detect particles with size higher than 1000nm, and if the observed particles are NPs generated from these secondary MPs there could be a delay in the generation.

No linear response-dose for the Schwarzschild's law was found.

Regarding the mean diameter (Figure 4.55), an oscillating behavior was visible, always around the mean pure seawater diameter (245nm). TPS NPs presents more fluctuations with respect to PLA, maybe due to its less homogeneous structure.

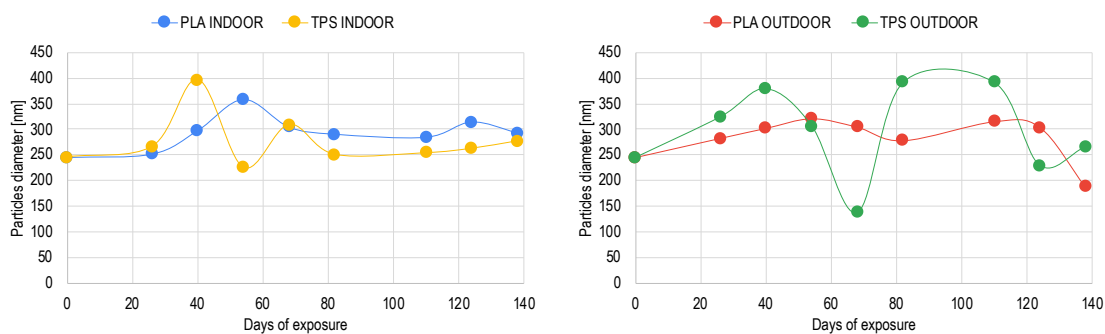


Figure 4.55. Particles diameter over the time for pelagic zone (NTA results).

No correlation between NTA diameter and DLS diameter was found, considering all results together. However, correlations between the two diameters (NTA and DLS) were found for single plastics: negative for PLA indoor (-0.94) , and positive for TPS indoor (0.95), highlighting the quite random behavior of bioplastics degradation in the marine environment

Advantages and limitation of the different techniques used for MPs/NPs detection and quantification

In Table 4.13 a summary of advantages and limitations in the use of the different techniques for MPs/NPs detection and quantification is presented.

Table 4.13. Advantages and limitation of the different techniques used for MPs/NPs detection and quantification. Table readapted from Fu et al., 2020.

Technique	Analytic capabilities	Advantages	Limitations
Fluorescence microscope with Nile Red	Concentration Size distribution	Low detection limit High sensitivity Fluorescence assures MPs detection	Sample preparation with dyes required Time consuming
Dynamic Light Scattering	Size distribution	Quick and easy Reliable estimation of the particle size distribution More accurate in detecting large aggregates	Large particles can obscure the presence of smaller particles No possibility to discriminate between different materials Not suitable for gravitationally settling or floating or aggregating particles
Nanoparticle Tracking Analysis	Concentration Size distribution Video of particles motion	Provides particle concentration and size of individual particles Direct visual information with the video Accurate in detecting small aggregates	The path of some particles might be out of the camera view and cannot be measured Set-up parameters need to be adjusted Not suitable for particles that are too disperse or too close in size

4.4. Sensitivity analysis

The results discussed in the previous sections were used to perform a sensitivity analysis using the Pearson correlation coefficient, introduced in Section 3.6. The results are shown in Figures 4.56, 4.57, 4.58, and 4.59, one for each plastic type and condition.

The fact that there are not many correlations highlights that bioplastics degradation (specifically hydrolysis and photo-oxidation) and MPs formation in the marine environments are complex phenomena difficult to explain and predict. As seen previously, the days of exposure (or light intensity) are negative correlated with the weight variation for PLA indoor coastal in Figure 4.56. The correlations between DLS diameter and the elements (such as Fe, Si, Ni, ...) is not meaningful, while the correlations among the elements could be interesting since they highlight a link among elements presence. For example, Iron can be found when there are also Nickel and Sulfur. In Figure 4.57, PLA outdoor coastal, shows an increase of S and Si, that are also correlated among them, over the time. This is less clear for PLA indoor since the presence of macroscopic sand particles on the pellets leads to a highly heterogeneous surface.

TPS indoor coastal (Figure 4.56) presents a good correlation between MPs concentration and weight variation. Again, elements (P, S, Si) are correlated among them, and they increase over the time. Regarding TPS outdoor coastal (Figure 4.57), an elemental correlation like the TPS indoor one is visible. Also, a correlation between DLS diameter and the time is highlighted.

		PLA INDOOR COASTAL													
		sampling #	days of exposure coastal	sunlight 4% (UV)	UV light	weight variation	Feret diameter	MPs concentration	Si	P	S	Cl	Fe	Ni	DLS diameter
PLA INDOOR COASTAL	sampling #	1.00	0.99	0.94	-0.77	0.00	0.39	0.37	-0.46	0.54	0.52	0.30	0.39	0.61	
	days of exposure coastal		1.00	0.94	-0.77	0.00	0.39	0.37	-0.45	0.55	0.52	0.30	0.40	0.61	
	sunlight 4% (UV)			1.00	-0.90	-0.01	0.37	0.36	-0.50	0.50	0.49	0.28	0.39	0.62	
	UV light				1.00	-0.85	-0.05	0.28	0.32	-0.41	0.48	0.43	0.22	0.36	0.65
	weight variation					1.00	0.51	-0.12	0.02	0.32	0.06	-0.37	0.22	0.16	-0.53
	Feret diameter						1.00	0.37	0.61	-0.23	0.62	-0.22	0.70	0.80	0.55
	MPs concentration							1.00	0.81	-0.35	0.21	0.63	-0.06	0.00	-0.34
	Si								1.00	-0.24	0.60	0.19	0.48	0.55	-0.41
	P									1.00	0.05	-0.16	-0.23	-0.24	-0.50
	S										1.00	0.25	0.76	0.81	-0.76
	Cl											1.00	-0.15	-0.24	-0.58
	Fe												1.00	0.91	0.94
	Ni													1.00	0.92
DLS diameter														1.00	

		TPS INDOOR COASTAL													
		sampling #	days of exposure coastal	sunlight 4% (UV)	UV light	weight variation	Feret diameter	MPs concentration	Si	P	S	Cl	Fe	Ni	DLS diameter
TPS INDOOR COASTAL	sampling #	1.00	0.99	0.94	0.00	0.11	0.28	0.40	0.71	0.77	0.57	0.31	0.02	0.48	
	days of exposure coastal		1.00	0.94	0.00	0.11	0.28	0.41	0.72	0.78	0.57	0.30	0.02	0.48	
	sunlight 4% (UV)			1.00	0.97	-0.04	0.14	0.25	0.32	0.69	0.70	0.54	0.37	0.05	0.48
	UV light				1.00	-0.18	0.18	0.13	0.21	0.66	0.60	0.50	0.43	0.11	0.50
	weight variation					1.00	-0.61	0.71	-0.07	0.01	-0.06	0.08	-0.14	0.13	
	Feret diameter						1.00	-0.29	-0.09	0.05	0.09	0.14	0.32	-0.02	0.36
	MPs concentration							1.00	0.30	0.26	0.30	0.61	-0.36	-0.26	-0.24
	Si								1.00	0.61	0.68	0.55	-0.13	-0.59	-0.11
	P									1.00	0.54	0.76	0.07	-0.45	0.68
	S										1.00	0.56	-0.13	-0.08	-0.21
	Cl											1.00	-0.04	-0.22	-0.18
	Fe												1.00	0.48	0.93
	Ni													1.00	0.76
DLS diameter														1.00	

Figure 4.56. Pearson correlation coefficient for PLA and TPS indoor coastal.

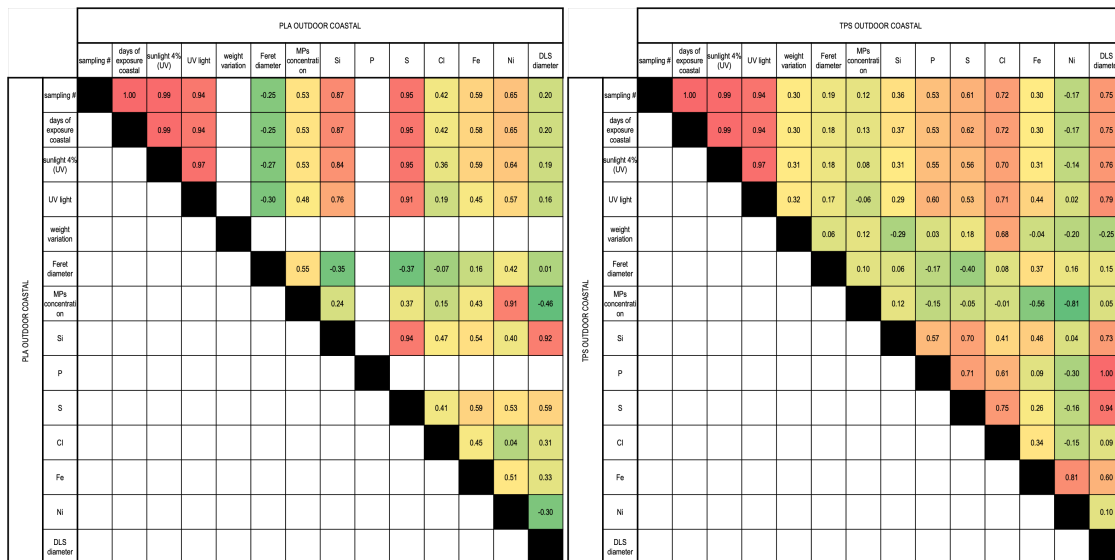


Figure 4.57. Pearson correlation coefficient for PLA and TPS outdoor coastal.

As highlighted from the results presented in the previous sections, the pellets degradation over the time was more visible for pelagic zone and this is also reflected in the correlations that the different variables have with the time (or light intensity).

For PLA indoor seawater (Figure 4.58) weight variation and size (Feret diameter) are negatively correlated with the time, while MPs concentration is positively correlated since it increases over time. Also, elements concentration is correlated with time and among them. Optical density from Crystal Violet test shows a good correlation with time. Also, MPs and elements concentrations increase over the time, and there is a strong correlation among the elements (especially for Si) in case of PLA outdoor seawater (Figure 4.59).

Like for PLA indoor, for TPS indoor seawater weight variation and Feret diameter are negative correlated with the time. DLS diameter is negatively correlated with exposure time. This negative correlation is also visible in case of TPS outdoor (Figure 4.59). Also, TPS outdoor shows correlations between the time of exposure and both MPs and elements concentration, and again, correlations among the elements themselves.

Briefly, due to the complexity of the phenomena occurring in the degradation of bioplastics, correlations are usually difficult to be detected. However, in most cases, elemental concentrations are correlated with time and among them since the elemental uptake increases over time and the particles are usually sand and salts. Negative correlations between weight variation (or size) and exposure time are more enhanced in the pelagic zone than in the coastal zone, as seen in the results section.

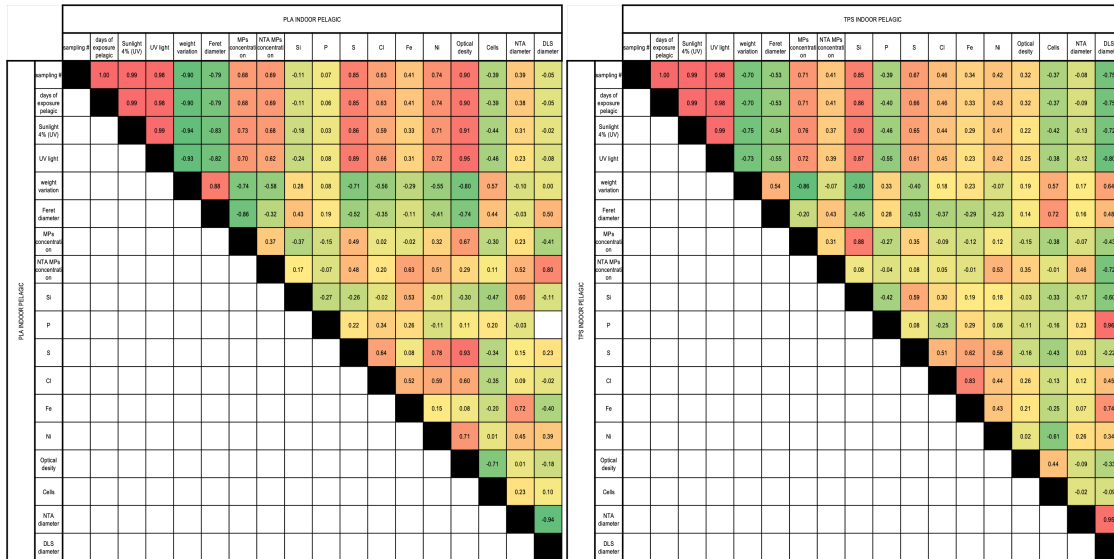


Figure 4.58. Pearson correlation coefficient for PLA and TPS indoor pelagic.

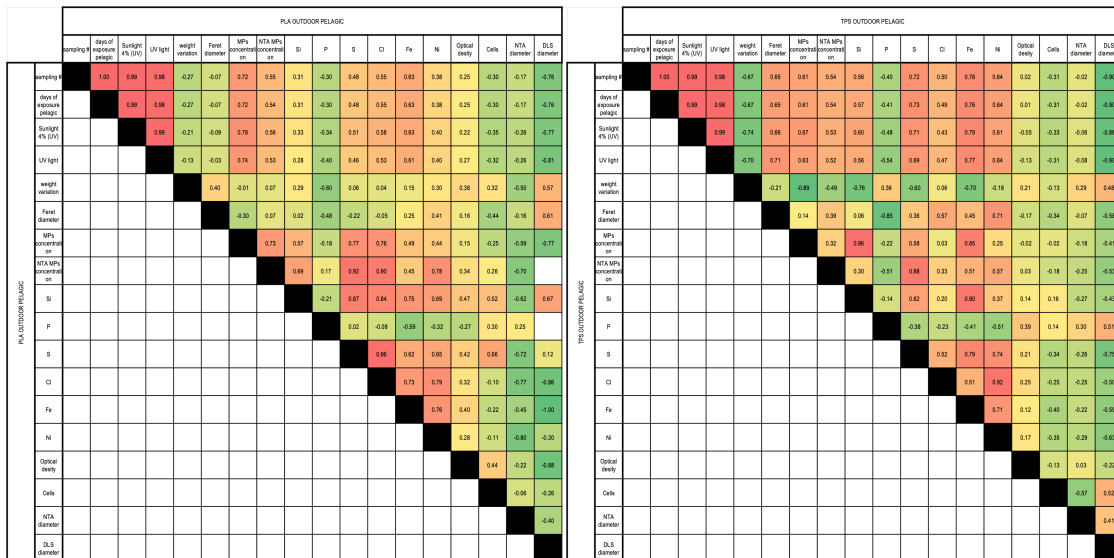


Figure 4.59. Pearson correlation coefficient for PLA and TPS outdoor pelagic.

6. Conclusions

The interest in biopolymers as sustainable alternatives to conventional fossil-based plastics is growing over the years in the market and in the research field. However, since bioplastics can often degrade quickly only under specific conditions and since the end-of-life of plastic waste is not always well managed, the fate on these plastics in the marine environment is arising concerns. Research is thus important to fill the lack of knowledge in the field of biopolymers degradation and bio-microplastics formation in the marine environments.

In this work, the degradation, mainly by photo-oxidation and hydrolysis, of bioplastic pellets (PLA and TPS) in the marine environment was studied in a 5-months experiments. The coastal zone (pellets over the beach sand) and the pelagic zone (pellets into aquariums filled with seawater) were simulated both in natural weathering in a greenhouse and accelerated weathering with UV lamps.

Pellets degradation was analyzed every two weeks by visual inspection, measuring weight and size, evaluating pellets topography (with SEM), chemical bonds (with ATR-FTIR) and elemental concentration (with XRF) changes along all the exposure periods. Secondary microplastics (MPs) and nanoplastics (NPs) concentration and size distribution were assessed every two weeks with Fluorescence microscope and Nile Red dye, Dynamic Light Scattering, and, only for pelagic zone, Nanoparticle Tracking Analysis.

During the 5 months of exposure, the color of TPS changed in different shadows of yellow in all the environments and conditions, except for TPS outdoor where a vivid green biofilm appeared over the time. PLA indoor coastal became yellowish and conglomerated with sand particles. Also, PLA indoor pelagic became from transparent to white.

Statistically significant weight reduction occurred only for PLA indoor in coastal zone (up to -7.6%), and for all the plastics in the pelagic zone. This effect was more pronounced in indoor conditions (up to -33.2% for PLA indoor and -16.8% for TPS indoor). Pellets exposed to pelagic indoor conditions also exhibited a size reduction. While the size increase of TPS outdoor pelagic pellets could be explained by water intrusion and biofilm formation.

Coastal pellets presented less signs of degradation than pelagic pellets, probably due to the hydrolysis effect. Also, pelagic degradation is more homogeneous than coastal one: pellets were free to move in water. Because of UV light, the indoor conditions showed a higher degradation than outdoor ones. Ruts and particles, shaped as the MPs visible under the Fluorescence microscope and with the same size, were detected on some pellets with SEM.

Some salts/sand particles were detectable on the pellets surface for both pelagic and coastal pellets. They become new pellets components and can act as contaminant carriers through the ecosystems. The elemental concentration (Ni, Si, S, Cl, Fe, P) on the surface of the pellets was assessed with XRF. TPS pellets showed an aptitude to absorb water with a consequent rapid increase of elemental concentrations. Pelagic TPS outdoor

showed the higher concentration increase since biofilm can enhance the elements trapping.

The FTIR spectra of degraded pellets exhibited significant changes in the carbonyl and hydroxyl bonds region. Also, the variation of chemical bond, quantified as Carbonyl Index (CI), was evaluated. For coastal zone, the CI increased from 0.30 to 0.85 and 0.47 for PLA indoor and outdoor pellets, respectively; while decreased from 5.60 to 3.40 and 4.90 for TPS indoor and outdoor pellets, respectively. For pelagic zone, the CI increased from 0.30 to 0.44 and 0.39 for PLA indoor and outdoor, respectively; while CI decreased from 5.60 to 3.20 and 4.74 for TPS indoor and outdoor, respectively.

MPs detection and quantification were challenging due to density separation procedure and the plastics aggregation, flotation or sedimentation. While Fluorescence microscope assures that plastics are measured thanks to Nile Red dye, NTA and DLS, despite the use of blank solutions, cannot guarantee that what the instruments are measuring is plastic or other particles. The use of fluorescence could overcome this problem. Secondary MPs formation (mainly in the form of fibers) was similar for the pelagic zone under indoor and outdoor conditions (from 10^4 MPs/ml of the pure seawater to 10^6) and its increase over the time was two orders of magnitude higher than in the coastal zone. NPs formation (with NTA) increased over the time but without a linear trend. While MPs concentration obeyed to Schwarzschild law for the pelagic zone, no linear dose-response was found for NPs. Due to faster degradation rates and different properties with respect to conventional plastics, the bioplastics behavior in the generation of micro-/nano-plastics could be more challenging to explain.

Briefly, the degradation mechanisms and the variations in the physico-chemical properties depend on the plastic type and on the environmental and exposure conditions. PLA pellets underwent more degradation effects than TPS. Also, the effects were more visible in the pelagic zone (hydrolysis effect) with respect to coastal zone and for indoor conditions (photodegradation effect) compared to outdoor ones. The potential of PLA and TPS to produce MPs is huge, posing a threat to the environment before they are fully degraded. Further research is needed to better understand all the mechanisms and rates of bioplastics degradation and microplastics formation in the different marine environments, along with their effects on the ecosystems and human health.

Bibliography

1. Accinelli, C., Saccà, M. L., Mencarelli, M., & Vicari, A. (2012). Deterioration of bioplastic carrier bags in the environment and assessment of a new recycling alternative. *Chemosphere*, *89*(2), 136–143. <https://doi.org/10.1016/j.chemosphere.2012.05.028>
2. Almond, J., Sugumaar, P., Wenzel, M. N., Hill, G., & Wallis, C. (2020). Determination of the carbonyl index of polyethylene and polypropylene using specified area under band methodology with ATR-FTIR spectroscopy. *E-Polymers*, *20*(1), 369–381. <https://doi.org/10.1515/epoly-2020-0041>
3. Al-Salem, S. M. (2020). *Biodegradable plastics fragmentation in soil and water: lessons learnt and comparative assessment with hydro-biodegradables*. 1–13. <https://doi.org/10.2495/WM200011>
4. Al-Salem, S. M. (2022). Study of the Degradation Behaviour of Virgin and Biodegradable Plastic Films in Marine Environment Using ASTM D 6691. *Journal of Polymers and the Environment*, *30*(6), 2329–2340. <https://doi.org/10.1007/s10924-021-02351-8>
5. Applied Rigaku technologies. (n.d.). *Elemental analysis by energy dispersive x-ray fluorescence (EDXRF)*. Rigaku. https://www.rigakuedxrf.com/?gclid=Cj0KCQjw39uYBhCLARIsAD_SzMQuP5wtAoeuyc5gqJsqMScJed7gmD5Dj2pQQT-cH7PKUGelcqwq5voaAjixEALw_wcB
6. Atiweh, G., Mikhael, A., Parrish, C. C., Banoub, J., & Le, T.-A. T. (2021). Environmental impact of bioplastic use: A review. *Heliyon*, *7*(9), e07918. <https://doi.org/10.1016/j.heliyon.2021.e07918>
7. Bahl, S., Dolma, J., Jyot Singh, J., & Sehgal, S. (2021). Biodegradation of plastics: A state of the art review. *Materials Today: Proceedings*, *39*, 31–34. <https://doi.org/10.1016/j.matpr.2020.06.096>
8. Banihashemi, K., & Gil, F. (2022). Biomass Estimation of Marine Biofilms on Plastic Surfaces. *Cal Poly Biological Science*, *23*.
9. Bao, R., Pu, J., Xie, C., Mehmood, T., Chen, W., Gao, L., Lin, W., Su, Y., Lin, X., & Peng, L. (2022). Aging of biodegradable blended plastic generates microplastics and attached bacterial communities in air and aqueous environments. *Journal of Hazardous Materials*, *434*, 128891. <https://doi.org/10.1016/j.jhazmat.2022.128891>
10. Beltrán-Sanahuja, A., Casado-Coy, N., Simó-Cabrera, L., & Sanz-Lázaro, C. (2020). Monitoring polymer degradation under different conditions in the marine environment. *Environmental Pollution*, *259*, 113836. <https://doi.org/10.1016/j.envpol.2019.113836>
11. Benítez, A., Sánchez, J. J., Arnal, M. L., Müller, A. J., Rodríguez, O., & Morales, G. (2013). Abiotic degradation of LDPE and LLDPE formulated with a pro-oxidant additive. *Polymer Degradation and Stability*, *98*(2), 490–501. <https://doi.org/10.1016/j.polymdegradstab.2012.12.011>
12. Bhatt, P., Pathak, V. M., Bagheri, A. R., & Bilal, M. (2021). Microplastic contaminants in the aqueous environment, fate, toxicity consequences, and remediation strategies. *Environmental Research*, *200*, 111762. <https://doi.org/10.1016/j.envres.2021.111762>
13. Cañado, N., Lizundia, E., Akizu-Gardoki, O., Minguéz, R., Lekube, B., Arrillaga, A., & Iturrondobeitia, M. (2022). 3D printing to enable the reuse of marine plastic waste with reduced environmental impacts. *Journal of Industrial Ecology*, *jiec.13302*. <https://doi.org/10.1111/jiec.13302>
14. Catarci Carteny, C., & Blust, R. (2021). Not Only Diamonds Are Forever: Degradation of Plastic Films in a Simulated Marine Environment. *Frontiers in Environmental Science*, *9*, 662844. <https://doi.org/10.3389/fenvs.2021.662844>
15. CFI Team. (2022, November 4). *R-squared*. CFI. <https://corporatefinanceinstitute.com/resources/data-science/r-squared/>
16. Chaplin, M. (2013). *Infrared Spectroscopy*. 85.
17. Cheng, J., Eyheraguibel, B., Jacquín, J., Pujo-Pay, M., Conan, P., Barbe, V., Hoypierres, J., Delige, G., Halle, A. T., Bruzard, S., Ghiglione, J.-F., & Meistertzheim, A.-L. (2022). Biodegradability under marine conditions of bio-based and petroleum-based polymers as substitutes of conventional microparticles. *Polymer Degradation and Stability*, *206*, 110159. <https://doi.org/10.1016/j.polymdegradstab.2022.110159>
18. del Rosario Salazar-Sánchez, M., Campo-Erazo, S. D., Villada-Castillo, H. S., & Solanilla-Duque, J. F. (2019). Structural changes of cassava starch and polylactic acid films submitted to biodegradation process. *International Journal of Biological Macromolecules*, *129*, 442–447. <https://doi.org/10.1016/j.ijbiomac.2019.01.187>
19. Delacuvellerie, A., Benali, S., Cyriaque, V., Moins, S., Raquez, J.-M., Gobert, S., & Wattiez, R. (2021). Microbial biofilm composition and polymer degradation of compostable and non-compostable plastics immersed in the marine environment. *Journal of Hazardous Materials*, *419*, 126526. <https://doi.org/10.1016/j.jhazmat.2021.126526>
20. Deroiné, M., Le Duigou, A., Corre, Y.-M., Le Gac, P.-Y., Davies, P., César, G., & Bruzard, S. (2014). Accelerated ageing of polylactide in aqueous environments: Comparative study between distilled water and seawater. *Polymer Degradation and Stability*, *108*, 319–329. <https://doi.org/10.1016/j.polymdegradstab.2014.01.020>

21. Di Cesare, A., Pinnell, L. J., Brambilla, D., Elli, G., Sabatino, R., Sathicq, M. B., Corno, G., O'Donnell, C., & Turner, J. W. (2021). Bioplastic accumulates antibiotic and metal resistance genes in coastal marine sediments. *Environmental Pollution*, 291, 118161. <https://doi.org/10.1016/j.envpol.2021.118161>
22. Duong, T. T., Le, P. T., Nguyen, T. N. H., Hoang, T. Q., Ngo, H. M., Doan, T. O., Le, T. P. Q., Bui, H. T., Bui, M. H., Trinh, V. T., Nguyen, T. L., Da Le, N., Vu, T. M., Tran, T. K. C., Ho, T. C., Phuong, N. N., & Strady, E. (2022). Selection of a density separation solution to study microplastics in tropical riverine sediment. *Environmental Monitoring and Assessment*, 194(2), 65. <https://doi.org/10.1007/s10661-021-09664-0>
23. Ebert, C., Tuchscher, L., Unger, N., Pöllath, C., Gladigau, F., Popp, J., Löffler, B., & Neugebauer, U. (2021). Correlation of crystal violet biofilm test results of *STAPHYLOCOCCUS AUREUS* clinical isolates with Raman spectroscopic read-out. *Journal of Raman Spectroscopy*, 52(12), 2660–2670. <https://doi.org/10.1002/jrs.6237>
24. Eich, A., Weber, M., & Lott, C. (2021). Disintegration half-life of biodegradable plastic films on different marine beach sediments. *PeerJ*, 9, e11981. <https://doi.org/10.7717/peerj.11981>
25. European Bioplastics. (2021a). *Applications for bioplastics*. European Bioplastics. <https://www.european-bioplastics.org/market/applications-sectors/>
26. European Bioplastics. (2021b). *Bioplastics market data*. European Bioplastics. <https://www.european-bioplastics.org/market/>
27. European Bioplastics. (2021c, December 6). *European Bioplastics Conference confirms bioplastics make significant contributions to the European Union's ambitious climate goals*. <https://www.european-bioplastics.org/european-bioplastics-conference-confirms-bioplastics-make-significant-contributions-to-the-european-unions-ambitious-climate-goals/>
28. European Commission. (n.d.). *Plastics*. European Commission Environment. https://environment.ec.europa.eu/topics/plastics_en
29. European Commission. (2022a). *Bio-based, biodegradable and compostable plastics*. European Commission. https://environment.ec.europa.eu/topics/plastics/bio-based-biodegradable-and-compostable-plastics_en
30. European Commission. (2022b). *Microplastics*. European Commission Environment. https://environment.ec.europa.eu/topics/plastics/microplastics_en
31. European Commission. (2022c). *Plastic bags*. European Commission Plastics. https://environment.ec.europa.eu/topics/plastics/plastic-bags_en
32. European Commission. (2022d). *Single-use plastics*. European Commission Environment. https://environment.ec.europa.eu/topics/plastics/single-use-plastics_en
33. Fu, W., Min, J., Jiang, W., Li, Y., & Zhang, W. (2020). Separation, characterization and identification of microplastics and nanoplastics in the environment. *Science of The Total Environment*, 721, 137561. <https://doi.org/10.1016/j.scitotenv.2020.137561>
34. Gallo, A. (2015, November 4). *A Refresher on Regression Analysis*. Harvard Business Review. <https://hbr.org/2015/11/a-refresher-on-regression-analysis>
35. Gardette, M., Perthue, A., Gardette, J.-L., Janecska, T., Földes, E., Pukánszky, B., & Therias, S. (2013). Photo- and thermal-oxidation of polyethylene: Comparison of mechanisms and influence of unsaturation content. *Polymer Degradation and Stability*, 98(11), 2383–2390. <https://doi.org/10.1016/j.polymdegradstab.2013.07.017>
36. Gewert, B., Plassmann, M. M., & MacLeod, M. (2015). Pathways for degradation of plastic polymers floating in the marine environment. *Environmental Science: Processes & Impacts*, 17(9), 1513–1521. <https://doi.org/10.1039/C5EM00207A>
37. Gorrasi, G., & Pantani, R. (Eds.). (2018). Hydrolysis and Biodegradation of Poly(lactic acid). In *Synthesis, Structure and Properties of Poly(lactic acid)* (Vol. 279, pp. 119–151). Springer International Publishing. <https://doi.org/10.1007/978-3-319-64230-7>
38. Guzman-Sielicka, A., Janik, H., & Sielicki, P. (2013). Proposal of New Starch-Blends Composition Quickly Degradable in Marine Environment. *Journal of Polymers and the Environment*, 21(3), 802–806. <https://doi.org/10.1007/s10924-012-0558-7>
39. Jacquin, J., Callac, N., Cheng, J., Giraud, C., Gorand, Y., Denoual, C., Pujo-Pay, M., Conan, P., Meistertzheim, A.-L., Barbe, V., Bruzard, S., & Ghiglione, J.-F. (2021). Microbial Diversity and Activity During the Biodegradation in Seawater of Various Substitutes to Conventional Plastic Cotton Swab Sticks. *Frontiers in Microbiology*, 12, 604395. <https://doi.org/10.3389/fmicb.2021.604395>
40. Janik, H., Sienkiewicz, M., Przybytek, A., Guzman, A., Kucinska-Lipka, J., & Kosakowska, A. (2018). Novel Biodegradable Potato Starch-based Compositions as Candidates in Packaging Industry, Safe for Marine Environment. *Fibers and Polymers*, 19(6), 1166–1174. <https://doi.org/10.1007/s12221-018-7872-1>
41. Kliem, S., Kreutzbruck, M., & Bonten, C. (2020). Review on the Biological Degradation of Polymers in Various Environments. *Materials*, 13(20), 4586. <https://doi.org/10.3390/ma13204586>

42. Li, Y., Yao, L., Li, Y., Wang, Y., Wang, L., Jiang, Z., Qiu, D., & Weng, Y. (2022). Degradation kinetics and performances of poly(lactic acid) films in artificial seawater. *Chemical Papers*, 76(9), 5929–5941. <https://doi.org/10.1007/s11696-022-02286-x>
43. Lobelle, D., & Cunliffe, M. (2011). Early microbial biofilm formation on marine plastic debris. *Marine Pollution Bulletin*, 62(1), 197–200. <https://doi.org/10.1016/j.marpolbul.2010.10.013>
44. Maes, T., Jessop, R., Wellner, N., Haupt, K., & Mayes, A. G. (2017). A rapid-screening approach to detect and quantify microplastics based on fluorescent tagging with Nile Red. *Scientific Reports*, 7(1), 44501. <https://doi.org/10.1038/srep44501>
45. Malvern Panalytical. (n.d.). *NanoSight NS300*. <https://www.malvernpanalytical.com/en/products/product-range/nanosight-range/nanosight-ns300?campaignid=166505820&adgroupid=12214296420&creative=562890761964&keyword=nanosight%20ns300&matchtype=e&network=g&device=c&gclid=CjwKCAjwrNmWBhA4EiwAHbjEQETpe4Nev7>
46. Mampel, J., Spirig, T., Weber, S. S., Haagensen, J. A. J., Molin, S., & Hilbi, H. (2006). Planktonic Replication Is Essential for Biofilm Formation by *Legionella pneumophila* in a Complex Medium under Static and Dynamic Flow Conditions. *Applied and Environmental Microbiology*, 72(4), 2885–2895. <https://doi.org/10.1128/AEM.72.4.2885-2895.2006>
47. Manohar, S. M., Shah, P., & Nair, A. (2021). Flow cytometry: Principles, applications and recent advances. *Bioanalysis*, 13(3), 185–203. <https://doi.org/10.4155/bio-2020-0267>
48. Martin, J. W., Chin, J. W., & Nguyen, T. (2003). Reciprocity law experiments in polymeric photodegradation: A critical review. *Progress in Organic Coatings*, 47(3–4), 292–311. <https://doi.org/10.1016/j.porgcoat.2003.08.002>
49. Martin, R. T., Camargo, L. P., & Miller, S. A. (2014). Marine-degradable polylactic acid. *Green Chem.*, 16(4), 1768–1773. <https://doi.org/10.1039/C3GC42604A>
50. Martinez Villadiego, K., Arias Tapia, M. J., Useche, J., & Escobar Macías, D. (2022). Thermoplastic Starch (TPS)/Polylactic Acid (PLA) Blending Methodologies: A Review. *Journal of Polymers and the Environment*, 30(1), 75–91. <https://doi.org/10.1007/s10924-021-02207-1>
51. Miksch, L., Köck, M., Gutow, L., & Saborowski, R. (2022). Bioplastics in the Sea: Rapid In-Vitro Evaluation of Degradability and Persistence at Natural Temperatures. *Frontiers in Marine Science*, 9, 920293. <https://doi.org/10.3389/fmars.2022.920293>
52. Mroczkowska, M., Germaine, K., Culliton, D., Kakouli Duarte, T., & Neves, A. C. (2021). Assessment of Biodegradation and Eco-Toxic Properties of Novel Starch and Gelatine Blend Bioplastics. *Recycling*, 6(4), 81. <https://doi.org/10.3390/recycling6040081>
53. Nasir, N. N., & Othman, S. A. (2022). Influence of Glycerol Contents on The Morphological (SEM) and Functional (FTIR) Properties of Corn-based Bioplastic. 43(1), 7.
54. National Geographic Society. (2022, May 20). *Microplastics*. National Geographic. <https://education.nationalgeographic.org/resource/microplastics>
55. Niu, X., Huan, S., Li, H., Pan, H., & Rojas, O. J. (2021). Transparent films by ionic liquid welding of cellulose nanofibers and polylactide: Enhanced biodegradability in marine environments. *Journal of Hazardous Materials*, 402, 124073. <https://doi.org/10.1016/j.jhazmat.2020.124073>
56. Pauli, N.-C., Petermann, J. S., Lott, C., & Weber, M. (2017). Macrofouling communities and the degradation of plastic bags in the sea: An *in situ* experiment. *Royal Society Open Science*, 4(10), 170549. <https://doi.org/10.1098/rsos.170549>
57. Pelegrini, K., Donazzolo, I., Brambilla, V., Coulon Grisa, A. M., Piazza, D., Zattera, A. J., & Brandalise, R. N. (2016). Degradation of PLA and PLA in composites with triacetin and buriti fiber after 600 days in a simulated marine environment. *Journal of Applied Polymer Science*, 133(15), n/a-n/a. <https://doi.org/10.1002/app.43290>
58. Phosri, S., Kunjiek, T., Mukkhakang, C., Suebthep, S., Sinsup, W., Phornsirigarn, S., & Charoeythornkhajhornchai, P. (2022). Biodegradability of bioplastic blown film in a marine environment. *Frontiers in Marine Science*, 9, 917397. <https://doi.org/10.3389/fmars.2022.917397>
59. Pickett, J. E. (2018). Chapter 8—Weathering of Plastics. In *Handbook of Environmental Degradation of Materials* (Third Edition, pp. 163–184). William Andrew Publishing. <https://doi.org/10.1016/B978-0-323-52472-8.00008-3>
60. Pinto, J., Dias, M., Amaral, J., Ivanov, M., Paixão, J. A., Coimbra, M. A., Ferreira, P., Pereira, E., & Gonçalves, I. (2022). Influence of UV degradation of bioplastics on the amplification of mercury bioavailability in aquatic environments. *Marine Pollution Bulletin*, 180, 113806. <https://doi.org/10.1016/j.marpolbul.2022.113806>
61. Pizzino, G., Irrera, N., Cucinotta, M., Pallio, G., Mannino, F., Arcoraci, V., Squadrito, F., Altavilla, D., & Bitto, A. (2017). Oxidative Stress: Harms and Benefits for Human Health. *Oxidative Medicine and Cellular Longevity*, 2017, 1–13. <https://doi.org/10.1155/2017/8416763>
62. Plastics Europe. (2021). *Plastics—The Facts 2021. An analysis of European plastics production, demand and waste data*. Plastics Europe. <https://www.google.com/search?client=safari&rls=en&q=Plastics+>

- +the+Facts+2021+An+analysis+of+European+plastics+production,+demand+and+waste+data&ie=UTF-8&oe=UTF-8
63. Pokora, M., Rheinberger, T., Wurm, F. R., Paneth, A., & Paneth, P. (2022). Environment-friendly transesterification to seawater-degradable polymers expanded: Computational construction guide to breaking points. *Chemosphere*, *308*, 136381. <https://doi.org/10.1016/j.chemosphere.2022.136381>
 64. Prieto, A. (2016). To be, or not to be biodegradable... that is the question for the bio-based plastics. *Microbial Biotechnology*, *9*(5), 652–657. <https://doi.org/10.1111/1751-7915.12393>
 65. QuestionPro. (2022). *Correlation analysis*. QuestionPro. <https://www.questionpro.com/features/correlation-analysis.html>
 66. Rheinberger, T., Wolfs, J., Paneth, A., Gojzewski, H., Paneth, P., & Wurm, F. R. (2021). RNA-Inspired and Accelerated Degradation of Polylactide in Seawater. *Journal of the American Chemical Society*, *143*(40), 16673–16681. <https://doi.org/10.1021/jacs.1c07508>
 67. Rodrigues, M. O., Gonçalves, A. M. M., Gonçalves, F. J. M., & Abrantes, N. (2020). Improving cost-efficiency for MPs density separation by zinc chloride reuse. *MethodsX*, *7*, 100785. <https://doi.org/10.1016/j.mex.2020.100785>
 68. Sandt, C., Waeytens, J., Deniset-Besseau, A., Nielsen-Leroux, C., & Réjasse, A. (2021). Use and misuse of FTIR spectroscopy for studying the bio-oxidation of plastics. *Spectrochimica Acta Part A: Molecular and Biomolecular Spectroscopy*, *258*, 119841. <https://doi.org/10.1016/j.saa.2021.119841>
 69. Sangkham, S., Faikhaw, O., Munkong, N., Sakunkoo, P., Arunlertaree, C., Chavali, M., Mousazadeh, M., & Tiwari, A. (2022). A review on microplastics and nanoplastics in the environment: Their occurrence, exposure routes, toxic studies, and potential effects on human health. *Marine Pollution Bulletin*, *181*, 113832. <https://doi.org/10.1016/j.marpolbul.2022.113832>
 70. Schirinzi, G. F., Pérez-Pomeda, I., Sanchis, J., Rossini, C., Farré, M., & Barceló, D. (2017). Cytotoxic effects of commonly used nanomaterials and microplastics on cerebral and epithelial human cells. *Environmental Research*, *159*, 579–587. <https://doi.org/10.1016/j.envres.2017.08.043>
 71. Shimadzu. (n.d.). *SALD-7500nano Nano Particle Size Analyzer*. <https://www.shimadzu.com/an/products/particle-size-analysis/particle-size-analyzer/sald-7500nano/index.html>
 72. Sin, L. T., Rahmat, A. R., & Rahman, W. A. W. (2012). *Polylactic Acid: PLA Biopolymer Technology and Applications* (1st ed.). St. Louis: Elsevier Science & Technology.
 73. Skariyachan, S., Manjunatha, V., Sultana, S., Jois, C., Bai, V., & Vasist, K. S. (2016). Novel bacterial consortia isolated from plastic garbage processing areas demonstrated enhanced degradation for low density polyethylene. *Environmental Science and Pollution Research*, *23*(18), 18307–18319. <https://doi.org/10.1007/s11356-016-7000-y>
 74. Smith, B. C. (2021). The Infrared Spectra of Polymers III: Hydrocarbon Polymers. *Spectroscopy*, *36*(11), 22–25.
 75. Thermo Scientific. (n.d.). *Nicolet™ iS50 FTIR Spectrometer*. ThermoFischer Scientific. <https://www.thermofisher.com/order/catalog/product/912A0760>
 76. Umamaheswari, S., & Murali, M. (2013). *FTIR spectroscopic study of fungal degradation of poly(ethylene terephthalate) and polystyrene foam*. 6.
 77. Wang, Z., Ding, J., Song, X., Zheng, L., Huang, J., Zou, H., & Wang, Z. (2023). Aging of poly (lactic acid)/poly (butylene adipate-co-terephthalate) blends under different conditions: Environmental concerns on biodegradable plastic. *Science of The Total Environment*, *855*, 158921. <https://doi.org/10.1016/j.scitotenv.2022.158921>
 78. Webb, H., Arnott, J., Crawford, R., & Ivanova, E. (2012). Plastic Degradation and Its Environmental Implications with Special Reference to Poly(ethylene terephthalate). *Polymers*, *5*(1), 1–18. <https://doi.org/10.3390/polym5010001>
 79. Yang, Y., Li, Z., Yan, C., Chadwick, D., Jones, D. L., Liu, E., Liu, Q., Bai, R., & He, W. (2022). Kinetics of microplastic generation from different types of mulch films in agricultural soil. *Science of The Total Environment*, *814*, 152572. <https://doi.org/10.1016/j.scitotenv.2021.152572>
 80. Zaaba, N. F., & Ismail, H. (2019). A review on tensile and morphological properties of poly (lactic acid) (PLA)/ thermoplastic starch (TPS) blends. *Polymer-Plastics Technology and Materials*, *58*(18), 1945–1964. <https://doi.org/10.1080/25740881.2019.1599941>